Section I

3.I.1 Importance of chiral molecules

The importance of chirality is now well recognised, mainly in connection with the fact that nearly all natural products are chiral and their physiological or pharmacological properties depend upon their recognition by chiral receptors, which will interact only with molecules of the proper absolute configuration. Hence, the use of chiral drugs or molecules in enantiopure form is now a standard requirement for every new chemical entity. Indeed, the preparation of chiral compounds is an important and challenging area of contemporary synthetic organic chemistry [1]. The extensive utility of synthetic chiral molecules as single enantiomer has been recognised by pharmaceuticals for the development of targeted key molecules. Many examples of compounds are known where one can note a different pharmacological response for two enantiomers. For instance, *S* warfarin is six times as active as an anticoagulant as its *R* enantiomer, while *S*-propranolol is antihypertensive and antiarrythmic which is used in the treatment of heart condition while the *R* enantiomer acts as a contraceptive.

Scheme 3.1: Structure of Warfarin and Propranolol

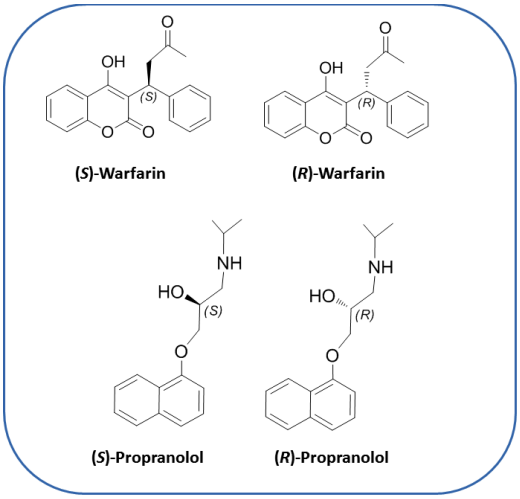

Along with this understanding there is constant need to develop reliable and quick methods to determine optical purity of the chiral molecules. The search for new and efficient methods for the purification and measurement of enantiomeric excess (ee) of chiral compounds has been an active area of research in organic synthesis.

3.I.2 Enantiomeric excess

The definite properties of chiral molecules are often linked with the particular optical isomer and depend on its purity. Chiral compounds have "*R*" and "*S*" enantiomers that may coexist in the same solution but not always in equal amounts. Enantiomeric excess is the most common way to report the level of enantioselectivity observed for a reaction. Enantiomeric excess is a measure of the extent to which a particular enantiomer dominates in the mixture. A racemic mixture has an *ee* of 0%, while a single completely pure enantiomer has an *ee* of 100%. A sample with 82% of one enantiomer and 18% of the other has an *ee* of 64%. Enantiomeric excess is used as one of the indicators of the success of an asymmetric synthesis. It is expressed as a percent enantiomeric excess.

$$ee\% = [(R - S) / (R+S)] \times 100$$

For mixtures of diastereomers, there are analogous definitions and uses for diastereomeric excess (*d.e.*%) and percent diastereomeric excess.

3.I.3 Analytical Methods

Over the past decade there has been a great interest in enantioselective synthesis which has led to an increased demand for accurate, reliable and convenient methods of measuring enantiomeric purity. The most suitable methods are chromatography on chiral stationary phases and spectroscopy. The other most employed techniques for enatiodiscrimination are High performance liquid chromatography, Gas chromatography [3], Polarimeter [4a], Circular dichroism [4b-4e] Electrophoresis [4f], X-ray crystallography and NMR spectroscopy. Methods of CD (circular dichroism) and VCD (vibrational circular dichroism) [2] are intrinsically chiral and avoid the need for an additional chiral reference. X-ray crystallography requires a single crystal of good quality and limiting its use for liquid samples and solutions. Among such HPLC, GC, polarimeter and NMR spectroscopy are most frequently used technique. Nevertheless, NMR spectroscopy although it is achiral method it is quite popular, because this technique is ubiquitous and easily available in nearly all laboratories around the world. Development of more powerful and more sensitive NMR machines has also an added advantage to this method of analysis of chirality. Recently some biochemical methods are also developed to determine ee of the chiral products [5].

3.I.3.2 Polarimeter, HPLC & GC method

The use of polarimeter to measure the optical activity is an old technique and also requires very large amount of compound [4a]. In HPLC direct enantiomeric resolutions are only feasible in chromatographic systems which contain an appropriate chiral selector. The latter can be incorporated into the stationary phase (chiral stationary phase) or be permanently bonded to or coated on to the surface of the column packing material (chiral bonded and chiral coated stationary phases). Gas chromatography (GC) is a technique in analytical chemistry used to separate the components in a mixture, to identify each product.

3.I.3.3 Limitation of HPLC & GC technique:

1. Its operation can be complex.
2. Requires different type of chiral column for different type of molecules.
3. Requires efforts for method development.

3.I.4 NMR as Analytical Technique

With the advent of NMR spectrometer most of the laboratories working in the area of chiral molecules have access to high resolution machines for this kind of analysis. The NMR spectra of the enantiomers display same pattern and chemical shifts, when recorded in achiral environment (solvent). However, the nuclei of diastereomeric compounds have slightly different environment and shows significant change in the signals. Therefore, for the utility of NMR for chiral analysis, the basic requirement is that enantiomers have to be converted into diastereomers.

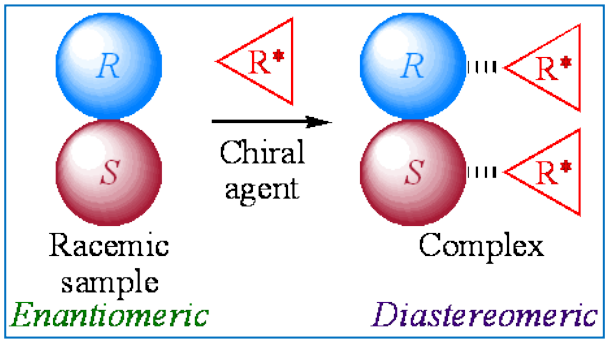

Application of NMR spectroscopy is convenient and straight-forward in many aspects, such as sample preparation and use of one dimensional NMR experiments. In this approach the conversion of enantiomer to diastereomers is carried out by using one of the chiral auxiliaries, viz., Chiral Derivatizing Agent (CDAs), Chiral Lanthanide shift Agent (CLSRs) or Chiral Solvating Agent (CSAs) [6].

One of the basic requirements of this approach is that chiral analyte must contain

certain functional group such as, -COOH, -OH, $–NH_2$, COOR etc. in order to convert them to diastereomers utilising the derivatization procedure or noncovalent interactions.

The NMR spectra of the enantiomers display the same pattern and chemical shifts, when recorded in achiral environment. However, the NMR active nuclei of diastereomeric compounds have slightly different environment and show significant change in the signals. Therefore, for accurate determination of the ratio of enantiomers by NMR spectroscopy, it is necessary to quantitatively convert the analyte to the diastereomers. This can be achieved by forming diastereomeric derivatives of the analyte with appropriate chiral additive.

In general chiral additive convert the mixture of enantiomers in a mixture of diastereomeric species in three different ways:

(a) By forming a covalent bond with the analyte, and in this case the additive is a "chiral derivatizing agent" (**CDA**) [7].

(b) By forming a labile supramolecular interaction, so it acts as "chiral solvating agent" (**CSA**) [8].

(c) A complex which can be formed between a paramagnetic material and substrate, to be used to differentiate enantiomers (**CLSR**) [9].

3.I.5 CHIRAL DERIVATISING AGENTS

A chiral derivatizing agent (CDA) is a chiral auxiliary used to convert a mixture of enantiomers into diastereomers in order to analyses the quantities of each enantiomer present within the mixture or analyte. Analysis can be conducted by chromatography or spectroscopy. If the NMR spectroscopy is available to chemists it is easier to analyze the sample of diastereomers. The CDA produces chemical shift difference between diastereomer of *R* and *S* of chiral substrate which can be utilized for measurement of *ee* and also for assignment of absolute configuration. In general, CDA forms a covalent bond with the substrate moiety by chemical reaction.

The first example of this technique was published in 1969 by Harry S. Mosher. The chiral agent used was a single enantiomer of MTPA (α-methoxy-α-(trifluoromethyl) phenylacetic acid), also known as Mosher's acid.

The corresponding acid chloride is also known as Mosher's acid chloride, and the resultant diastereomeric esters are known as Mosher's esters [10].

Scheme 3.2: Structure of Mosher`s acid [MPTA] and Mosher`s acid chloride

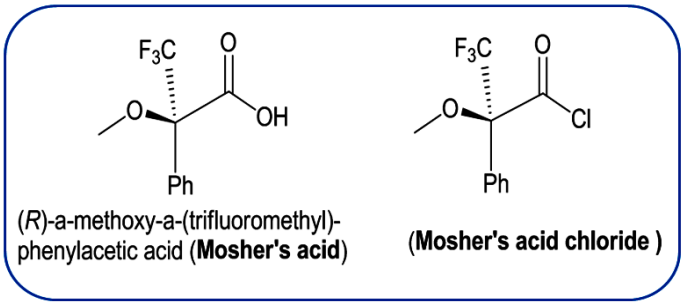

3.I.5.1 Condition for CDA

The general use and design of CDA should obey following rules so that CDA can effectively determine optical purity [11].

1. The CDA should be enantiomerically pure, or (less satisfactorily) its enantiomeric purity must be accurately known.

2. The reaction of the CDA with both enantiomers should proceed to completion under reaction conditions. If not this can give error in the measurement of enantiomeric excess.

3. CDA must not racemize under derivatization process. Its attachment should be mild enough so that the substrate does not racemize either. If analysis is performed by HPLC, the CDA must contain a chromophore to enhance detectability.

4. The CDA should have a functional group that gives a singlet signal in the resultant NMR spectrum, where the new signal must be well resolved from other peaks.

3.I.5.2 Limitation of chiral derivatizing agent

(1) The use of CDAs can involve kinetic resolution of the substrate.

(2) It requires purification of the sample.

(3) The structure of CDA should contain functional group.

3.I.6.1 Chiral Lanthanide Shift Reagent

In earlier decades more focus was on the use of chiral lanthanide shift reagent for determination of enantiomeric excess [12]. If the ligand in the lanthanide complex is chiral then it is possible to obtain diastereomeric complex.

A complex formed between a paramagnetic material and substrate can be used to differentiate enantiomers.

Scheme 3.3: Structure of Chiral Lanthanide reagent

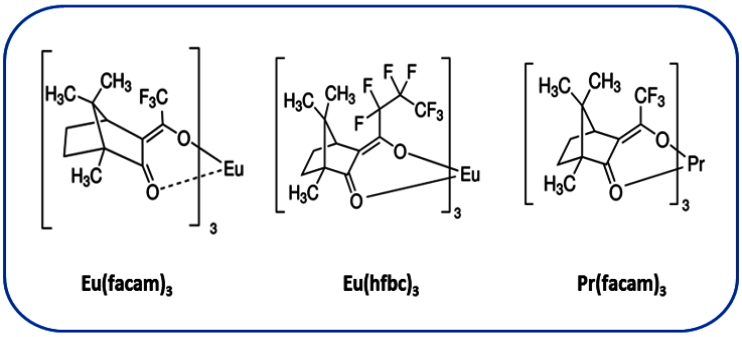

3.I.6.2 Limitation of chiral lanthanide shift reagent

CLSRs are paramagnetic in nature and cause excessive broadening of NMR peaks of chiral substrate. Their limited availability and some operational difficulties such as high cost and sometime lower solubility make them less popular.

3.I.7.1 Chiral Solvating Agents [CSAs]

During the last couple of decades, steroselective synthesis of chiral compounds has been one of the major challenges in modern organic, pharmaceutical and medicinal chemistry. Such syntheses need to be supported by suitable analytical methods; in other words, they are effective only if they are accompanied by quick and easy ways to determine enantiomeric purity and where ever relevant, the absolute configuration. The use of CDAs can involve kinetic resolution of the substrate and requires purification of the sample, whereas CSAs do not pose such disadvantages and the sample can be easily recovered after the analysis. It is a nondestructive technique.

Chiral solvating agents [CSAs] essentially have potential for this purpose because the enantiomeric purity can be determined just by adding the reagent to a chiral compound in a small amount while recording the NMR spectra. This technique is simple compared to the above mentioned methods.

Chiral solvating agent involves the formation of diastereomers through non-covalent interaction such as hydrogen bonding, -CH-π ion pairing, π-π interaction etc. It involves straight forward protocol that is "*mixing of analyte with CSA*".

A practical expression of this idea was pioneered by Pirkle who used 2,2,2-trifluoro-1-(9-anthryl)ethanol (TFAE) as a chiral solvating agent (CSA) for the determination of enantiomeric purity [13a].

To achieve discrimination of different molecules various CDAs, CSAs, CLSRs, are available in literature and discussed in book and reviews [13b]. There are different type of available molecules such as amine, crown ether, amide, alcohol which were screened as chiral solvating agent.

3.I.7.2 Crown ether as CSAs

Chiral macrocyclic compounds have been recognised as successful and promising chiral selectors for molecular recognition, mainly because of their inherent reduced flexibility and complexation ability. In literature different type of crown ethers and aza crown ethers (scheme 3.4, **52a** to **52d**) were reported [14].

Scheme 3.4 Structures of different macrocyclic compounds

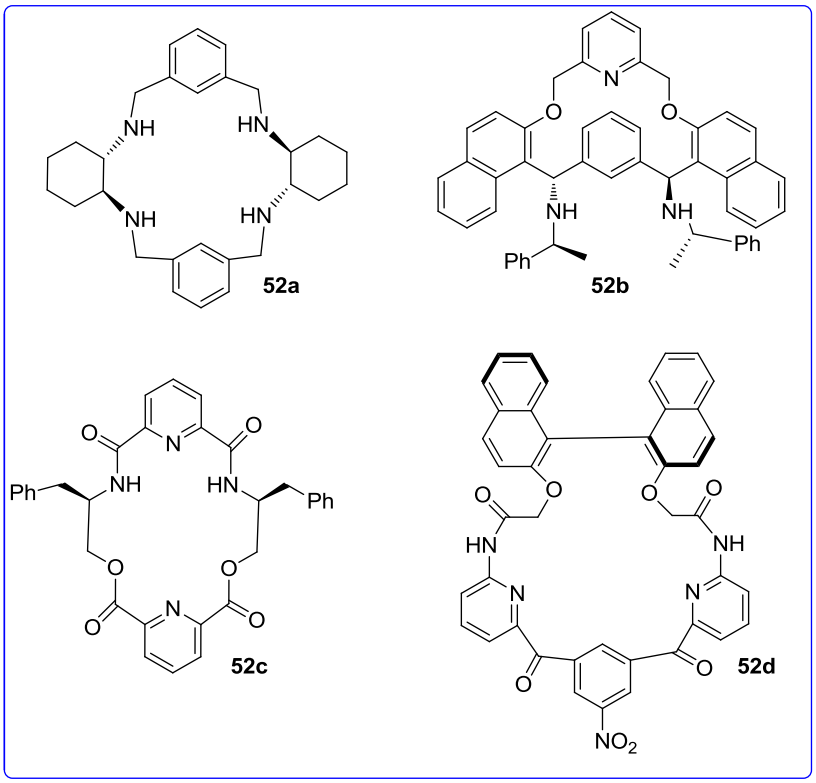

3.I.7.3 Chiral amine as CSA

Among different class of compounds chiral amines were exploited by many researchers in designing and preparing a series of molecules to act as CSA for various acids [15, 16]. Primarily, chiral amine binds with acid to form diastereomeric salt that is responsible for separation of signals in NMR (scheme 3.6). The separation in

analyte also depends on intermolecular supramolecular interactions such as dipole-dipole, charge transfer, van der Waals, π-π stacking and formation of H-bonding etc.

Scheme 3.6: Formation of diasteremeric salt

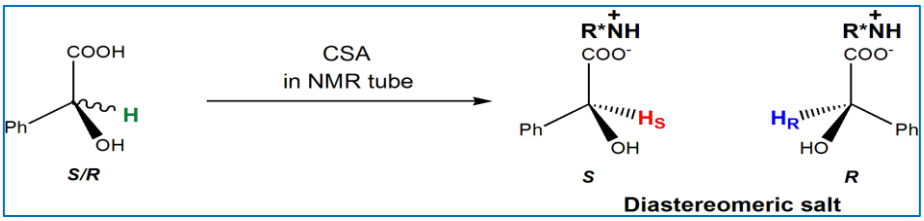

Scheme 3.5: Structure of different chiral amine motif screened as CSA

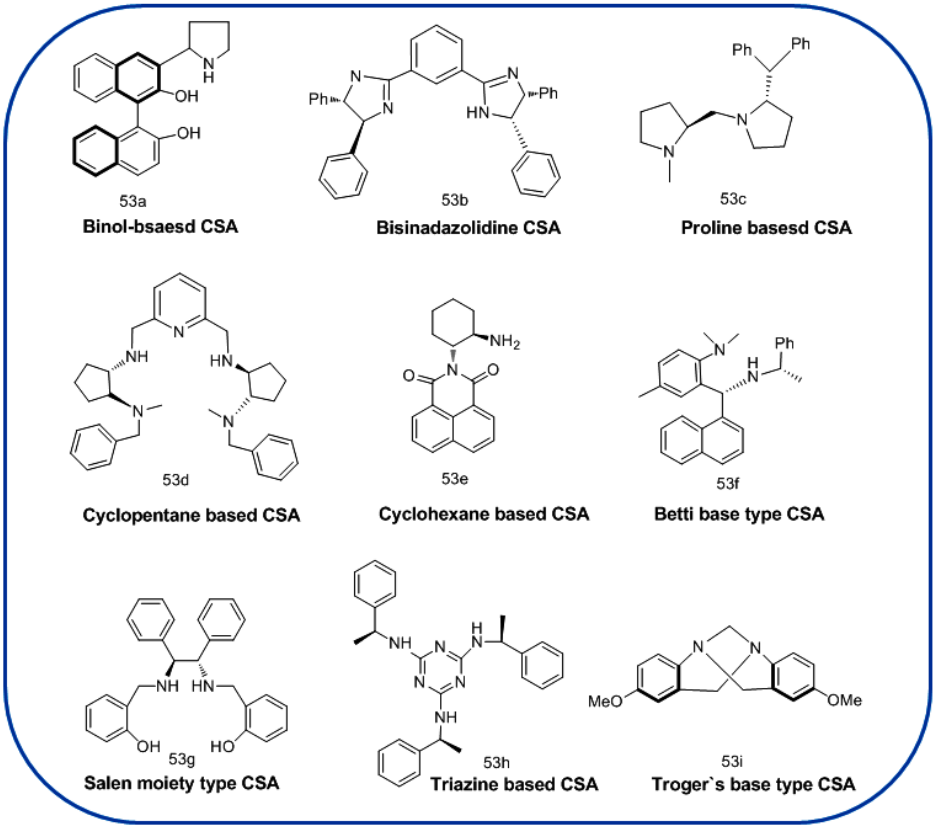

3.I.7.4 Advantage of CSAs

1. The use of CDAs can involve kinetic resolution of the substrate and requires purification of the sample, whereas CSAs do not present such disadvantages and the sample can be easily recovered after the analysis.

2. The use of CSAs does not require need of functional group like in CDAs.

3. The advantages of the method are that it is quick and simple to perform, with no issue of kinetic resolution or sample racemization, provided that the complexes

remain stable in solution.

4. Even the enantiomeric purity of the CSA is not critical, if it is less than 100% then only the size of the chemical shift non-equivalence is reduced.

3.I.7.5 Limitations of Chiral Solvating Agent

1. The discrimination ability of CSA depends on its concentration and the temperature. Higher the concentration of CSA results in larger chemical shift difference. In some cases this is not economically practical.

2. In other cases spectrum may be complex and might be difficult to interpret. Sometime chemical shift difference is relatively less for the precise measurement of enantiomeric excess.

3. Baseline separation is needed for accurate measurement.

4. One of the drawbacks of these methods is the small values of the signal discrimination, however, advent of high-field, sensitive NMR instruments the minute data can be amplified and measured.

3.I.8 Development of New Chiral Solvating Agent

There is pool of chiral auxiliaries or ligand available in the literature, each of which is specific to molecules containing the particular functional group. Nevertheless, there is continuous research to discover new molecules or ligands to add to CSA library.

In chapter 2 we have mentioned the efficient conditions for selective separation of roof shape diol and alcohol into enantiomers and their stepwise conversion to few amines and diamines.

3.I.9 Objective

Since the basic skeleton of the roof shape molecules offer

1. Two aromatic rings for possible $\pi-\pi$ interaction with another system.
2. The three dimensional bicyclic shape is also quite rigid to favour and control the intermolecular interactions.

Amongst the most successfully used CSAs are amines, because they form first diasteremeric complex with racemic acid with non-covalent interactions. Theoretically, a chiral solvating agent should form stable complex with the enantiomers due to combine effect of noncovalent interactions. Thus, the structure of the diastereomeric complex should be well suited to produce selective shielding effects on the protons of the substrate moiety. Since the structure of roof shape amine

and diamines are rigid, they offer two aromatic planes on the unsymmetrical space of the amine and hence probably suitable as CSAs. With this concept we have screened two sets of roof shape amines (and diamines) as CSA for a range of chiral analytes to study discrimination of signals in NMR analysis.

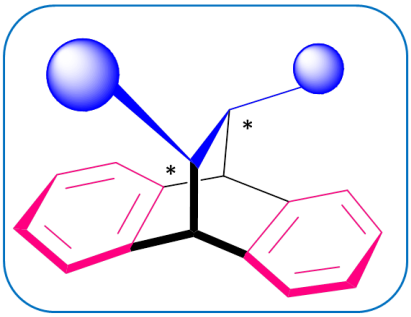

Figure 3.1: Basic Skeleton of Roof Shape Molecules

In this chapter (Section I & II) we have discussed the utility of various types of roof shape amino ligands in NMR analysis as Chiral Solvating Agents (CSA) for the discrimination of α–functionalized acids.

3.1.10 Importance of α–Functionalized acids

Chiral carboxylic acids are important natural products, constituents of drugs and key building blocks for the preparation of a wide range of important compounds [17]. Different type of acid and their derivatives are present in alkaloids, amino acids, peptides. Therefore, the chiral acids are significantly important in chemical industry, as they are building block of new pharmaceuticals and agrochemicals. They are also key intermediate in synthetic chemistry. The investigation of chiral recognition of carboxylic acids by artificial receptor was of critical importance in the preparation, separation and analysis of acids.

3.I.11 Chemical Shift

In CSA two different types of abbreviations are used.

1. Induced Chemical shifts [Δδ]

The difference between the signals in a solution of the acid and the average of the signal of the two discriminated enantiomers after mixing the chiral additive which is represented as Δδ and often expressed in ppm.

2. Chemical shift nonequivalence [ΔΔδ]

It is the difference between two resolved peaks after mixing the chiral additive. Chemical shift non-equivalence is represented by **ΔΔδ** (ppm) or **Δ(Δδ)**. When this value is multiplied with operating frequency then the ΔΔδ is expressed in Hz.

In chiral solvating agent this value is important to check different CSA structure which cause signal to separate. Larger the separation, it will produce more value of ΔΔδ, hence it will allow the operator to accurately measure the exact composition of non-racemic sample.

Figure 3.2 : Diagrammatic representation of the appearance of ^{1}H-NMR peaks for calculation of chemical shift nonequivalence (ΔΔδ) and induced chemical shift (Δδ)

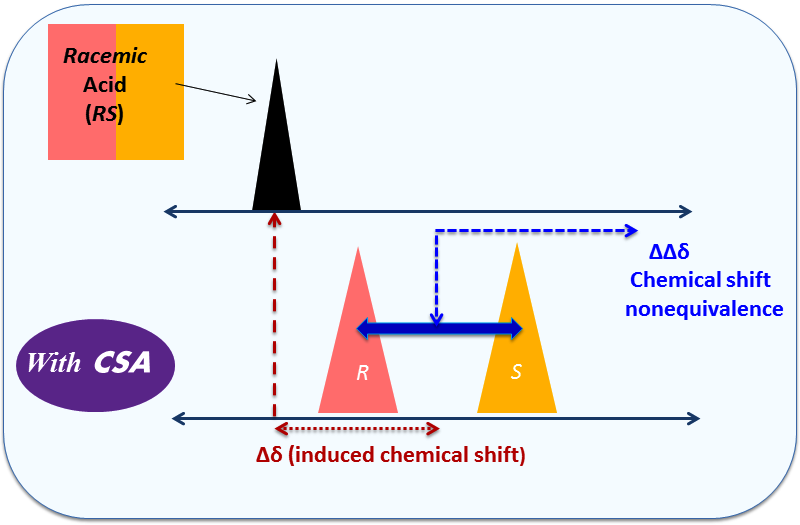

3.I.12 Experimental

The commercially available racemic α functionalized acid such as Mandelic acid, 4-triflouro mandelic acid, chloro propionic acid were purchased and used as received. 4-Bromo mandelic acid was prepared according to literature procedure [18a]. Two derivatives of mandelic acid where the hydroxyl group is blocked by methyl ether and by acetyl ester were prepared according to literature procedure. Some other acids and their derivative are prepared according to literature procedure. Amino acids were protected using standard protocol (18b). Drugs and their intermediates were arranged from local pharmaceutical firms.

^{1}H NMR spectra were recorded on 400 MHz NMR Avance Bruker spectrometer and

resonance peaks were referenced to TMS (0.00 ppm) as internal standard. ^{13}C NMR spectra were obtained at 100 MHz, all the ^{19}F spectra were obtained at 376 MHz and all the ^{31}P Spectra were recorded at 162 MHz. For screening all the chiral solvating agent $CDCl_3$ was used which was purchased from Eurotopspin and directly used. ^{1}H NMR spectra is recorded after preparing stock solution in $CDCl_3$.

3.I.13 Discrimination of Carboxylic acids

This section of the chapter 3 reports the result obtained on the chiral discrimination of acids such as acids, hydroxy acid, diacid, amino acid derivative.

Chart 1: Structure of Roof shapes amine/ diamine/ amide/diamide screened as CSA

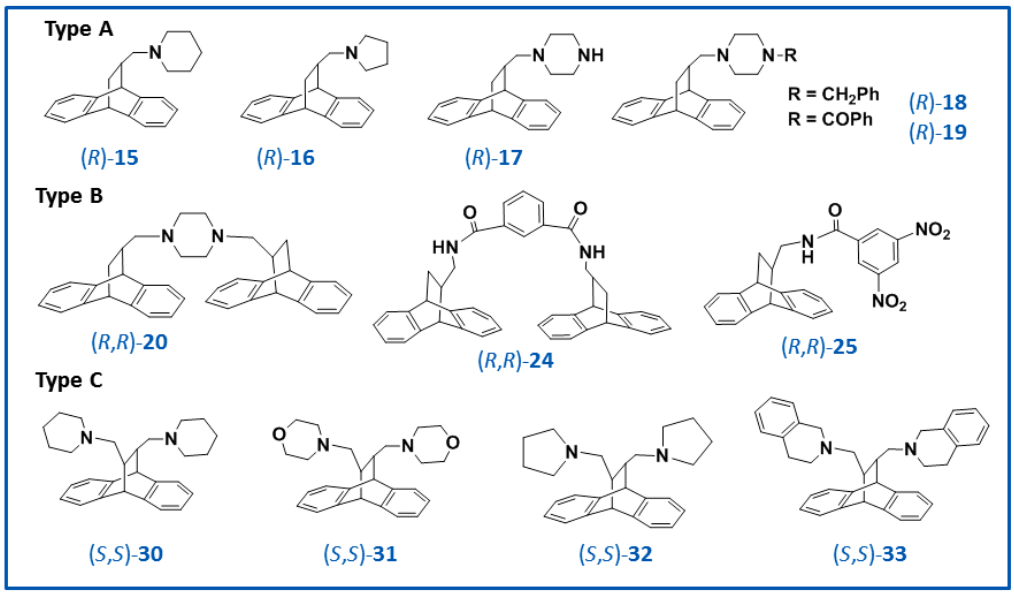

^{1}H-NMR protocol

The scope of the ability of optically pure roof shape amines and diamines to discriminate the chiral substrates such as α-substituted carboxylic acids was investigated by performing few NMR experiments at ambient conditions. The screening process was conducted with the racemic sample of mandelic acid (±) **54** as the standard substrate with the amines or di-amines (Type A & Type B) and the results are presented schematically in Figure 3.3 as well as the data is summarized in Table 3.1. The solution of (±)-**54** in $CDCl_3$ (20 mmol) was mixed with the test amine (or di-amine) whose solution is also prepared in the same solvent in the same concentration.

Table 3.1: Effect of the roof shape chiral amines (Type A) and di-amines (Type B) on the α-proton of the *rac* mandelic acid **54**. [Δδ = induced chemical shift[a]; ΔΔδ = chemical shift non-equivalences.]

No	Amine/di-amine	Ratio of amine: **54**	Probe Signal PhC*H*(OH)COOH	
			Δδ (ppm)	ΔΔδ (ppm)
	Type A			
1	(*R*)-**15**	1:1	-0.15	--[b]
2	(*R*)-**15**	2:1	-0.33	--[b]
3	(*R*)-**16**	1:1	-0.19	0.007
4	(*R*)-**17**	1:1	-0.16	--[b]
4	(*R*)-**18**	1:1	-0.21	--[b]
5	(*R*)-**19**	1:1	-0.18	--[b]
	Type B			
1	(*R*,*R*)-**20**	1:1	-0.18	0.008
2	(*R*,*R*)-**21**	1:1	-0.16	--[b]
3	(*R*,*R*)-**24**	1:1	-0.15	--[b]

[a]The difference between the signals of **54** in $CDCl_3$ solution and the average of the signals of the two enantiomers after the addition of the amine or di-amine. [b]Not resolved

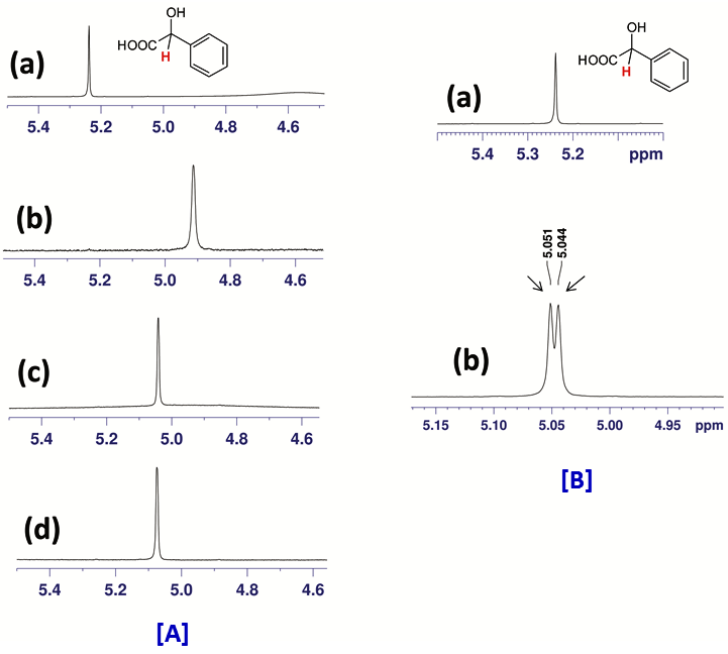

Figure 3.3: (A) Selected region of ^{1}H-NMR spectra in presence of roof shape amine ligand (a) blank **54** (b) with (*R*)-**15** (2:1) (c) (*R*)-**18** (1:1) (d) (*R*)-**19** (1:1) **(B)** (a) Blank **54** (b) with (*R*)-**16** (1:1) in $CDCl_3$ at 20 mM, 400MHz.

The ^{1}H NMR of the mixture is recorded at 400 MHz at ambient conditions, the C$^{\alpha}H$ of (±)-**54** show a slight shift towards the high field region. The induced chemical shift (Δδ) is expressed in terms of the difference between the C$^{\alpha}H$ signal of (±)-**54** measured in $CDCl_3$ and the average of the separated signals of the two enantiomers, while the chemical shift non-equivalences (ΔΔδ) is the difference between the two resolved peaks. The effect of amines (*R*)-**15** to (*R*)-**19** on mandelic acid (±)-**54** was restricted mainly to the small shift of the C$^{\alpha}H$ signals to the up field region but failed to resolve them significantly.

3.I.13.2 Effect of rigid amide ligand

Similarly use of Type B ligand also fails to discriminate between two isomer of racemic mandelic acid. It is noteworthy to observe the methine signals of mandelic acid slightly splitting in to two sets on complexation with type B ligand (*R*,*R*-**20**). Addition of these roof shape analogues to *rac*-mandelic acid (1 equiv.) induced small upfield shifts in the NMR signals of the substrate (Figure 3.4) but the separation of the enantiomer signals is almost negligible.

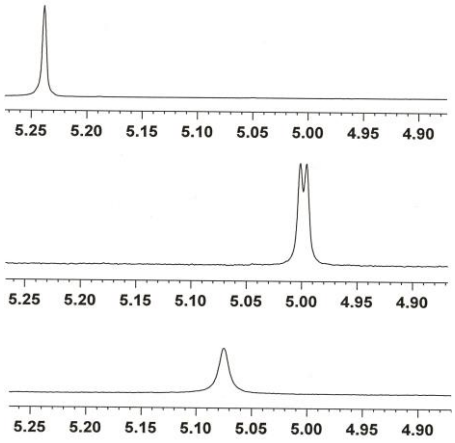

Figure 3.4: Selected region of ^{1}H NMR spectra in presence of roof shape amine ligand (upper trace) blank **54** (middle trace) with (bottom trace) (*R*,*R*)-**20** (2:1) (c) (*R*,*R*)-**21** (1:1) in $CDCl_3$ at 20 mM, 400MHz.

3.I.13.3 Effect of Type C ligand

Amines of Type A and Type B failed to distinguish between two isomer of mandelic acid but in some cases showed small separation of racemic analyte. In next stage Type C ligands were screened as chiral solvating agent and result are summarized in Table 3.2.

Table 3.2: Effect of the roof shape chiral amines and di-amines on the α-proton of the racemic mandelic acid **54**. [**Δδ** = induced chemical shift[a]; **ΔΔδ** = chemical shift non-equivalences.]

No	di-amine	Ratio of amine/di-amine	Probe Signal PhC*H*(OH)COOH	
			Δδ (ppm)	ΔΔδ (ppm)
1	(*S*,*S*)-**30**	1:2	-0.26	0.056
2	(*S*,*S*)-**31**	1:2	-0.15	0.044
3	(*S*,*S*)-**32**	1:1	-0.21	0.032
4	(*S*,*S*)-**32**	1:2	-0.28	**0.071**
5	(*S*,*S*)-**33**	1:2	-0.21	0.024

[a]The difference between the signals of **54** in $CDCl_3$ solution and the average of the signals of the two enantiomers after the addition of the amine or di-amine

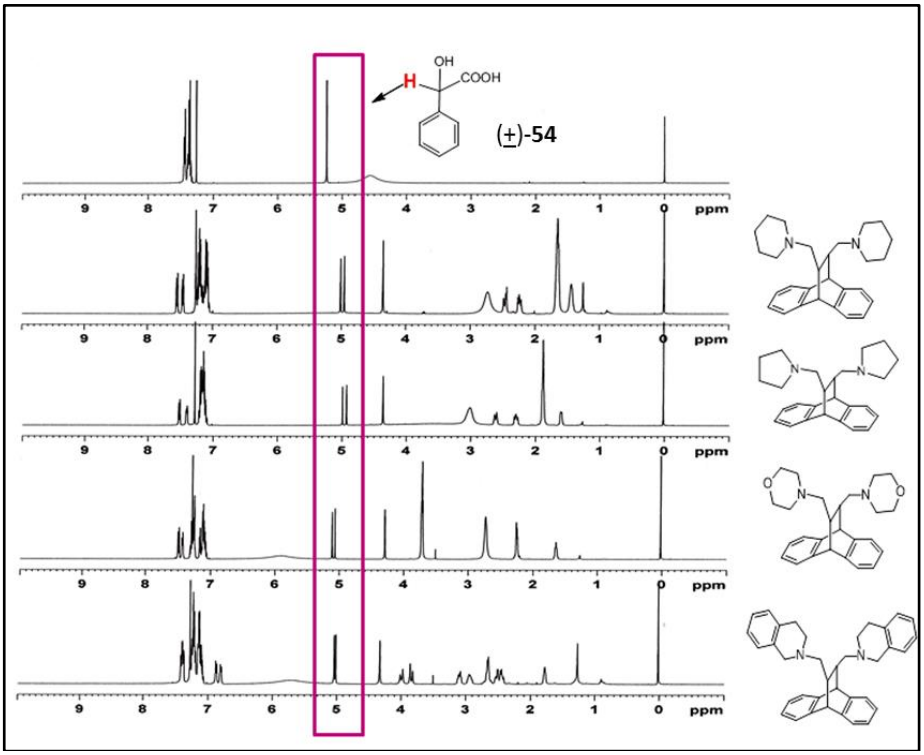

Figure 3.5: Effect of the roof shape chiral amine on the $C^{\alpha}H$ of the racemic mandelic acid (**54**) recorded at 20 mM, $CDCl_3$, 400 MHz.

The Type A & B amines failed to discriminate $C^{\alpha}H$ signals of mandelic acid (±)-**54**. However, addition of di-amine (*S*,*S*)-**30** considerably enhanced the induced chemical

shift of the C$^{\alpha}$*H* signals to the up field region but also caused a good separation of the signals. Similar but marginally lower resolution of the same signals was observed with morpholine derived di-amine (*S*,*S*)-**31**. However, the pyrrolidine derived di-amine (*S*,*S*)-**32** improved the separation to more extent. This may be attributed to the envelope like, slightly rigid form of the five member ring as against the other two six member chair like conformations (Table 3.2, entry 1 & 3).

The ^{1}H NMR spectrum of mandelic acid exhibited a single peak around 5.238 ppm, (upper most part of Figure 3.5), in presence of Type C ligand the ^{1}H NMR spectrum gives two well resolved peaks and also with proper baseline resolution, one for each enantiomer.

Table 3.3: Effect of the roof shape di-amines (Type C) on the α-proton of the racemic mandelic acid **54** (expanded region).

Entry	Ligand	Probe Signal	ΔΔδ(ppm)
1	(*S*,*S*)-**30**	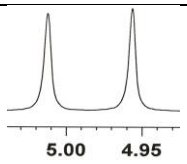	0.056
2	(*S*,*S*)-**31**	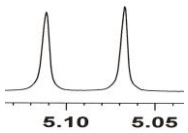	0.044
3	(*S*,*S*)-**32**	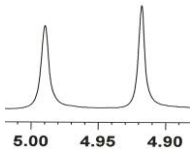	0.071
4	(*S*,*S*)-**33**	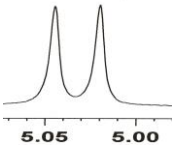	0.024

Generally two basic information are obtained in NMR spectroscopy

1. Difference between two resolved peaks (chemical shift non equivalence)
2. Area under two peaks (to measure the enantiomeric ratio.)

Using this two paremeter we can calculate compostion of different enatiomers of analyte.

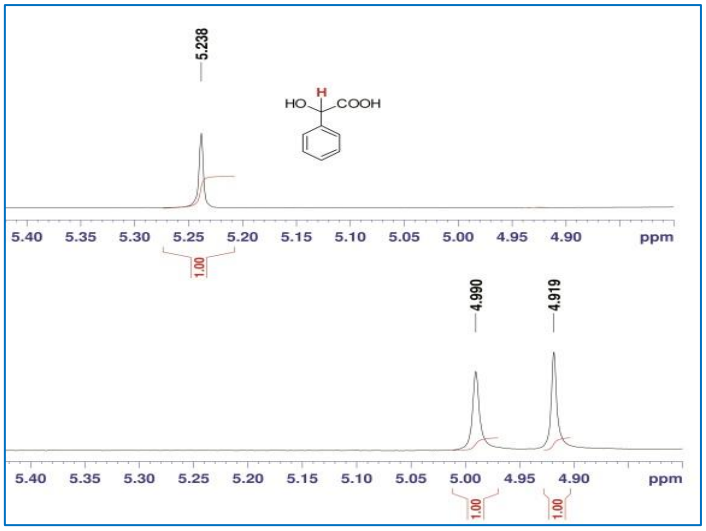

Figure 3.6: The ^{1}H-NMR Spectra of racemic mandelic acid recorded at 20 mM, $CDCl_3$, 400 MHz, (top) pure (±)-**54**, (lower) (±)-**54** with (*S*,*S*)-**32** ratio (2:1) Measurement of area under two resolved peak of mandelic acid **54.**

3.I.14 Effect of concetration

When chiral additive was used as auxiliary the extent of discrimination also depends on its concentration where the detected NMR signal will be the considered as the average of complexed and uncomplexed species/ion that exist in equilibrium in the solution state [19, 20]. The optimization of the concentration of CSA was performed by carrying out the experiments at different concentrations. The standard experiment of (±)-mandelic acid with (*S*,*S*)-**32** in the ratio of 1:2 at varying concentrations. The values of chemical shift non-equivalences were summarized in Table 3.4. Hence, further study was performed at 20.0 mmol scale.

Table 3.4: Value of different with different concentration

No	Con.(mmol)	Chemical shift non-equivalences
1	5.0	0.048
2	10.0	0.068
3	20.0	0.071
4	40.0	0.074
5	100.0	0.074

3.I.15 Implementation on derivative of Mandelic acid

In order to validate the protocol of chiral solvating agent, some other derivatives of mandelic acid were screened as acid analytes. The roof shape amines which show promise for (±)-mandelic acid **54** were then screened for few derivatives of mandelic acid to study the effect of substitution (Scheme 3.7).

Scheme 3.7: Structure of derivative of mandelic acid

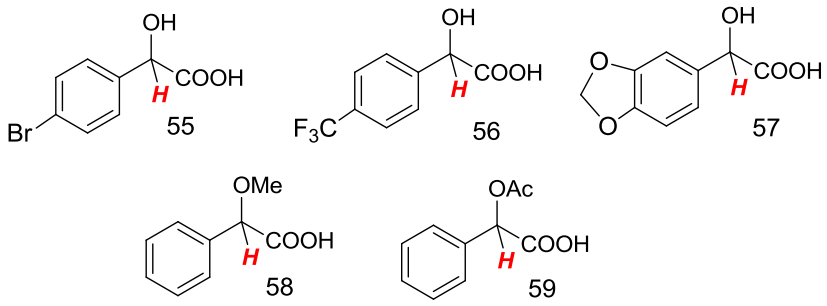

For most of the cases it was observed that the presence of electron withdrawing group (CF_3 or Br) showed enhanced degree of the shift of the signals as well as chemical shift non-equivalences compared to mandelic acid (Table-3.5).

Table 3.5: Value of different chemical shift value in ^{1}H NMR

No	Amine/diamine	4-Br-PhC*H*(OH)COOH		4-CF_3PhC*H*(OH)COOH	
		Δδ (ppm)	ΔΔδ (ppm)	Δδ (ppm)	ΔΔδ (ppm)
1	(*R*)-**15**	-0.11	--[a]	-0.09	--[a]
2	(*R*)-**16**	-.012	--[a]	-0.07	--[a]
3	(*S*,*S*)-**30**	-0.31	0.058	-0.32	0.048
4	(*S*,*S*)-**31**	-0.22	0.051	-0.22	0.043
5	(*S*,*S*)-**32**	-0.34	0.076	-0.36	0.058
6	(*S*,*S*)-**33**	-0.20	0.017	-0.21	0.019

[a]Not resolved

In most of the cases of mandelic acid derivatives with the diamines were more effective in causing discrimination between C$^{\alpha}$*H* signals of the two isomers.

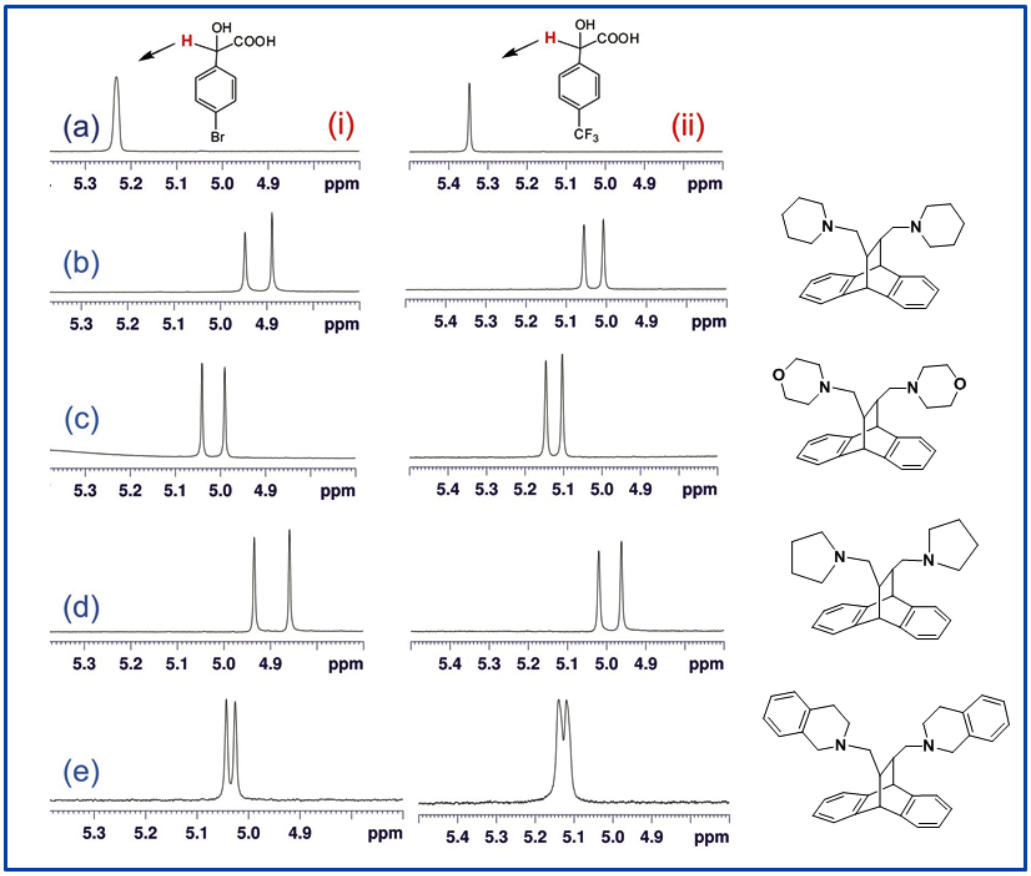

Figure 3.7 Selected region of ^{1}H-NMR spectra (i) 4-Bromo mandelic acid **55** (ii) 4- triflouro mandelic acid **56** (a) pure (±)-acid (b) in presence of (*S*,*S*)-**30** (c) (*S*,*S*)-**31** (c) (*S*,*S*)-**32** (c) (*S*,*S*)-**33** in the ratio of (2:1).

In case of racemic sample of triflouromandelic acid **56** where pyrrolidine based roof shape diamine ligand produce maximum chemical shift nonequivalence. However, we could not establish a clear pattern between the aromatic substituents of mandelic acid and the efficiency of discrimination. We observed that in some cases larger size of bromine atom seems to be making the difference as against the stronger electron withdrawing nature of trifluoromethyl group. Interestingly the signals of the aromatic protons of (±)-**56** also exhibited considerable discrimination in ^{1}H NMR spectrum when recorded with the CSAs of Type-C. The three representative examples of CSA are investigated. The signals with CSA (*S*,*S*)-**30** ($\Delta\delta$ = -0.096 and 0.197) and (*S*,*S*)-**31** ($\Delta\delta$ = -0.082 and 0.103) were slightly overlapping but with (*S*,*S*)-**32** a clear and complete separation for the two sets of signals (eight lines) were seen ($\Delta\delta$ = -0.170 and $\Delta\Delta\delta$ = 0.202). In Figure 3.8(a) the comparison of aromatic hydrogens of (±)-**56** without and with CSA (*S*,*S*)-**32** is presented.

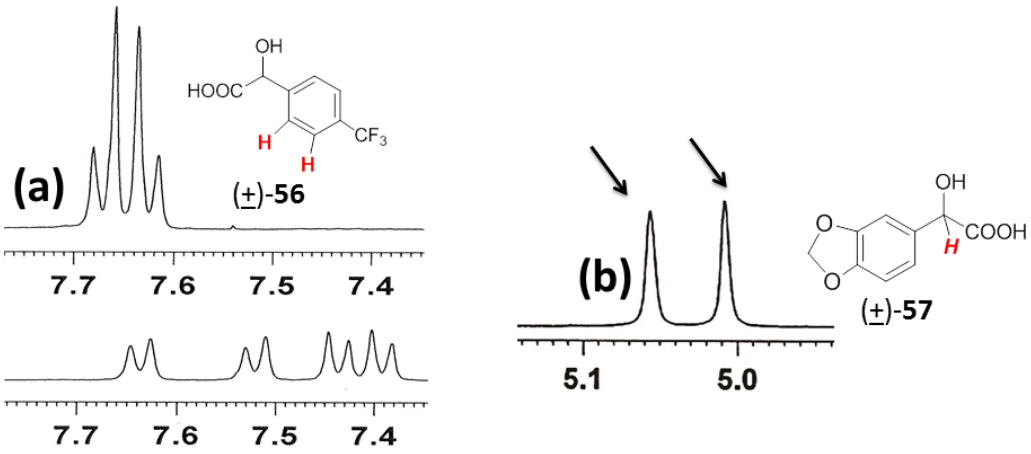

Figure 3.8: Selected region of ^{1}H-NMR spectra (a) {top} Aromatic region of **56** (two doublet) [bottom] after addition of (*S*,*S*)-**32** (b) after addition of (*S*,*S*)-**32** in (±) **57** (2:1).

In view of this observation, the CSA (*S*,*S*)-**32** was also scanned for 2-(benzo[*d*][1,3]dioxol-6-yl)-2-hydroxyacetic acid (±) **57**, where the amine (*S*,*S*)-**32** was found suitable. (Chemical shift nonequivalence 0.040) (Figure 3.8**b**). It was also noteworthy to observe the O-CH_2-O signals getting split in to two sets of two doublets on complexation with (*S*,*S*)-**32**.

3.I.15.2 Study of O-derivative of Mandelic acid

Such type of C-2 symmetrical ligand showed good chiral discrimination of mandelic acid and their derivative in NMR analysis. In next stage some of the mandelic acid derivative where OH group was protected (or blocked) and investigated this change on the selectivity of (*S*,*S*)-**32**.

The ^{1}H NMR spectra of -OMe derivative of mandelic acid **58** and -OAc derivative mandelic **59** acid were given. Both the protons of methyl ether derivative **58**, i.e. C$^{\alpha}H$ and C$^{\alpha}$OCH_3 showed discrimination in ^{1}H NMR ($\Delta\Delta\delta$ = 0.074 for C$^{\alpha}$***H***, 0.063 C$^{\alpha}$O**C*H*$_3$**). Similar results were observed for *O*-acetyl derivative **59** (($\Delta\Delta\delta$ = 0.045 for C$^{\alpha}$***H***, 0.004 COC***H*$_3$**). This study further establishes that our system detects more than one set of hydrogen discrimination in ^{1}H NMR analysis.

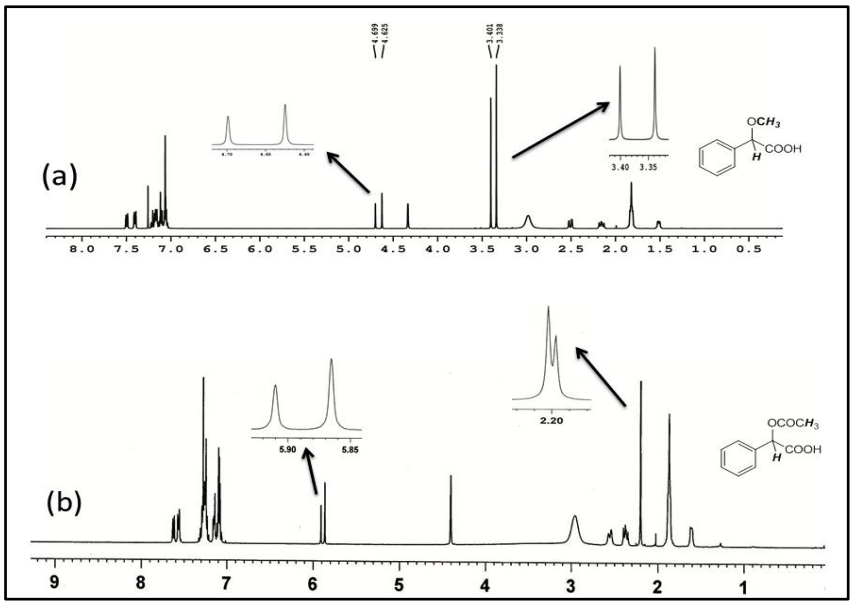

Figure 3.9: ^{1}H-NMR spectra (a) with α-OMe mandelic acid **58** (b) α -OAc mandelic acid **59** in presence of (*S*,*S*)-**32** in $CDCl_3$.

3.I.16 Amino Acid derivative

In view of this observation, we are interested in extending the range of substrates where such type of ligand discriminate proton of some important acid moiety. It is often seen that the region of ^{1}H NMR spectrum where the differentiation is observed is overlapped with the area covering the signals of CSA. The analysis will be more accurate if it is confirmed by checking the ratio of more than one protons of the sample [21]. Hence it is more useful to examine different signals which shift on the addition of CSA for more effective analysis of chiral compounds. For that purpose amino acids were chosen as acid component.

Amino acids are at the basis of all life process, as they are essential for every metabolic process. Amino acid and their derivative are important intermediates in organic synthesis, which have been used in various areas such as peptide synthesis [22], medicinal chemistry [23], as chiral sources [24b] & polymer materials [24c]. Detection of the optical purity of natural and unnatural amino acids and their derivatives is of prime importance since they are used for the synthesis of many pharmacologically active molecules. Since amino acids are not freely soluble in deuterated chloroform and may limit the scope of this analysis. To overcome this difficult by increase its solubility, their N-Ts derivatives, were prepared [18b]

Scheme 3.8: Chemical structure of N-Ts amino acids

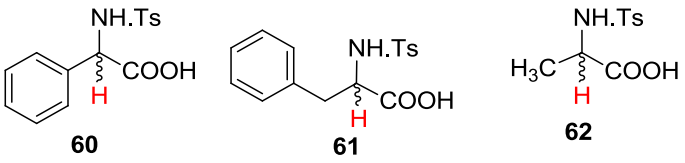

In order to develop a facile method of determining optical purity by NMR analysis, we have taken N-Ts phenyl glycine as acid component and (*S*,*S*)-**32** as CSA for enatio discrimination. In the present study we are also looking at exploring the applications of roof shape chiral amines to discriminate protons located at different positions of the N-Ts derivative of α-amino acid such as phenyl glycine (Figure 3.10).

In order to correlate the signals with the two enantiomers of **60** a sample of N-Ts phenyl glycine was prepared by mixing its *D* and *L* isomers in a fix ratio (2:1). Careful investigation of ^{1}H NMR spectra of Phenyl glycine-N-Ts with (*S*,*S*)-**30** revealed that discriminations were observed not only at stereogenic proton but also at multiple site which are remote to sterocentre (Figure 3.11). Such observation were rare in literature, hence consistently effective diamine based CSAs (*S*,*S*)-**31** and (*S*,*S*)-**32** are also screened to examine chiral recognition of **60** and to examine shift of its protons.

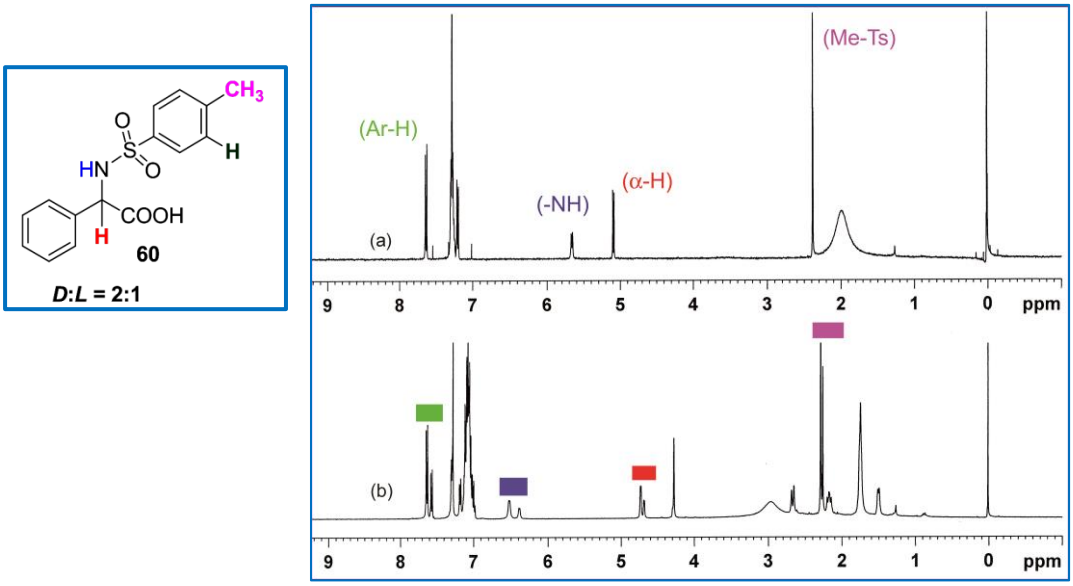

Figure 3.10: (a) ^{1}H NMR spectra of N-Ts Ph-glycine **60** (b) ^{1}H NMR spectra of N-Ts Ph glycine in presence of (*S*,*S*)-**32**

3.I.16.1 Discrimination of Ar-*H* signal

The structure of the CSA for the present study was designed in such a way as to offer a three dimensional motif and present an aromatic plane for the effective π-π interaction with the analyte. Due to this interaction we expect some shift in the signals of the aromatic protons of **60**. Although the protons *meta* to the SO_2N group of N-Ts were merged with the aromatic signals of the CSAs, the protons *ortho* to SO_2N group appeared separately at the downfield region and were quite suitable for this study. These protons appeared as a doublet and as the most downfield well resolved signal of the spectra. The same set of CSAs was scanned for these protons and results clearly indicate resolution of the two doublets for the two isomers of **60** (Figure 3.11a). Since these protons are not attached to any electronegative atoms there was no significant shift (Δδ) but reasonable base line separation of the signal was observed for (*S*,*S*)-**30** and (*S*,*S*)-**32**, with substantial chemical shift non-equivalences (ΔΔδ = 0.063 and 0.064).

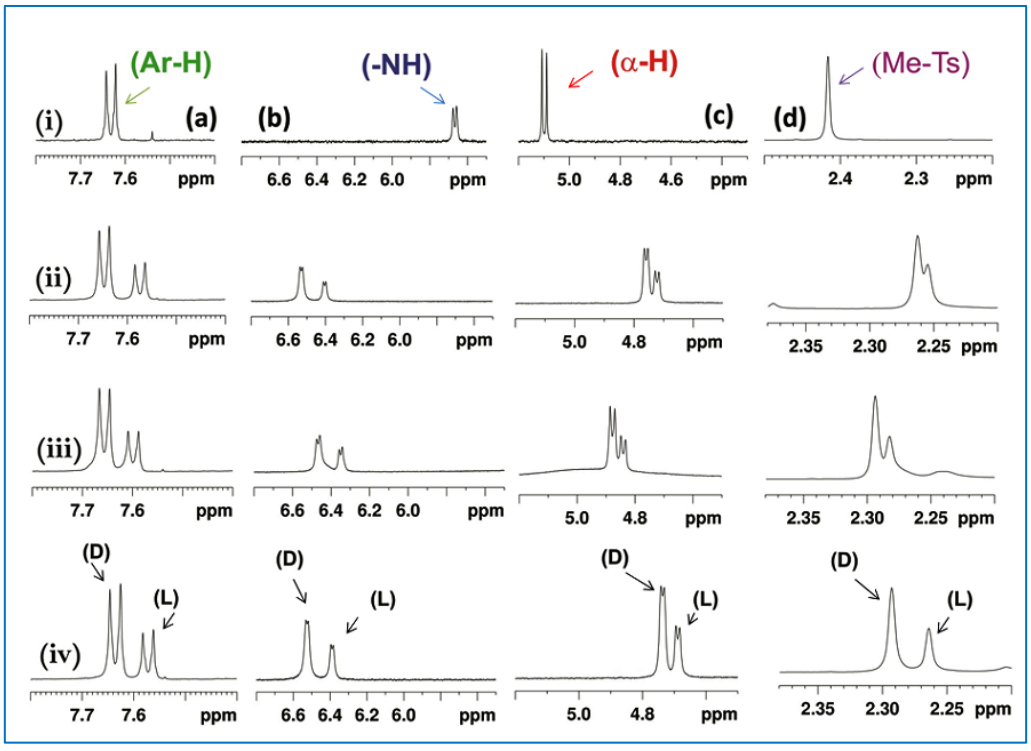

Figure: 3.11 ^{1}H-NMR spectra of **60** with three CSAs: (a) signal of Ar-*H* of **60** (D:L= 2:1) with (i) blank, (ii) (*S*,*S*)-**30**, (iii) (*S*,*S*)-**31** and (iv) (*S*,*S*)-**32**; (b) signal of N-*H* of **60** (D:L= 2:1) with (i) blank, (ii) (*S*,*S*)-**30**, (iii) (*S*,*S*)-**31** and (iv) (*S*,*S*)-**32**; (c) signal of C$^{\alpha}$*H* of **60** (D:L= 2:1) with (i) blank, (ii) (*S*,*S*)-**30**, (iii) (*S*,*S*)-**31** and (iv) (*S*,*S*)-**32**; (d) signal for C*H*$_3$ of **60** with (i) blank, (ii) (*S*,*S*)-**30**, (iii) (*S*,*S*)-**31** and (iv) (*S*,*S*)-**32**; (*D*:*L* ratio 2:1)

3.I.16.2 Discrimination of -N*H* signal

In the next set of study we observed the shifting of the position of the signal of -N*H* hydrogen on addition of CSA (Figure 3.11b). These are the only signals which move to down field region indicating stronger intramolecular hydrogen bond with carboxylate as compared to carboxylic acid in the absence of CSA. In this case all the three CSAs showed more or less same effect.

3.I.16.3 Discrimination of C$^{\alpha}$*H* signal

In comparison the C$^{\alpha}$*H* directly attached to the chiral centre observed a significant shift for (*S*,*S*)-**30** ($\Delta\delta$ = -0.39 and 0.048) and for the piperidine derived (*S*,*S*)-**30** ($\Delta\delta$ = -0.36 and 0.036). It is interesting to see a small shift in the pattern for morpholine derived (*S*,*S*)-**31** ($\Delta\delta$ = -0.24 and 0.038) probably the presence of oxygen atom of the CSA is responsible for this deviation. The upfield shift of the C$^{\alpha}$*H* proton in all the cases is consistent due to the deprotonation of the acid group as the shielding effect is more in case of carboxylate ion.

3.I.16.1 Discrimination of Methyl signal

Firstly the methyl protons of the N-Ts moiety of **60** was observed with the three different CSAs in the molar ratio of 2:1 (**60**:CSA) (Figure 3.11d). The single unresolved signal at δ 2.39 ppm of **30** shifted up field with all the three CSAs, but most effective separation was observed with pyrrolidine derived (*S*,*S*)-**32** ($\Delta\delta$ = -0.11 and $\Delta\Delta\delta$ = 0.029). It is noteworthy to observe such pronounced effect on the methyl protons which are located far away from the chiral center of α-amino acid.

Further exploration of application of CSA for other amino acids, such as N-Ts alanine **61** and N-Ts phenyl alanine **62**, revealed that the presence of a rigid π-system near to chiral centre is required for effective interaction. Both these showed lesser degree of discrimination compared to N-Ts phenyl glycine **60** for all the four protons under study. In both the cases signals of methyl protons of Ts group showed discrimination with (*S*,*S*)-**32** similar to N-Ts phenyl glycine.

We have also screened representative CSAs from our Type-A & Type-B. The Type-A and B ligand show discrimination at only one of the position of amino acid, namely the methyl signal. Results of chemical shift nonequivalence of amino acids with different CSAs are summarized in Table 3.6. These results also prove that rigid and

geometrically fused structures were more favorable for effective and multiple chiral discriminations.

Table 3.6: Enatiodiscrimination of various amino acids with chiral roof shape Amine

No	Amino Acid	CSA	ΔΔδ(ppm) α-*H*	ΔΔδ(ppm) N*H*	ΔΔδ(ppm) Ar-*H*	ΔΔδ(ppm) *CH*$_3$
1	Phenyl Glycine.Ts	(*S*,*S*)-**30**	0.036	0.125	0.063	0.022
2	Phenyl Glycine.Ts	(*S*,*S*)-**31**	0.038	0.117	0.057	0.011
3	Phenyl Glycine.Ts	(*S*,*S*)-**32**	0.048	0.136	0.064	0.029
4	Phenyl Glycine.Ts	(*R*)-**15**	-NR-	-NR-	-NR-	0.040
5	Phenyl Glycine.Ts	(*R*,*R*)-**20**	-Merge-	-NR-	-NR-	0.037
6	Phenyl Alanine.Ts	(*S*,*S*)-**32**	--[a]	-NR-	0.084	0.038
6	Alanine.Ts	(*S*,*S*)-**32**	-Merge-	-NR-	-NR-	0.037

[a]-complex pattern; NR = not resolved.

Encouraged by successful chiral discrimination of mandelic acid derivative and amino acid derivative, our aim was to screen variety of different acids where such amino ligand could work. Present system of CSAs were tested for three different racemic acid which were structurally different to each other under the influence of effective (*S*,*S*)-**32** ligand.

Scheme 3.9: Structure of different acids studied.

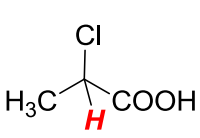

63

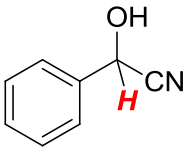

64

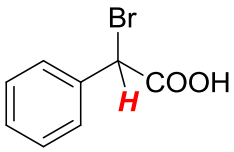

65

In case of chloro propionic acid **63** our system failed to discriminate the proton of acid which indicate positive role of aromatic system of the α-functionalized acids for effective binding. This assumption indicates that these CSAs failed to recognise α-chloro propionic acid, where there is no π-π interaction. In another case, mandelonitrile **64** was tested with (*S*,*S*)-**32** which show lesser degree of chemical shift nonequivalence (ΔΔδ = 0.013) as compare to mandelic acid (ΔΔδ = 0.071). These

observations support the tightly held acid-base interaction between the roof shaped diamines and carboxylic acid. A racemic sample of α-bromo phenyl acetic acid **65** was studied with the same CSA, which showed negligible discrimination (ΔΔδ = 0.004), it also indicate that role of type of atom and size of atom on α position.

3.I.17 Understanding cause of signal separation

Once the efficacy of chiral recognition had been demonstrated, we attempted to gain better understanding of the diasteremeric complexes formed in the solution. With this aim, we have done three different experiments.

1. IR study 2. 2D NOSEY 3. Job plot

3.I.17.2 Infrared study

We focused on the complex formed between the enantiomer of acid and receptor. The formation of diastereomeric host guest complexes possibly occurs through interaction of the basic nitrogen atom in chiral receptors and the carboxyl group in the chiral carboxylic acid. The protonated amine groups would lead to the formation of the corresponding diastereomeric salt with chiral carboxylic acids. The C=O stretch (1716 cm^{-1} for mandelic acid) in IR spectra of a 1 : 1 mixture of (*S*,*S*)-**32** and mandelic acid **54,** shifted to 1624 cm^{-1} (the COO^- stretch) which confirmed that the carboxyl group of the acid was ionized (Figure 3.12).

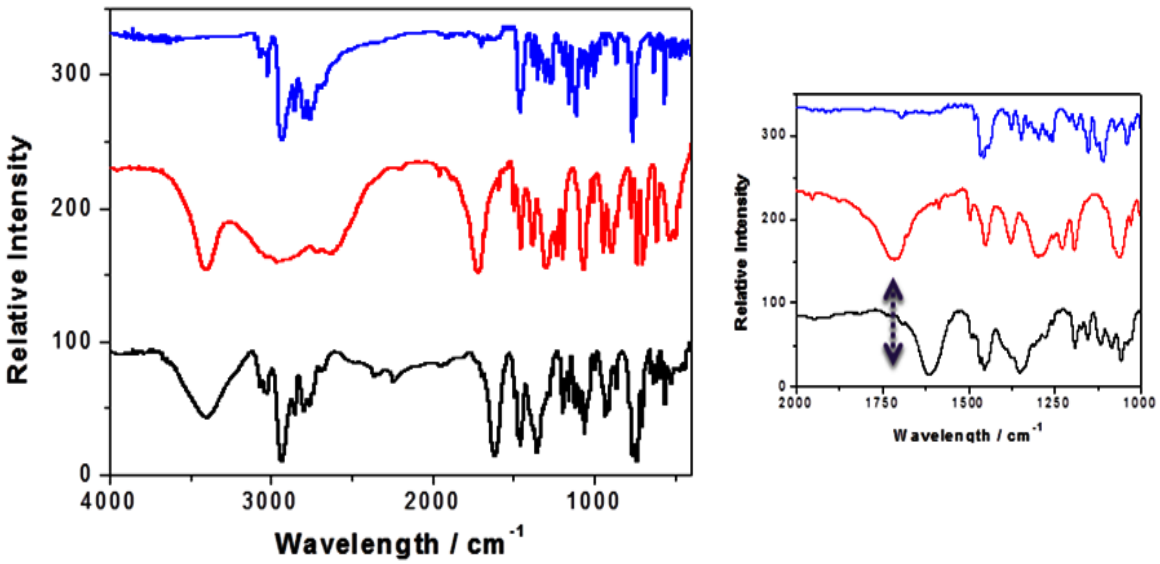

Figure 3.12: IR spectra between *rac*- mandelic acid and (*S*,*S*-**32**) [Right]-Full spectra [Left] Enlarge region of the shift.

3.I.17.3 2D NOSEY

Further information about the nature of the complex between CSAs and mandelic acid was obtained by performing 2D-NOESY experiment. Analysis of the spectra clearly showed cross peak between protons of C3-C4-C3 methylenes of pyrrolidine ring of (*S*,*S*)-**30** with $C^{\alpha}H$ of (±)-**54** and its aromatic protons. Along with this, the CH-π interaction between the aromatic ring of (*S*,*S*)-**30** and mandelic acid is also seen.(Figure 3.13).

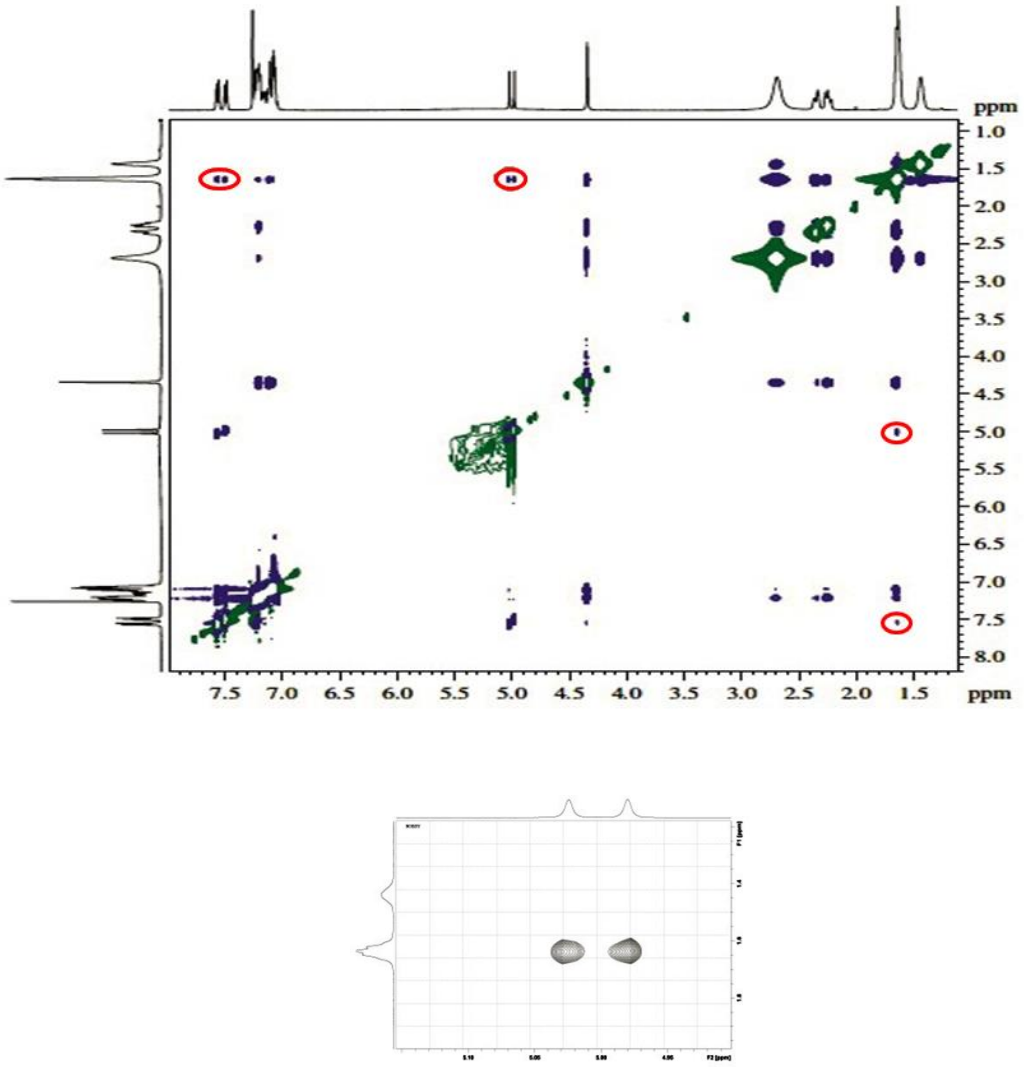

Figure 3.13: 2D-NOESY spectra between *rac*- mandelic acid **54** and (*S*,*S*-**30**). Upper trace show full spectra and lower trace show enlarge region where cross peaks are occurred.

3.I.17.4 Job Plot

The stoichiometry of the complex formed between (*S*,*S*)-**30** and Mandelic acid **54** was determined according to Job's method of continuous variations. Equimolar amounts

of (*S*,*S*)-**30** (0·020 M) and (*S*)-Mandelic acid (0·020 M) were prepared in $CDCl_3$ (5 mL). These solutions were distributed among thirteen NMR tubes in such a way that the mole fractions (X) of (*S*,*S*)-**30** and (*S*)-**54** in the resulting solutions increased from 0·1 to 0·9. The complexation induced shifts of the methine signal (Δδ) were multiplied by the mole fraction of the acid (X) and plotted against X to obtain the Job's plot, Which shows a maxima at X = 0.67 (Figure 3.14). This indicates that (*S*,*S*)-**30** and the mandelic acid bind in a (1:2 Complex) under these conditions.

Table 3.7: Chemical shift value of methine signal

No.	Mole fractions of acid (54)	Mole fractions of amine (*S*,*S*-30)	α-H signal (Δδ)
1	0.1	0.90	0.157
2	0.2	0.80	0.161
3	0.3	0.7	0.154
4	0.4	0.60	0.170
5	0.45	0.55	0.178
6	0.50	0.50	0.199
7	0.55	0.45	0.219
8	0.60	0.40	0.261
9	0.65	0.35	0.336
10	0.70	0.30	0.327
11	0.75	0.25	0.287
12	0.80	0.20	0.230
13	0.90	0.10	0.111

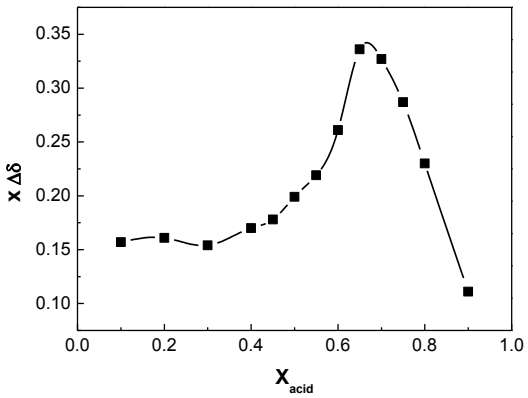

Figure 3.14: Job plot graph

3.I.18 In view of understanding of the structural requirement of the acid component, we were interested in extending the range of substrates where such type of ligand discriminate proton of drug molecules or its intermediate such as dibenzoyl derivative of tartaric acid **66**, 2-hydroxy-3-methoxy-3,3-diphenylpropanoic acid **67** and ibuprofen **68**.

Scheme 3.10: Structure of different acids.

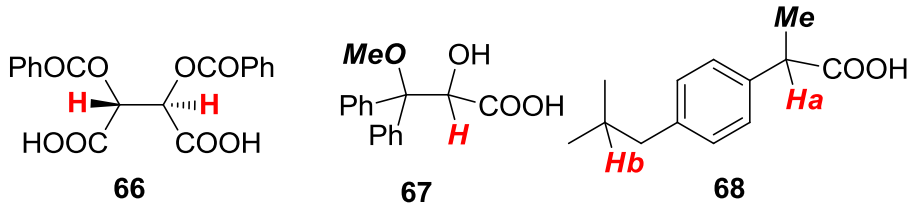

3.I.19 Study of Tartaric acid derivative

Tartaric acid played an important role in the discovery of chemical chirality. This property of tartaric acid was first observed in 1832 by Jean Baptiste Biot who observed its ability to rotate polarized light. Since then tartaric acid and its derivatives have a plethora of uses in the field of chiral chemistry and pharmaceuticals [25], hence it is important to develop a reliable method to quickly determine its optical purity.

For this study, a nonracemic sample of dibenzoyl tartartic acid was prepared (20% excess in D-isomer). It is apparent that the chemical shift changes of (*D*)-dibenzoyltartaric acid were greater than that of the corresponding (*L*)-dibenzoyltartaric acid ($\Delta\Delta\delta = 0.043$) (Figure 3.15).

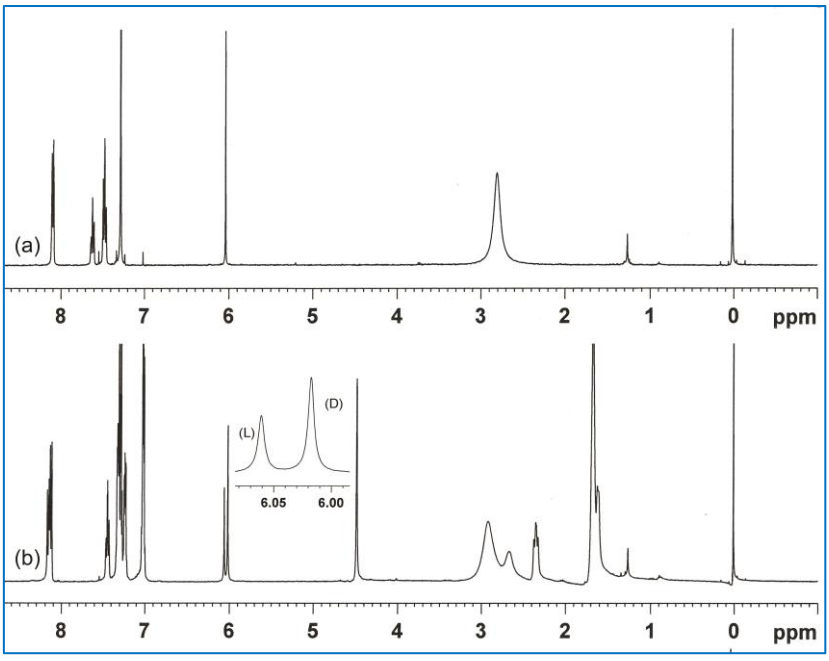

Figure 3.15: ^{1}H NMR spectra of dibenzyol tartaric acid (a) blank **66**; (b) in presence of (*S*,*S*)-**32**, the expanded region of peak pertaining to α proton is also given. Ratio is (1:1).

3.I.20 Study of 2-hydroxy-3-methoxy-3,3-diphenylpropanoic acid 67.

In case of 2-hydroxy-3-methoxy-3,3-diphenylpropanoic acid **67** which is an intermediate for few pharmaceutical entities with Type A ligand [26]. It was observed that ligand (*R*)-**15** & (*R*)-**16** gave better discrimination as compared to other ligands. Similarly some extent of separation was also observed for -OMe signal particularly in presence of ligand (*R*)-**15**.

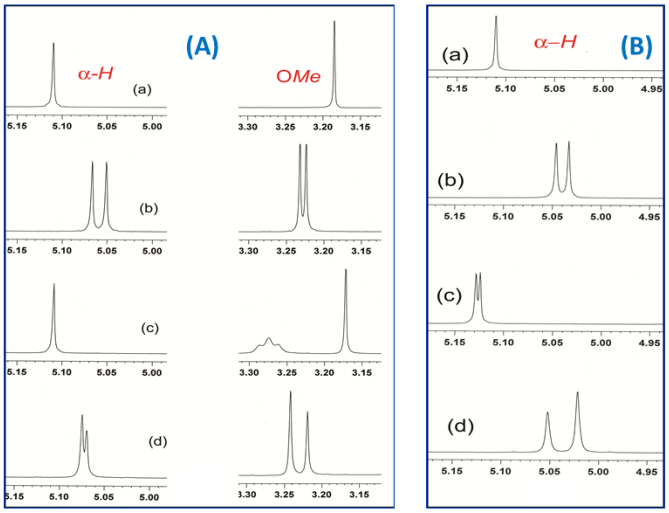

Figure 3.16 Selected region of compound **67** in presence of CSA **(A)** in presence of Type A ligand (b) with (*R*)-**15** (c) (*R*)-**17** (d) (*R*)-**16. (B)** In presence of Type C ligand (b) with (*S*,*S*)-**30** (c) (*S*,*S*)-**31** (d) (*S*,*S*)-**32**

Similarly when Type B ligand were screened, in particular the most effective (*S*,*S*)-**30** and (*S*,*S*)-**32** were screened, base line resolution were observed in both the case (Figure 3.16B), particularly the two hydrogen signals of C$^{\alpha}$*H* showed base line separation with (*S*,*S*)-**32** while the ratio of non-racemic mixture (20% excess of '*S*' isomer of **67**) was also determined indicating a defined control over the interactions [Figure 3.16B(d)].

Table 3.8: Screening of amines and di-amines as CSA for **67**

Entry	CSA	ΔΔδ (ppm) **α-H**	ΔΔδ (ppm) **OMe**
1	(*R*)-15	0.015	0.008
2	(*R*)-16	0.005	0.013
3	(*R*)-22	0.008	0.006
4	(*S*,*S*)- 30	0.013	0.008
5	(*S*,*S*)- 31	0.004	0.002
6	(*S*,*S*)- 32	0.020	0.006

NMR were performed with $CDCl_3$ for entry 1 to 3 (CSA:analyte 1:1) for entry 4 to 6 (1:2).

3.I.21 Study of Ibuprofen

The racemic sample of ibuprofen **68**, a widely used non steroidal anti-inflammatory agent, was also analyzed for the chiral recognition with the synthesized roof shape amines. There are three hydrogens of the molecule of **68** which showed discrimination on the recognition with the CSA. The $C^{\alpha}Me$ of **68** appeared as two doublets under the influence of (*R*)-**15** or (*R*)-**16** (entry 1, 2, Table 3.9). The $C^{\alpha}H_a$ showed slightly more resolution with (*R*)-**15** compared with (*S,S*)-**30** as clearly eight lines were seen corresponding to the two separated quartets for the enantiomers (entry 3,4). It is significant to note that the proton present on the alkyl substituent on the aromatic ring of **68** also indicated discrimination. The methine proton (CH_b of **68**) which should show a multiplet in ^{1}H NMR showed two sets of signals with CSA (entry 3 to 5). This observation is probably due to the CH_b-π interaction between the methine proton and the aromatic ring of the CSA [Figure 3.27 (c)].

Table 3.9: Screening of amines and di-amines as CSA for Ibuprofen

No	CSA	Probe Signal *H* in bold	
		Δδ (ppm)	ΔΔδ (ppm)
1	(*R*)-**13**	-0.012	0.011 ($C^{\alpha}CH_3$)
2	(*R*)-**15**	-0.015	0.007 ($C^{\alpha}CH_3$)
3	(*S,S*)-**30**	-0.011	0.007 (*Ha*)
4	(*R*)-**13**	-0.052	0.007 (*Ha*)
5	(*S,S*)-**30**	-0.062	0.007 (*Hb*)

All experiments were performed with $CDCl_3$ for entry 1, 2,4 (1:1) for entry 3 & 5 (CSA:analyte 1:2)

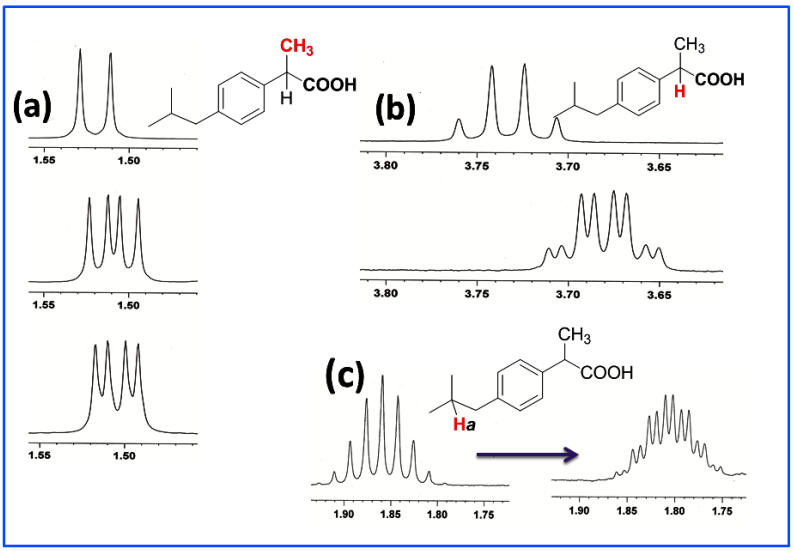

Figure 3.27: Selected region of Ibuprofen in ^{1}H NMR signal

3.I.22 Measurement of enantiomeric excess

The proposed CSA has also been applied to evaluate its limit in the accuracy of the measurement of *ee*. Seven samples containing mandelic acid with 0%, 20%, 40%, 60%, 80%, 90%, 95% ee purity were prepared.These samples were analysed with 0.5 equiv of (*S*,*S*)-**30** by recording their ^{1}H NMR. Integration of the corresponding C$^{\alpha}$*H* ^{1}H NMR signals rendered measured *ee* showing an excellent linear correlation with the prepared samples (R^2= 0.9998). Such linear relationship confirms the possible practical use of these CSAs for determination of purity of unknown samples.

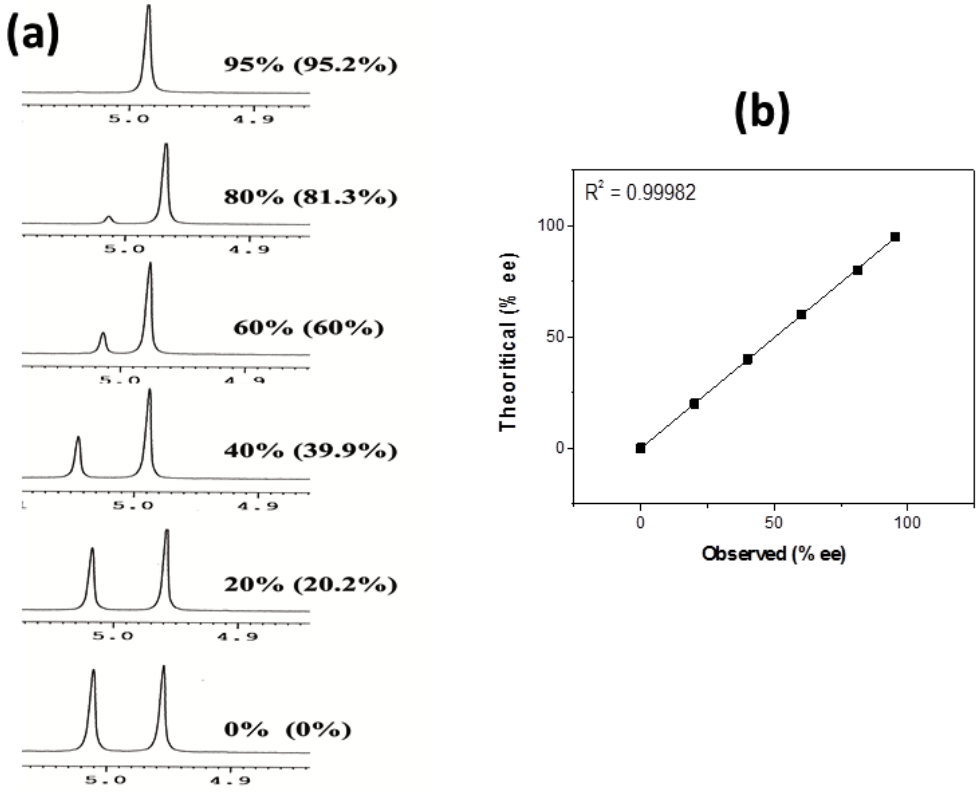

Figure 3.18: Correlation between observed and theoretical value [Right]. Selected region of ^{1}H NMR spectra of mandelic acid with various enantiomeric purities [Left]

Section-II

3.II.1 Background

The use of chiral solvating agent for ^{1}H NMR spectroscopy is one of the most convenient methods to achieve rapid determination of enantiomeric excess of chiral compounds. This method has an advantage of easy performance without using any chiral derivatization of the analyte. The importance of chiral discrimination and measurement of *ee* have been discussed in section-I.

High sensitivity, high natural abundance and ubiquitous presence of protons in majority of chiral molecules render the use of ^{1}H NMR by default as most favorable choice.

The use of chiral solvating agent for effective analysis requires large chemical shift nonequivalence and the spectrum should not become too complex due to overlap of multiple pattern of host structure signals. When any of these requirements were not fulfilled, the NMR utility was severely hampered for chiral analysis.

This problem can be addressed by targeting NMR probes, other than proton by selecting suitable examples. The use of heteronuclei NMR may be preferred where ever feasible. Given the encouraging result obtained in the enatiodiscrimination in proton spectroscopy, we investigated the utility of different roof shape amine and diamines by selecting probes of other nuclei such as ^{13}C, ^{19}F, and ^{31}P for NMR spectroscopy. Performing the analysis of chiral molecules by considering two (or more) different nuclei and comparing the data can result in more accurate analysis.

The objectives of NMR experimental technique in chiral discrimination are:

(i) measurement of chiral composition
(ii) simplification of spectral complexity
(iii) straightforward or direct identification of peaks

The present section discusses the utilisation of heteronuclei for identification of peaks pertaining to two enantiomers facilitating the determination of enantiomeric excess.

3.II.2 Objective

While dealing with the study of complex chiral molecules using ^{1}H NMR, often one might encounter situations where the spectra are extremely complex due to multiple pattern or poor resolution due to much overlap of different peaks.

During our studies of CSA in ^{1}H NMR spectroscopy we had observed that CSA (*S*,*S*)-**32** appeared to give best results in most of the examples, but in case of ibuprofen peaks of ligand structure merge with acid component, *see* Figure 3.28 (B). At the same time when ^{1}H NMR spectra of racemic sample of trifluoro mandelic acid recorded with (*S*,*S*)-**32**, interesting pattern of signals of the aromatic protons of (±)-**55** showed considerable discrimination. The signal of (±)-**55** in presence of (*S*,*S*)-**32** gave clear spectra with complete separation for the two sets of signals at remote position from sterocentre Figure 3.28 (**A**-Right).

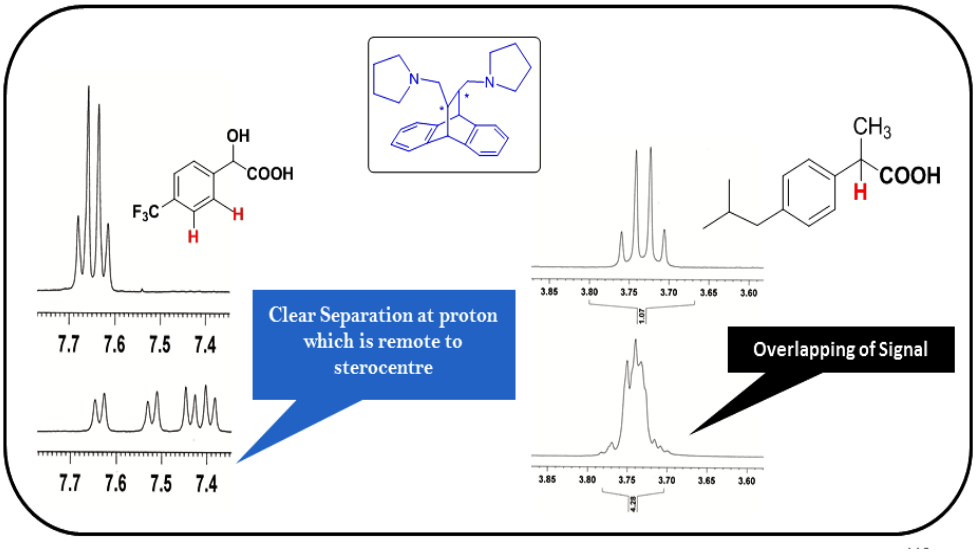

Figure 3.28: (A-Right) Discrimination of Aromatic proton (B-Left) overlapping of signal.

In continuation of our study of discrimination of signals of α-functionalized acid derivatives we further examined other nuclei ^{13}C, ^{19}F and ^{31}P under the effect of CSA interactions.

3.II.3 ^{13}C NMR Study

Study of molecular recognition of chiral isomers by ^{13}C NMR spectroscopy is not well studied; probably such analysis would be more qualitative in nature. The screening process was conducted with the racemic sample of 4-trifloro mandelic acid **55** as the standard substrate to study its ^{13}C NMR spectra. The carbonyl carbon and $^{\alpha}$C of (±)-4-triflouromandelic acid **55**, are expected to show two single peaks in ^{13}C NMR were split in the presence of (*S*,*S*)-**32**. The signals of carbonyl and $^{\alpha}$C appear as two sets of well separated peaks on treatment with (*S*,*S*)-**32** (Table 3.10; Figure 3.29).

Table 3.10: Chemical shift nonequivalence in ^{13}C- NMR for compound **55**

Entry	Carbonyl carbon of ^{13}C-NMR (ΔΔδ)	$^{\alpha}$C of ^{13}C-NMR (ΔΔδ)
1	**0.11**	**0.20**

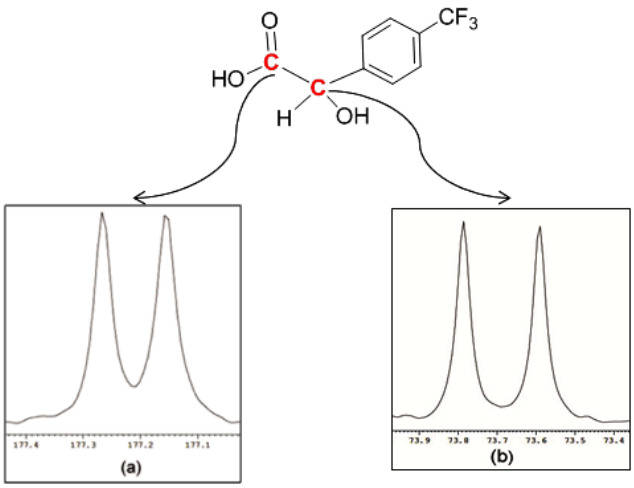

Figure 3.29: (a) Carbonyl carbon of ^{13}C NMR with (*S*,*S*)-**32**; (b) $^{\alpha}$C of ^{13}C NMR with (*S*,*S*)-**32**.

3.II.4 ^{19}F NMR Study

There is a substantial advantage of employing ^{19}F NMR, when compared other less abundant nuclei, which makes it most favorable nucleus for investigation because of the following benefits;

- It has 100% natural abundance and no labeling is required.
- Its sensitivity is similar to proton.
- It has very large chemical shift range (~500 pm). .
- The spectra are quite less complicated, as compared to ^{1}H and ^{13}C NMR.

For exploring the utilization of ^{19}F NMR we have chosen the readily available 4-trifluoro mandelic acid. The three representative examples of (*S*,*S*)-**30,** (*S*,*S*)-**31,** (*S*,*S*)-**32** and (*R*)-1**6** were investigated (Table 3.11).

Table 3.11: Screening of different CSAs for (±)-**55** to measure shift in ^{19}F NMR

No	CSA	ΔΔδ (ppm)
1	(*S*,*S*)-**30**	0.054
3	(*S*,*S*)-**32**	0.052
4	(*R*)-**16**	0.010

All experiments were performed with $CDCl_3$ for entry 1 and 2 (1:2) for entry 3 (1:1) (CSA: analyte)

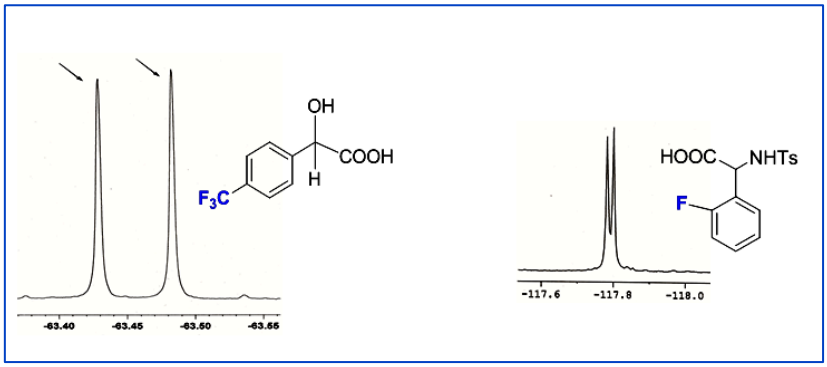

Figure 3.30: ^{19}F NMR spectrum (376 MHz) of (±)-**55** with (*S*,*S*)-**32**

We also examined the ^{19}F NMR of an amino acid derivative (2-flouro N-Ts phenyl glycine **69** under the effect of (*S*,*S*)-**32** where the fluorine showed two sets of signals with considerable separation.The chemical shift nonequivalence (ΔΔδ) was recorded to be 0.017 ppm.

3.II.5 ^{31}P NMR Study

Since many biologically significant compounds and ligands for asymmetric synthesis also have phosphorous, we have extended our investigations to study ^{31}P NMR of such molecules. To assess the ability of our systems to recognize phosphorous containing acids we chose racemic sample of (±)-1,1'-binaphthyl-2,2'-diyl hydrogenphosphate **70** and studied its ^{31}P NMR (at 174 MHz in $CDCl_3$).

Scheme 3.11: Structure of phosphorous containing compound **70**

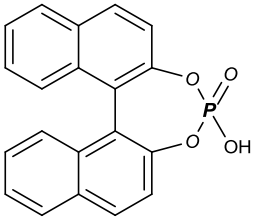

The chiral molecule of acid has recently been widely used in asymmetric transformations [27] and hence it is important to develop a reliable method for quick determination of its optical purity.

We examined our efficient (*S*,*S*)-**32** for the discrimination of the signal of phosphorous of the racemic sample and found good resolution. In order to assign the configuration to the signals we scanned a non-racemic sample (2:1 for *R:S* isomer) with optically pure (*S*,*S*)-**32** and detected a good separation of signals upto 0.69 ppm (Figure 3.31).

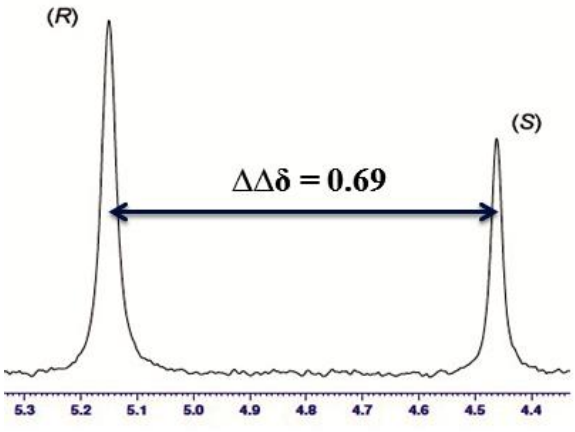

Figure 3.31: ^{31}P NMR of spectra of compound **70** in presence of ligand (*S*,*S*)-**32**

Table 3.12: Screening of different CSAs to measure shift in ^{31}P-NMR

No	CSA	ΔΔδ (ppm)
1	(*S*,*S*)-**30**	0.60
2	(*S*,*S*)-**32**	0.69
3	(*R*)-**16**	0.15

Consistently good separation of signals for ^{31}P NMR with different CSAs is observed (Table 3.12) confirming the generality of our system (Figure 3.32).

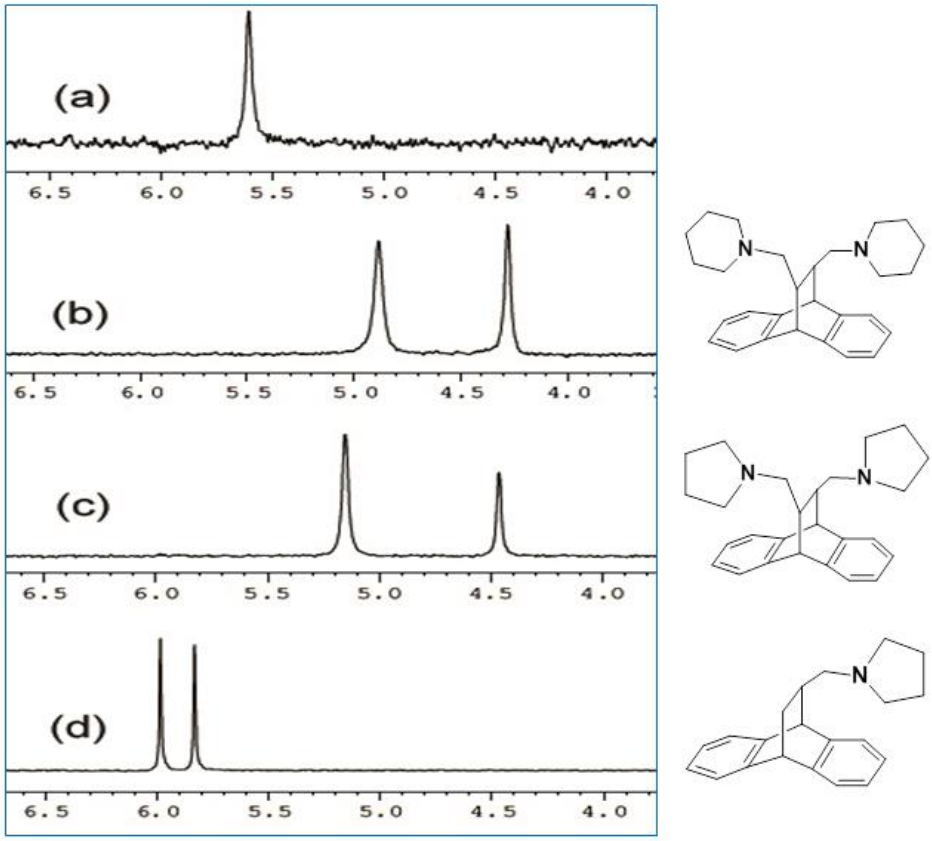

Figure 3.32: ^{31}P NMR spectrum (174 MHz) (a) blank, (b) (*S*,*S*)-**30,** (c) (*S*,*S*)-**32** (d) (*R*)-**16** in $CDCl_3$

Section-III

3.III.1 Introduction to crown ethers

Crown ethers are compounds that, known form, are cyclic oligomer of ethylene oxide. The essential repeating unit of several simple crown ether is ethyleneoxy group, i.e (-CH_2CH_2O-)$_n$.

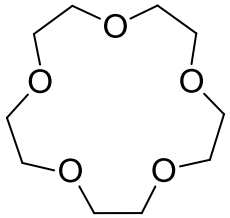

15-crown-5

The supramolecular chemistry involves the study involves design and synthesis of receptor suitable for particular analytes and investigation their interactions. If the receptors are chiral in nature one may extend their interactions with chiral analytes. The most common of these receptors are crown ethers that are able to form complexes in an enantioselective manner with chiral analytes, such as amines and amino acid derivatives [28].

The chiral crown ethers have been widely applied as chiral selectors in differentiating the enantiomers of racemic mixtures containing a primary amino group. However, these crown ethers are shape and size selective in their molecular recognition. Hence, there is a constant need to synthesize and screen novel chiral crown ethers.

Crown ethers can complex with cations, especially alkali and alkaline metal ions, in routine organic solvents. In 1967, Pedersen's papers on crown ether described the synthesis of crown ethers, their complexation behaviour with metal cations and ammonium salts [29].

In this effort we have synthesized and characterized crown ether anchored to our roof shape diol with a hope to study its utility for the enantioselective interaction with amino acids.

3.III.2 Synthesis of crown ether

We designed the synthesis of crown ether based on the cyclization of di-tosyl derivative of ethylene glycol derivative. The macrocycle can be synthesized by

cyclization on these tosyl-diol by substitution reaction with alkoxide derived from the roof shape chiral diol. Hence, the efforts to construct the macrocyclic ether began by synthesizing different di-tosyl derivative of ethylene glycol and its oligomers. We prepared OTs- derivative of di, tri and tetra ethylene glycol and preformed reaction for construction of crown. Attempts to synthesize crown with diethylene and triethylene glycol tosylate with (*S*,*S*)-**27** at different dilution conditions were not successful. We further attempted reaction of tosyl derivative of tetra ethylene glycol with roof shape diol. In this case we were successful to prepare the desired crown ether. Crown ether **71** was obtained as white solid and the structure of this new roof crown was consistent with data obtained from ^{1}H and ^{13}C NMR, Mass spectral analysis and single crystal X-ray diffraction data. Slow evaporation of compound **71** in Pet Ether–Ethyl acetate gave transparent crystal which was suitable for single crystal analysis.

Scheme 3.12: Synthesis of crown ether

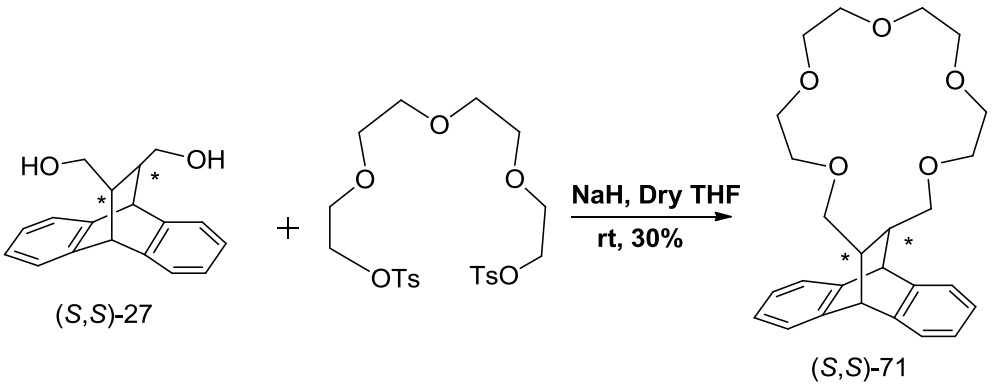

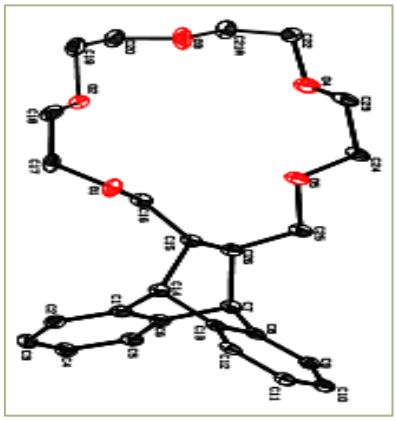

Figure 3.33: ORTEP diagram of crown ether

It is well known in literature such type of crown ethers is capable of forming complexation with cation [28d].

To test the ability of crown ether for discrimination of signals in NMR spectroscopy, few derivatives of ammonium cation of amino acid, were screened. The above mentioned racemic ammonium cation was added in CD_3OD with ratio 1:1 to crown ether, but separation was found to be negligible. Addition of chiral crown ether to amino acid salt induced small up field shifts in the NMR signals of the analyte, but the separation of the enantiomer signals was not detected. A similar result is also obtained when ammonium salt of racemic α-methyl benzyl ammonium hydrochloride was tested.

Scheme 3.13: Structure of different analyte tested

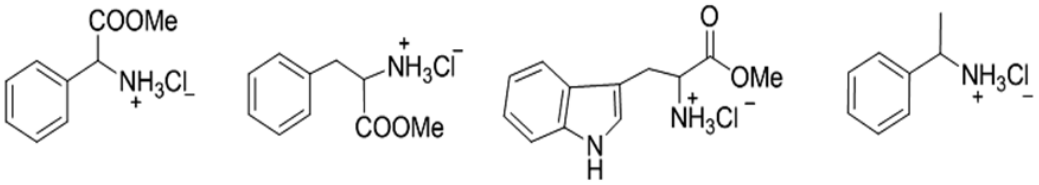

72a 72b 72c 72d

3.III.3 Experimental Section:

To a solution of diol **27** (0.30 g, 1.12 mmol) in dry THF (10 ml) under N_2 atmosphere sodium hydride (0.112 g, 2.8 mmol) was added in one portion. The above solution was stirred for one hour and then a solution of tetra ethylene glycol ditosylate (0.56 g 1.12 mmol) in dry THF (10 ml) was added slowly. The reaction mixture was stirred for another 30 h at room temperature. After the reaction water was added to the mixture and extracted with ethyl acetate (2X100 mL) dried over sodium sulphate and purified over silica gel chromatography.

White solid (0.145 g, 30 % Yield). $[\alpha]_D$ = +55.2 (c = 1.0, MeOH)

^{1}H NMR (400 MHz, $CDCl_3$): δ 1.71-1.77 (m, 2H), 2.97 (m, 1H), 3.28-3.30 (m, 2H), 3.42-3.47 (m, 2H), 3.58-72 (m, 14 H), 4.27 (s, 2H), 7.09-7.24 (m, 4H), 7.12-7.28 (m, 4H).

^{13}C NMR (100 MHz, $CDCl_3$): δ 43.8, 45.9, 70.2, 70.7, 70.9, 74.6, 76.7, 123.4, 125.2, 125.5, 125.8, 141.1, 143.7

HRMS (EI^+): Calculated for $C_{26}H_{32}O_5$ $(M+Na)^+$ 447.2147, observed 447.2130

IR (KBr): υ 2896, 2870, 1466, 1353, 1133, 986, 762, 569 $cm.^{-1}$

Spectral chart

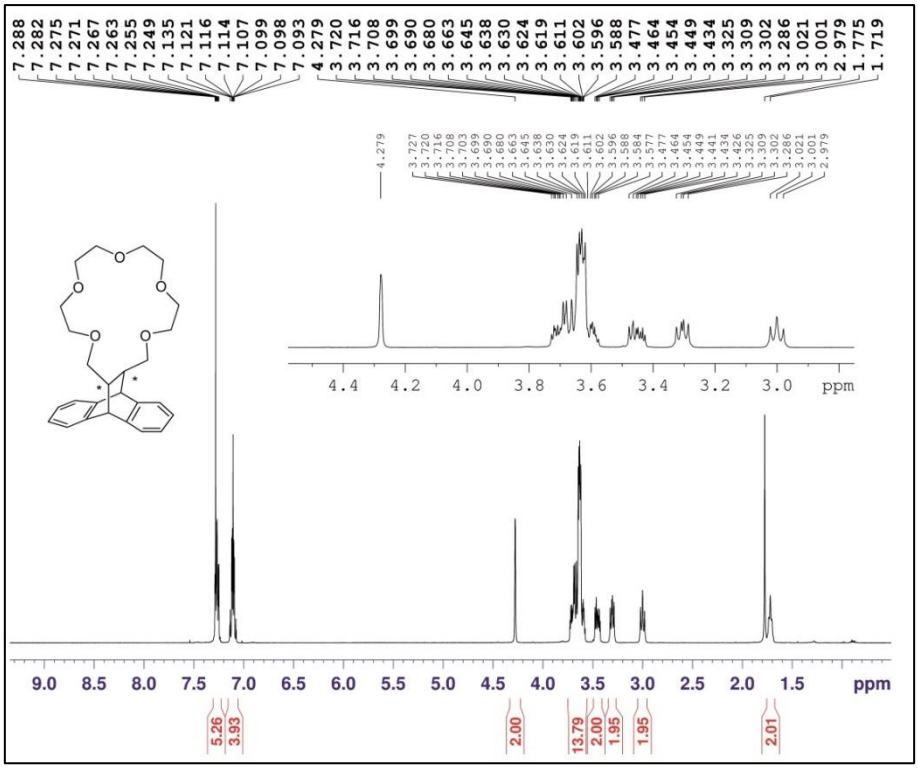

^{1}H NMR spectra of compound 71

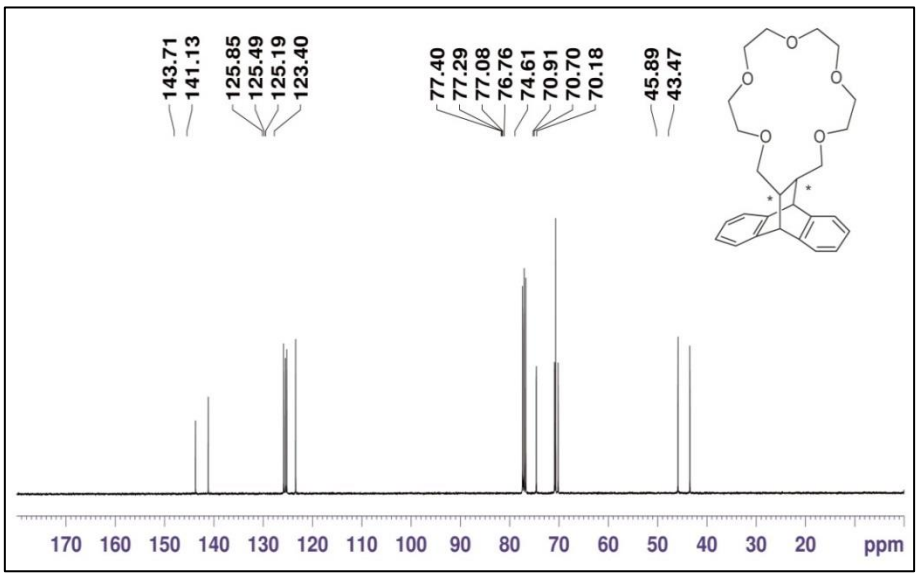

^{13}C NMR spectra of compound 71

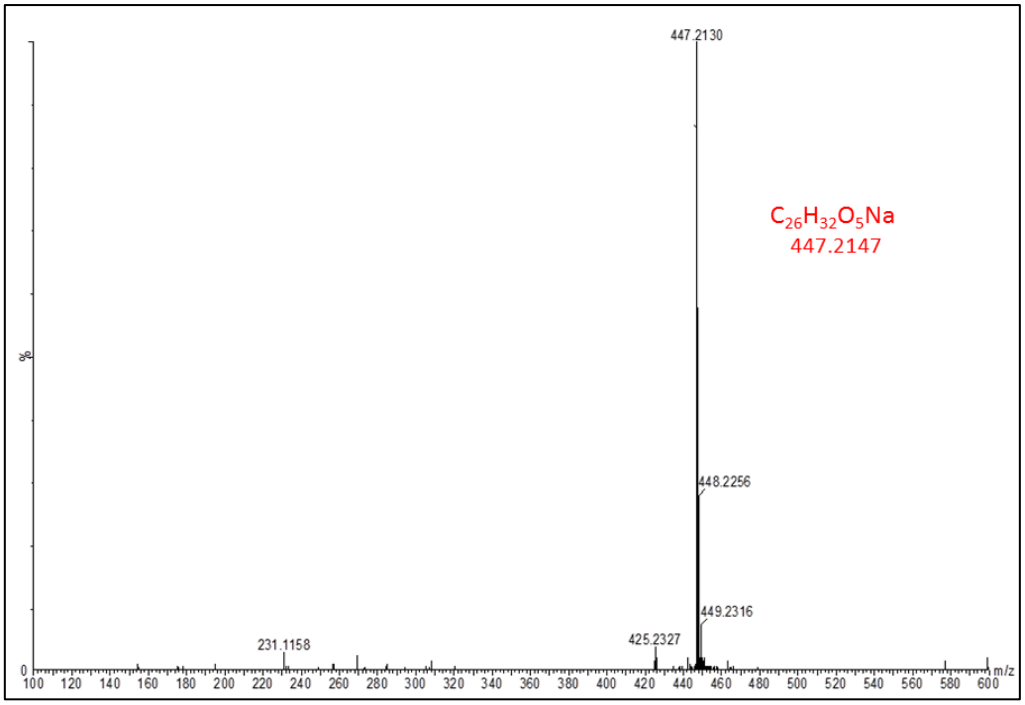

Mass spectra of compound 71

Section-IV

3.IV.1 Hydrogen bonding based CSA

Non covalent interaction such as hydrogen bond, π-π, CH-π and van der Waal`s force are classified as supramolecular interactions. Among non-covalent interactions hydrogen bonds (HBs) play an important role in chemical reactivity, solvation, and molecular self-assembly [30a]. Such interactions are also fundamental in determining biomolecular structure, upon which biological function is ultimately dependent.

The description of hydrogen bonds is still evolving and a more inclusive definition has been recently proposed by the IUPAC [30b]. However, the general viewpoint remains very close to the definition already proposed more than a century ago. A hydrogen bond is understood as the *attractive interaction involving an electronegative proton donor and an electronegative proton acceptor*.

According to IUPAC definition of H–bond "The hydrogen bond is an attractive interaction between a hydrogen atom from a molecule or a molecular fragment X-H in which X is more electronegative than H, and an atom or a group of atoms in the same or a different molecule, in which there is evidence of bond formation."

To understand such interaction numerous technique are available. Among them X-ray crystallography and IR spectroscopy are widely used. These techniques need a certain type of structural requirement such as good quality crystal or depend on the presence of certain functional group in the analyte or molecules.

The technique of Nuclear Magnetic Resonance (NMR) spectroscopy, with its highly advance and sensitive mode of analysis, also offers an alternative method of quick and accurate determination of non-covalent interaction which causes chiral discrimination [31]. In the present section, the study of different type of non-covalent interactions in which analyte and chiral solvating agent particularly capable of forming hydrogen bond are discussed. The adduct formed between analyte and CSA was stabilized by an intermolecular H-bonding and other non-covalent interactions that leads to considerable discrimination in ^{1}H NMR spectroscopy.

Hydrogen bond is one of the primary intermolecular forces. The first definitive paper on hydrogen bonding was published in 1920 by Latimer and Rodehush [32]. They applied the concept of hydrogen bonding for association of water molecules, although understanding different aspects of molecular structure by hydrogen bonding is now

grown in to an advance field. Thousands of papers have been published on various aspects of hydrogen bonding [33].

In organic chemistry the strong and directional nature of H-bonds is exploited in number of ways. Hydrogen bond between different molecules is commonly found such as acid-acid, acid-amide, amide-amide, amide-sulphoxide [34]. The Amide–amide hydrogen bonding had been explored over decades and was recognized as building block in determining peptide secondary structure, DNA base pairs, protein folding, and also found as binding component in molecular recognition. For instance a simple molecule of acetic acid is well known to form hydrogen bonded dimer in carbon tetra chloride [35].

In this section chiral discrimination by amide-amide H-bonding, amide-sulphoxide & amide-carbonyl H-bonding are discussed. Along with amide to carboxylic acid hydrogen bonding, in the presence of external base are also explored.

This section is divided into two parts: Part I and Part II

Part I

3.IV.2 Kagan's Amide and its modification

Chiral amide of 3,5-dinitro benzoic acid **73** reported by Kagan (Figure 3.33) was one of the earliest and well-studied CSA for efficiently discriminating several types of molecules by NMR analysis [36]. This is a simple molecule with basic functional units present to enable H-bonding and offer π-π interactions with substrates for tight complex formations in NMR conditions.

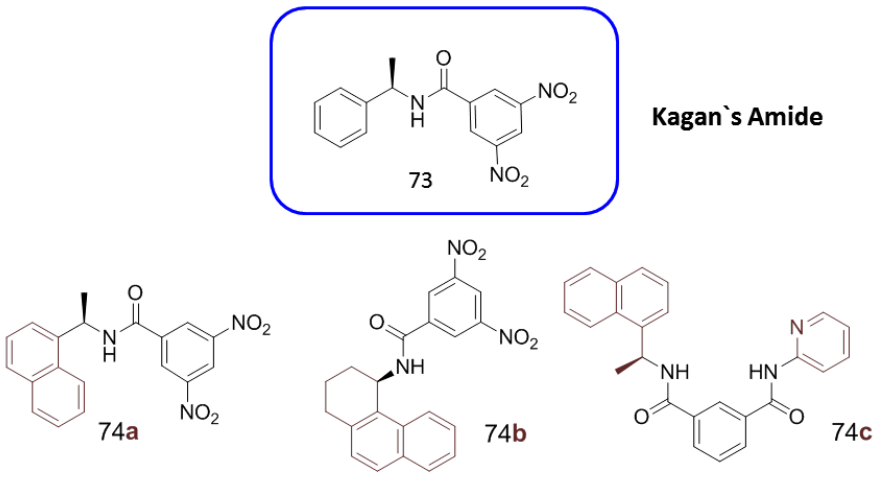

Figure 3.33: Structure of Kagan amide **73** and Modification in Kagan`s amide **74**a -**74**c

These types of compounds were first developed by Pirkle for the Whelk-O type materials for separation of chiral compounds on HPLC columns [37]. Over the years few more derivatives of Kagan's amide **74a** to **74c** have been explored with good success in molecular recognition of chiral compounds [38]. Different ranges of chiral analytes screened with these CSAs include amides [39], sulfoxides [36b, 36d] multifunctional *tert*-alcohols [38d], and phosphine oxides [36c].

3.IV.3 Modification in Kagan Amide

Generally accepted mode of interaction between the two molecules involve hydrogen-bonding between the CSA and the analyte, N-H·····O=X (X = C or S of analyte), and the π-π interaction between the aromatic units [39]. It was also proposed that the analyte fits between the cleft type conformation created by perpendicularly arranged dinitro benzoyl and the naphthalene rings in case of **74a** [39]. In the case of **74c**, cleft between the dinitrobenzoyl and phenanathrene moieties account for it unusual ability to cause high degrees of enantiomeric discrimination in many classes of substrates [40] (Figure 3.33). The proposed interactions were also corroborated by up-field and down-field shifts of appropriate examples in the ^{1}H NMR experiments.

Based on these proposed models (**A** Figure 3.34) we propose to introduce a modification in Kagan's amide where the chiral amine portion had an aromatic ring with two strongly electron withdrawing groups. With this modification the hydrogen attached to the nitrogen of the amide group of CSA will be more electron deficient due to the inductive effect and may form stronger hydrogen bonding with the carbonyl of the test sample (**B** in Figure 3.34).

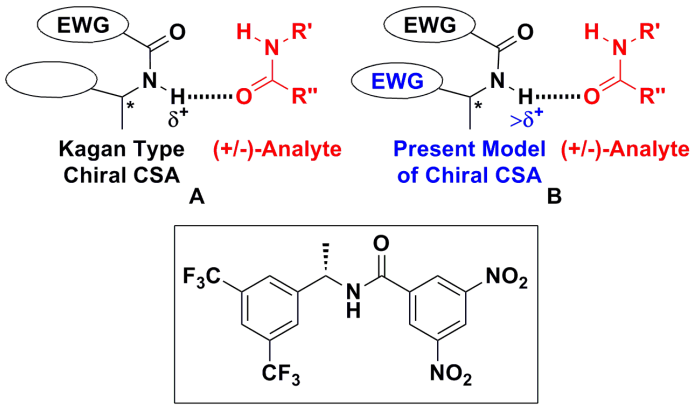

Figure 3.34: H-bonding and proposed modification in Kagan type CSA

We introduced two trifluoromethyl groups at the *meta* positions of aromatic ring at the amine portion of the amide unit keeping the chiral centre unchanged. In earlier chapter 2 we have shown resolution of triflouromethyl alcohol and stepwise conversion into amides. In this section evaluation of **50** & **51** as CSA for determining chiral purity of suitable range of substrates by ^{1}H NMR are discussed.

3.IV.4 Single crystal analysis

As mention in previous chapter that single crystal of (*S*)-**50** was developed by slow evaporation in toluene and its X-ray diffraction analysis was performed (Figure 3.35) [42]. The single crystal analysis of **74**a indicated a cleft-like arrangement caused by having the 3,5-dinitrobenzoyl group placed orthogonal to the naphthalene plane [39]. The selective recognition of the two isomers of chiral amide analyte was attributed to this arrangement and was proposed to be responsible for the supramolecular interactions.

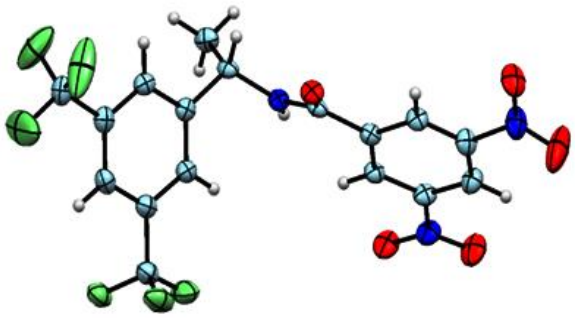

Figure 3.35: ORTEP diagram of (*S*)-**50**

We observed that the planes passing through the two aromatic rings bisecting each other at an angle of 119.6^{o} making the arrangement of the aromatic rings quite open compared to **74a**, where the same angle was noted to be 99.9^{o} (Figure 3.36). The intramolecular hydrogen bonding N-H·····O=C was detected with the bond distance of 2.104 Å.

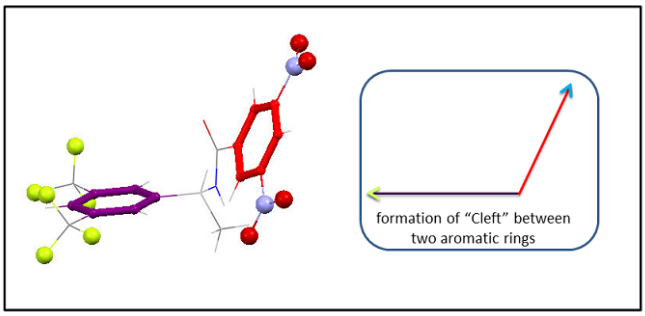

Figure 3.36: Orientation of compound showing cleft between two aromatic ring [$(CF_3)_2$ in purple color & $(NO_2)_2$ as red color]

Experimental

Commercially available (*S*) and (*R*) α–Methyl benzyl amine are purchased and used as received. Both the isomer are mixed in 2:1 (*S*:*R*) ratio and used for the preparation of non-racemic sample of amide using standard protocol. Methyl phenyl sulphoxide was prepared by methylation of thiophenol followed by oxidation of thioanisole [43a]. The other analytes were prepared according to literature procedures and purified by column chromatography before use.

3.IV.5 Implementation of Amide derivative

Having prepared two derivatives of modified CSAs, (*S*)-**50** and (*S*)-**51**, we next screened them to test their ability to discriminate the signals of chiral amide analytes. We made four types of the chiral amides Ph*C***H**(***CH*$_3$**)NHCOR (**75a**-**75m**) in the unequal ratio of its enantiomers and tested them with CSAs (Table 3.13 to 3.16).

3.IV.5.1 Effect of aromatic amide

The first set of amides is made with aromatic acid moieties (**75a - 75c**) being phenyl, naphthyl and anthryl. The recognition study was conducted in $CDCl_3$ (400 MHz; 10 mmol concentration; ratio of 1:1). As can be seen from Table 3.13 there is not much difference in case of benzene and naphthalene derivatives (**75a** and **75b**) while the signals (of C*<u>*Me*</u>) are much resolved in case of anthracene derivative (**75c**).

Table 3.13: ^{1}H NMR induced chemical shift (Δδ) and nonequivalences (ΔΔδ) of amides **75a** – **75c** in presence of CSA (*S*)-**50**

No	Amide **75**	ArC<u>***H***</u>MeNHCOR		ArCH<u>***Me***</u>NHCOR	
		Δδ	ΔΔδ	Δδ	ΔΔδ
1	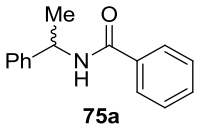 **75a**	-0.086	0.060	-0.018	0.025
2	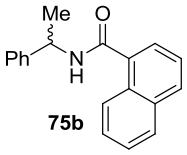 **75b**	-0.084	0.063	-0.018	0.022
3	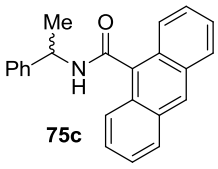 **75c**	--[a]	--[a]	-0.049	0.045

[a-] Not resolved

3.IV.5.2 Effect of electron withdrawing & donating group in analyte

The second set of amides investigated had the phenyl substituted with electron releasing and withdrawing groups (**75d-75i**). When the aromatic ring is attached with electron withdrawing group the degree of induced chemical shift (Δδ) and nonequivalence (**ΔΔδ**) for both sets of protons was observed to be marginally on the lower side (**8d** and **8f**) (Table 3.14, entry 1 to 4) while with electron releasing group attached showed considerably enhanced shifts in both the parameters (**75g** and **75i**) (Table 3.14, entry 5 to 7).

Table 3.14: ^{1}H NMR induced chemical shift (Δδ) and nonequivalences (ΔΔδ) of amides **75d -75i** in presence of CSA (*S*)-**50**

No	Amide **8**	ArC***H***MeNHCOR		ArCH***Me***NHCOR	
		Δδ	ΔΔδ	Δδ	ΔΔδ
1	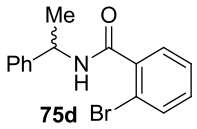 **75d**	-0.077	0.043	-0.025	0.015
2	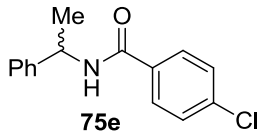 **75e**	-0.072	0.044	-0.012	0.017
3	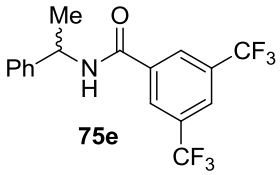 **75e**	-0.015	--[a]	-0.014	0.021
4	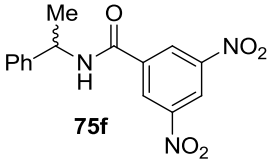 **75f**	-0.046	--[a]	-0.014	0.018
5	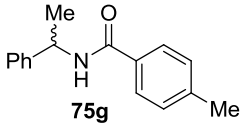 **75g**	-0.090	0.059	-0.021	0.024
6	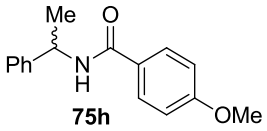 **75h**	-0.091	0.059	-0.019	0.025
7	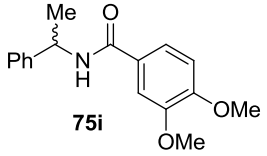 **75i**	-0.067	0.076	-0.016	0.030

[a]Not resolved.

The pattern observed for the second set of amide analytes was consistent with the proposed hydrogen bonding model (Figure 3.34), where the electron releasing groups on the amide (ArCO) would make the oxygen of carbonyl more electron rich and hence should favor the interaction by becoming better hydrogen bond acceptor. The opposite phenomena supported the lower values in case of electron withdrawing substituents.

3.IV.5.3 Effect of alkyl amide

The third set of amides was made where the alkyl acids were condensed with α-methyl benzyl amine (**75j-75m**) targeting two protons $C^{\alpha}H$ of Ph*C*H*(CH$_3$)NHCOR and methyl protons attached to the chiral center of Ph*CH(C*H*$_3$)NHCOR. In case of alkyl derivatives a pattern was observed where both the parameters were seen to increase with increase in the size of R group (**75j** and **75m**, Table 3.15a). Higher values were seen in case of pivaloyl (**75l**) and adamantyl (**75m**) supporting this trend (Table 3.15, entry 3 & 4 and Figure 3.15a entry 3 & 4).

Table 3.15: ^{1}H NMR induced chemical shift (Δδ) and nonequivalences (ΔΔδ) of amides **75j** to **75m** in presence of CSA (*S*)-**50** and in some cases (*S*)-**51**[b].

No	Amide **8**	ArC***H***MeNHCOR		ArCH***Me***NHCOR	
		Δδ	ΔΔδ	Δδ	ΔΔδ
1	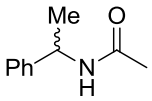 **75j**	-0.110 (-0.004)[b]	0.081 (--[a,b])	-0.028 (-0.004)[b]	0.034 (--[a,b])
2	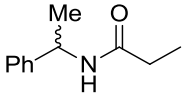 **75k**	-0.154	0.108	-0.046	0.047
3	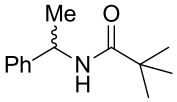 **75l**	-0.158 (-0.007)[b]	0.156 (--[a,b])	-0.047 (-0.004[b])	0.057 (--[a,b])
4	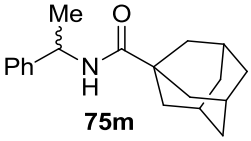 **75m**	-0.174	**0.163**	-0.018	**0.059**

[a]Not resolved. [b]with (*S*)-**51.**

Table 3.15a: Selected portion of ^{1}H NMR with (*S*)-**50** as CSA with **75**j to **75**m

No.	Amide	ArC***H***MeNHCOR	ArCH***Me***NHCOR
1	**75j**	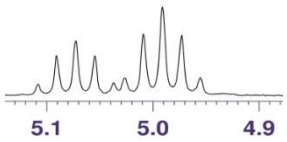	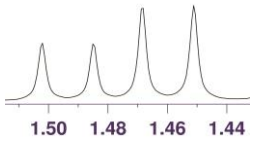
2	**75k**	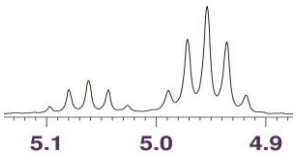	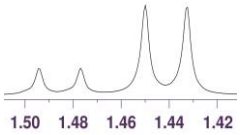
3	**75l**	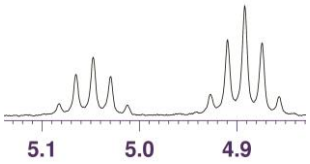	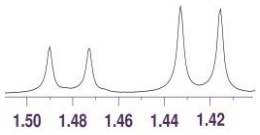
4	**75m**	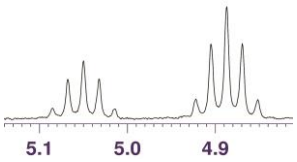	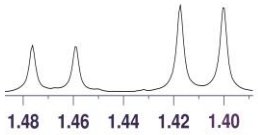

NMR in $CDCl_3$ at 10 mM (1:1), 400 MHz: Ratio of *S*:*R* for **75j**, **75l**, **75m** 1(***R***):2(***S***) & for **75k** 1(***R***):3(***S***)

3.IV.5.4 The fourth set of amides was made where adamantyl chloride is condensed with two different amine 4-flouro α–Methyl benzyl amine **75n** and α-methyl napthyl amine **75o** targeting two protons C$^{\alpha}$*H* of R*C***H**(C***H*$_3$**)NHCO adamantyl and fluorine attached to in case of **75o** (Table 3.16 & Figure 3.37 & 3.38).

Table 3.16: ^{1}H NMR induced chemical shift (Δδ) and nonequivalence (ΔΔδ) of amides **75m** - **75o** in presence of CSA (*S*)-**50**.

No	Amide	ArC***H***MeNHCOR		ArCH***Me***NHCOR	
		Δδ	ΔΔδ	Δδ	ΔΔδ
1	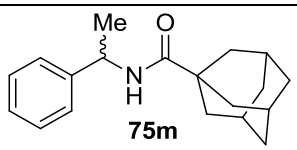 **75m**	-0.174	0.163	-0.018	0.059
2	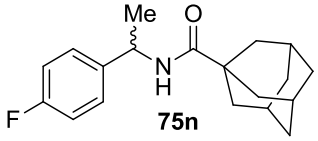 **75n**	-0.061	0.157	-0.036	0.053
3	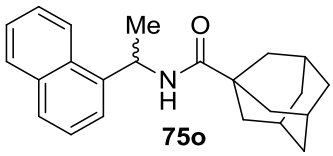 **75o**	**-0.39**	**0.502**	**-0.212**	**0.241**

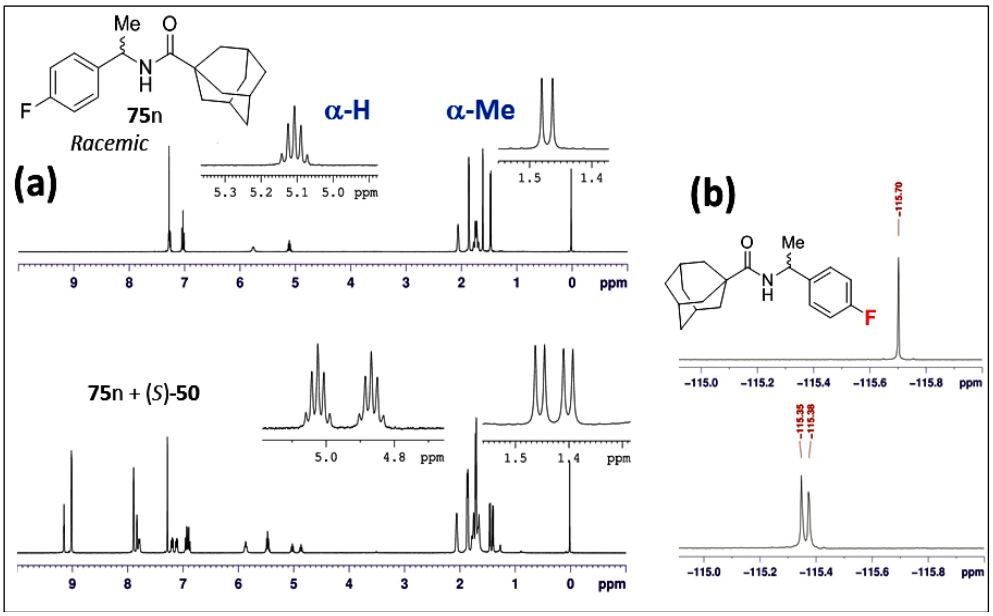

Figure 3.37: (a) ^{1}H NMR of **75n** [top], after addition of (*S*)-**50** [left] **(b)** ^{19}F NMR of **75n** [top], after addition of (*S*)-**50** [Right]

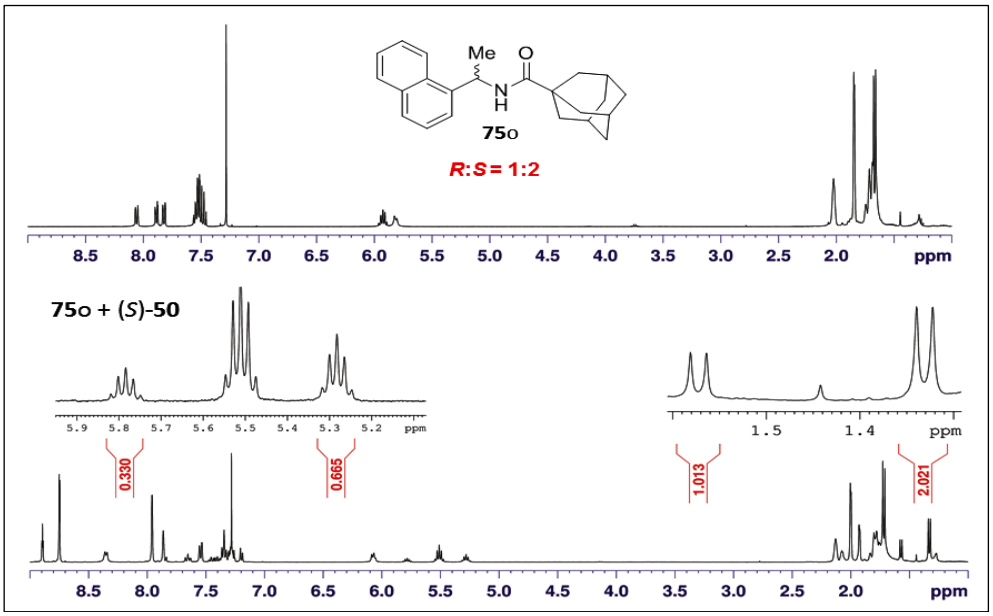

Figure 3.38: ^{1}H NMR of **75o** [top], after addition of (*S*)-**50**

3.IV.6 Comparison study

The hypothesis of designing the present modification in the Kagan's amide hinges on making the aromatic ring of CSA (ArNHCO-) more electron deficient by attaching two strongly electron withdrawing groups in (*S*)-**50** (B of Figure 3.34). By making this ring electron deficient and the subsequent inductive effect (-*I*) it is expected that

hydrogen of N-H acquire more +δ character and hence becoming a better hydrogen-bond donor. This hypothesis is then tested by comparing the CSA activity of Kagan's amide **73**, the known data for **74a**, [37] and our present study for (*S*)-**50** for the pivaloyl (**75l**) analyte derivative (Table 3.17). Another analogue is prepared without nitro groups (*S*)-**51** and also scanned for the comparison. The present modified Kagan's amide (*S*)-**50** showed marginally better values of the nonequivalences (ΔΔδ) for the amide **75l** for both the targeted hydrogens in the ^{1}H NMR analysis supporting the concept. The other derivative (*S*)-**51** failed to effect the discrimination in both the protons of **75l** indicating the need of strongly electron withdrawing groups on the ArC=O to make the carbonyl carbon sufficiently electron deficient (+δ) for effective hydrogen bond formation. Similar phenomenon is also observed for **75j** when (*S*)-**50** and (*S*)-**51** are tested (Figure 3.38). The role of hydrogen bond in the mechanism of the action of recognition of isomers for chiral solvation has been well established [44] and our observations corroborate the known observations.

Table 3.17: Comparison of CSA activity of **73**, **74a**, (*S*)-**50** and (*S*)-**51** for amide **75l**.

No	CSA	ArC*H*MeNHCOR	ArCH*Me*NHCOR
		ΔΔδ	ΔΔδ
1	**73**	0.061	0.023
2	**74a**	0.141	0.049
3	(*S*)-**50**	0.156	0.057
4	(*S*)-**51**	--[a]	--[a]

[a]Not resolved.

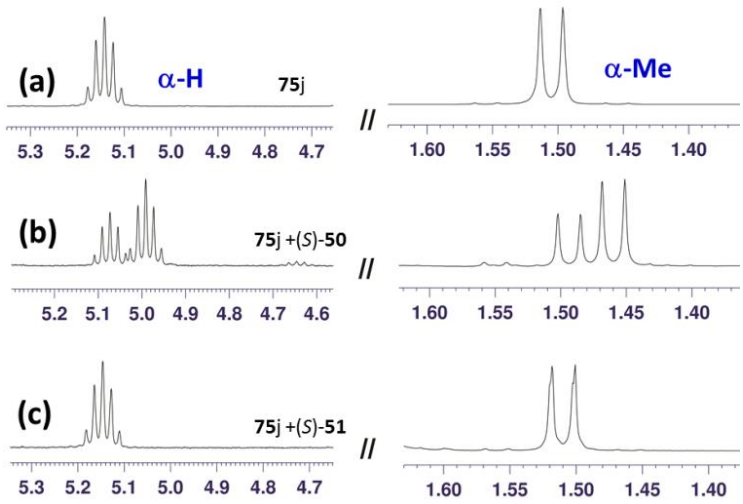

Figure 3.38: ^{1}H NMR of [a] blank **75j** [b] after addition of (*S*)-**50** [c]after addition of (*S*)-**51**.

3.IV.7 Solvent study

Further evidence of effect of polarity of solvent is studied with conducting ^{1}H NMR experiments in different solvents (Table 3.18). Very poor resolution is observed in polar solvents such as acetone-d_6 which is capable of forming hydrogen bond, while better separation is found in less polar benzene-d_6 (Table 3.18, Figure 3.39). However, due to the high cost of benzene-d_6 we have focused on the use of more commonly available chloroform-*d* for further study.

Table 3.18: Effect of solvent on the CSA activity of (*S*)-**50** for amide **75l**

No	Solvent	ArC*H*MeNHCOR	ArCH*Me*NHCOR
		ΔΔδ	ΔΔδ
1	$CDCl_3$	0.156	0.057
2	C_6D_6	0.201	0.070
3	CD_3COCD_3	--[a]	--[a]
4	$CDCl_3$ + DMSO-d_6 (9:1)	--[a]	--[a]

[a]Not resolved.

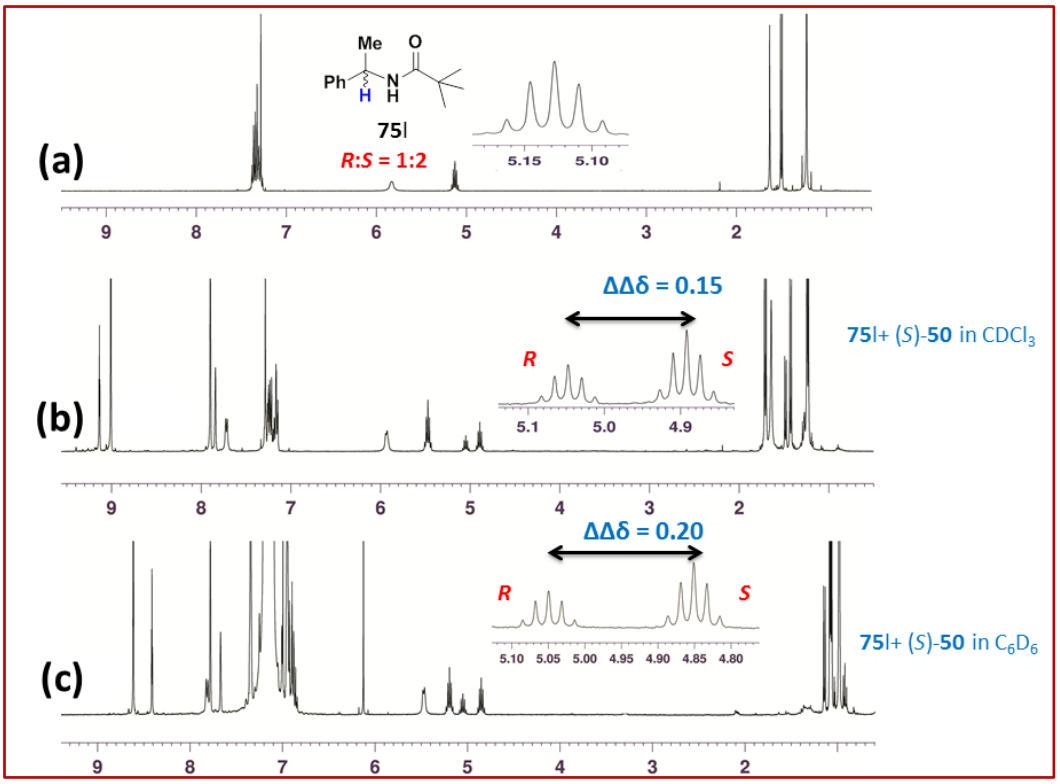

Figure 3.39: ^{1}H NMR spectra of pivaloyl derivative (a) blank in $CDCl_3$ (b) with (*S*)-**50** in $CDCl_3$ (c) with (*S*)-**50** in C_6D_6.

3.IV.8 Assignment of *R* & *S*

The two sets of signals in ^{1}H NMR of pivaloyl derivative **75l** and (*S*)-**50** in equimolar ratio are well resolved (Figure 3.40). In which both the signals C$^{\alpha}$*H* and the methyl signals of "*S*" isomer experienced up-field shift, more than the other isomer (Figure 3.40d).

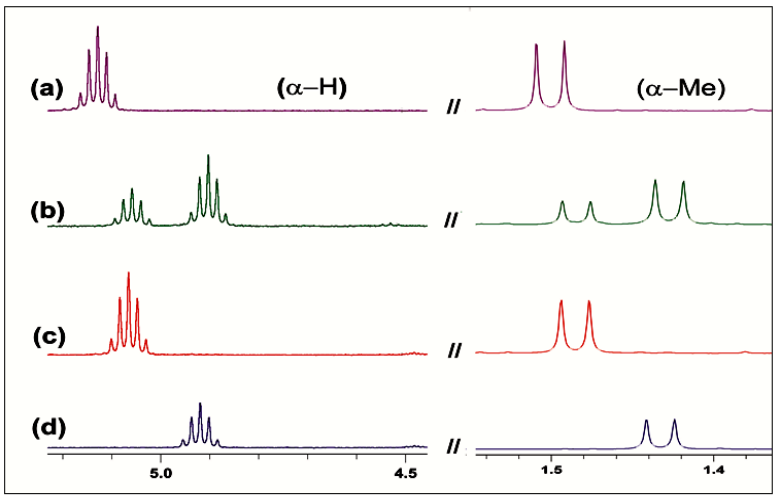

Figure 3.40 Selected region of ^{1}H NMR of **75l** in $CDCl_3$ (1:1 ratio, 10 mM): (a) blank **75l**; (b) non racemic sample of **75l** ratio of *S*:*R* [2:1] in presence of (*S*)-**50**; (c) *R*-isomer of **75l** with *S*-**50**; (d) *S*-isomer of **75l** with (*S*)-**50**.

3.IV.9 Study of Chiral Sulfoxide

The scope of the present CSA was further explored with chiral sulfoxides to determine their efficacy in recognition of the isomers. Since sulfoxides are also effective acceptors of hydrogen bonding we believe the mode of action of molecular recognition of the present CSA will be on the similar lines [36c]. Few derivatives of CSA are available to determine the enantiomer ratio by ^{1}H NMR analysis [46, 47 & 36b]. To test the efficiency we screened a sample of unsymmetrical sulfoxides **76** with (*S*)-**50** in $CDCl_3$ under the established conditions (Figure 3.41). A distinct shift of the signals of alkyl protons was observed with base line separation of the two sets of signals corresponding to the two enantiomers, but the values were on the lower side compared to the amide analytes **75**. This could be attributed to the possibility of two point hydrogen bonding in **75** rather than one point attachment in sulfoxides **76a**. For comparison, our molecule showed similar values ($\Delta\Delta\delta$ = 0.008 ppm or 3.2 Hz) compared to the **73** for separation of signals for **76a** [36b].

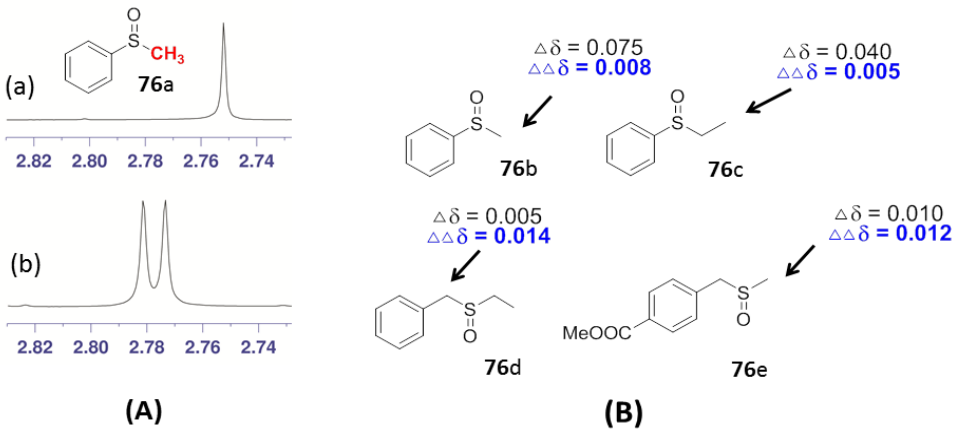

Figure 3.41: **(A)** ^{1}H NMR spectra (a) blank **76a** (b) with (*S*)-**50** **(B)** Structure of different sulphoxide and value of chemical shift nonequivalence after addition of CSA (*S*)-**50** (1:1)

Since the present CSA has worked well in differentiating the methyl phenyl sulphoxide, we further investigated application of (*S*)-**50** to check separation of signals of some other sulphoxide. All the three tested analyte showed some discrimination of signals in ^{1}H NMR (Figure 3.35).

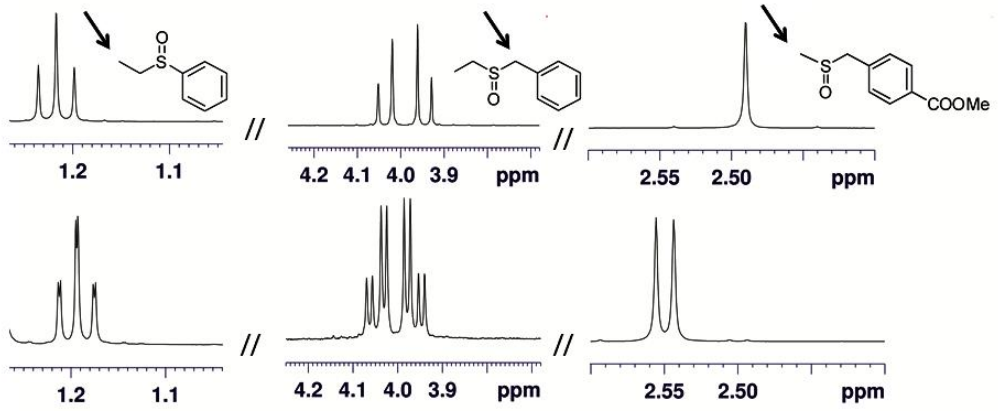

Figure 3.35: Discrimination of different sulfoxides with (*S*)-**50**.

Many optically active drugs possess sulfoxide chiral center and the activity is linked with the isomers. One of these classes of drugs is used as proton pump inhibitor to treat gastroesophageal reflux disease, peptic ulcers, erosive asophagitis and Zollinger-Ellison syndrome [48]. Omeprazole **76f** is one such active drug commercially available. We scanned (*S*)-**50** to detect discrimination of the signals in ^{1}H NMR of **76f** **(**Figure 3.42). However, the expected split for the α-protons of SOCH_2- is not observed but the aromatic methyl signals get separated with small chemical shift

nonequivalences (0.008 ppm). Although this separation and resolution is low, it is encouraging to widen the scope of the present study.

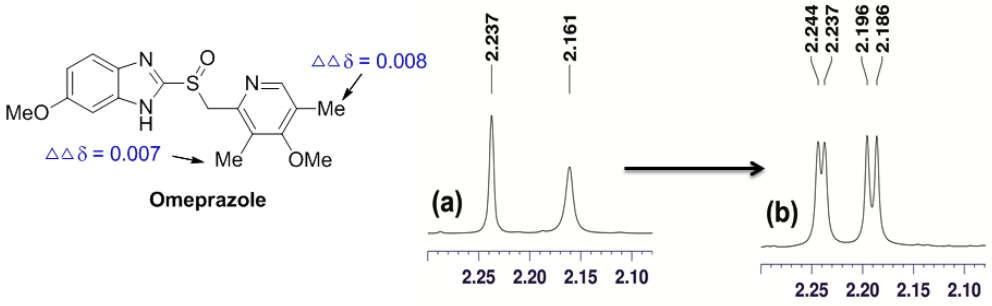

Figure 3.42: Value of discrimination of Omeprazole **76f** with (*S*)-**50** and corresponding NMR spectra. (a) blank Omeprazole (b) in presence of (*S*)-**50.**

3.IV.10 Study of Benzoin & Keto Epoxide

There were very few reports of the methods to use NMR to discriminate isomers of benzoin for analytical purpose [49]. Since our CSA has worked well in differentiating the isomers based on hydrogen bonding we scanned (*S*)-**50** with racemic benzoin **77** under similar conditions and observed small shift in the signals of the $C^{\alpha}H$ in ^{1}H NMR (Figure 3.43a). We further investigated application of (*S*)-**50** to check separation of signals in case of keto epoxide **78** a product of Darzen condensation, where the carbonyl is expected to be less polarized compared to other substrates and hence may have weaker hydrogen bonding. Although a tendency to detect the split in the signals was observed the range of the value of nonequivalence was low and there was no overlap of the signals.

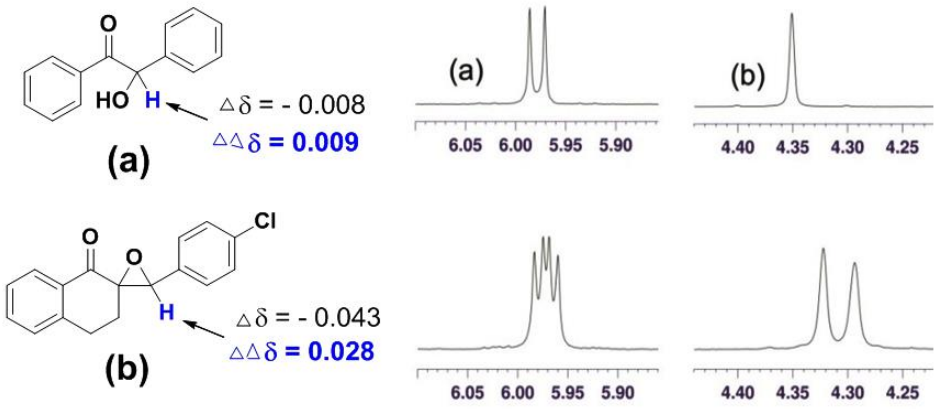

Figure 3.43: (a) Discrimination of benzoin **77** (b) Discrimination of keto epoxide **78;** with (*S*)-**50**. The top represents the select signal of the ^{1}H NMR spectra without CSA and the bottom with CSA (1:1, $CDCl_3$, 10 mM).

3.IV.11 Measurement of enantiomeric excess

To demonstrate practical utility of the present CSA for the quantitative determination of enantiomeric excess (***ee***) of **75l** pivaloyl derivative was performed. Thus different scalemic mixtures were prepared using enantiopure (*S*) and (*R*) derivative. These sample were analyzed with (*S*)-**50** by recording their ^{1}H NMR (Figure 3.45a). The experimentally measured ee were in accordance with the theoretical values as can be seen from the Figure 3.45b.

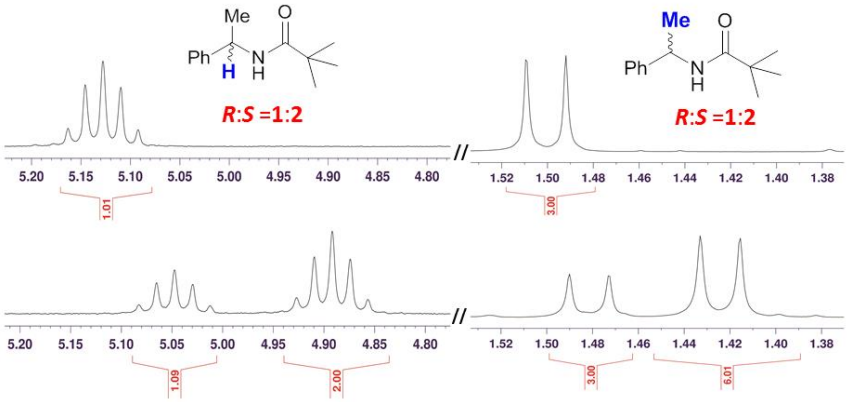

Figure 3.44 Measurement of area under two peaks of **75l**

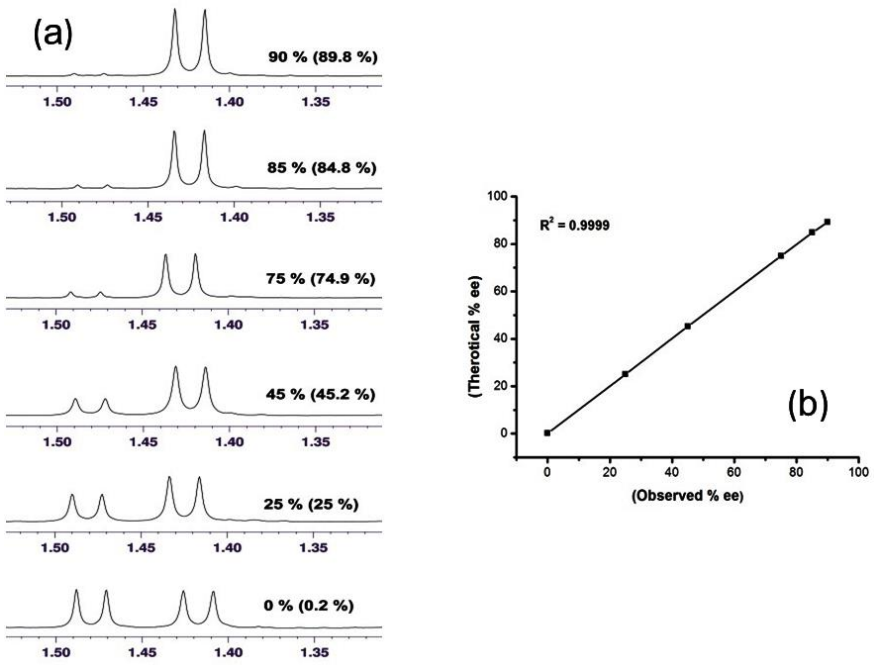

Figure 3.45: (a). Selected region of ^{1}H NMR spectra of scalemic mixture of **75l** in presence of (*S*)-**50** (b) its correlation between theoretical and observed % ee values.

3.IV.12 Study of Mandelic acid & their derivative

The use of chiral solvating agents (CSA) for determining optical purity by ^{1}H NMR analysis is emerging as a useful tool and hence we need to scan different types of analytes to explore its wider applicability. Hence we further scanned the present CSA (*S*)-**50** for α-substituted acids as they form an important class of chiral compounds. Usually the CSAs used for analyzing chiral acids are basic in nature and the mode of interactions are based on the formation of diastereomeric complex or salt with the substrates. The nature of (*S*)-**50** is neutral and hence our initial experiment of mixing only mandelic acid **54** and (*S*)-**50** in $CDCl_3$ and recording ^{1}H NMR did not result in any separation of signals, although a small degree of up field shift was recorded (Δδ = - 0.019 ppm).

The use of external base to help abstraction of acidic proton of such analytes, making the hydrogen bonding possible with the carboxylate with hydrogen bond donor bis-thiourea type CSA was reported [50]. For similar action in the present study we initially used DMAP along with (*S*)-**50** to determine if the C$^{\alpha}$*H* of mandelic acid can be distinguished in ^{1}H NMR. Indeed the C$^{\alpha}$*H* proton is observed to shift much upfield and two distinct singlets were seen for the two isomers (Table 3.19, entry 1).
Further improved resolution was observed when the base is replaced with DABCO, with equimolar quantity and even better separation with excess of CSA (Table 3.19, entry 3).

Table 3.19 Chemical shift non-equivalence of **54** in presence of (S)-**50** and external Base

No.	Acid	CSA (eq.)	Base (1 eq.)	ArC***H***(OH)COOH Δδ	ΔΔδ
1	Mandelic acid **54**	1.0	DMAP	-0.278	0.022
2	**54**	1.0	DABCO	-0.384	0.040
3	**54**	2.0	DABCO	-0.425	0.047

Number of derivative of α-hydroxy aryl acetic acids, **55** to **58**, were scanned to establish generality of the analysis (Table 3.20, Figure 3.26).

Table 3.20: Study of CSA activity of (*S*)-**2** for α-hydroxy/alkoxy acids.

No	α-hydroxy/alkoxy acid	CSA (eq.)	Base (1 eq.)	ArC***H***(OH)COOH Δδ	ΔΔδ
1	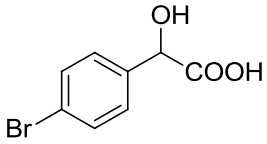	2.0	DABCO	-0.430	0.056
2	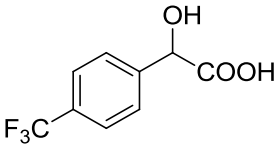	2.0	DABCO	-0.402	0.030
3	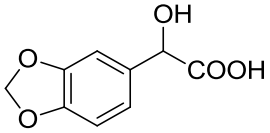	2.0	DABCO	-0.441	0.048
4	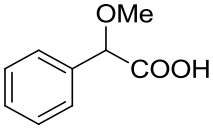	2.0	DABCO	-0.250	0.066

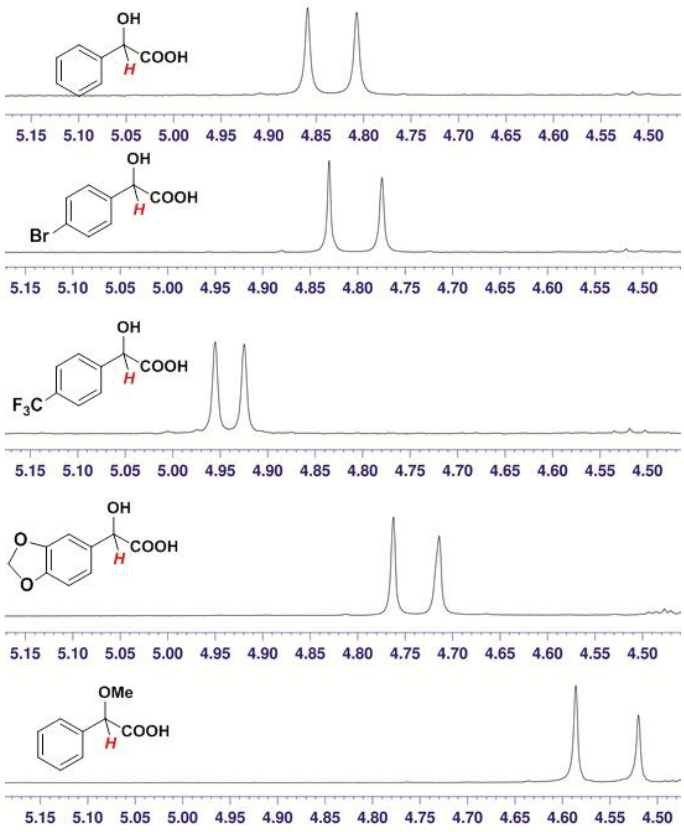

Figure 3.46: Selected region of ^{1}H-NMR spectra in presence of (*S*)-**50 &** DABCO in $CDCl_3$ **(a)** with **54** (b) **55** (c) **56** (d) **57** (e) **58.**

An example of α-chloro phenyl acetic acid **79** was also scanned with good separation (Figure 3.47). All these molecules showed a clear base line separation of the $C^{\alpha}H$ signals for practical and accurate determination of optical purity.

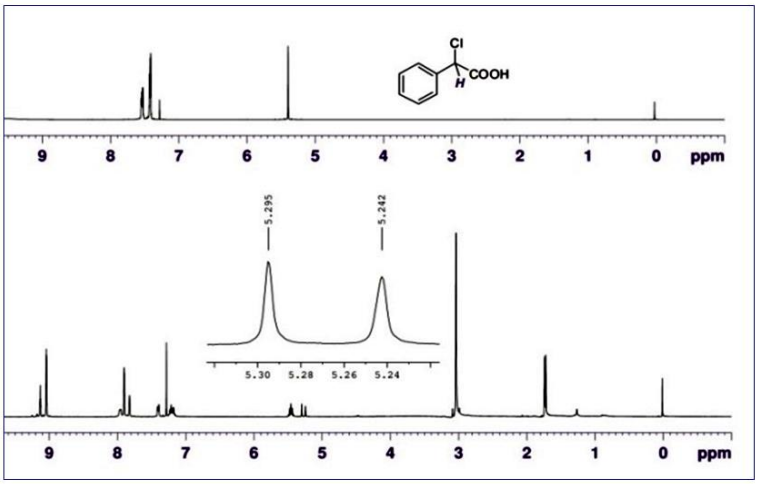

Figure 3.47: ^{1}H NMR spectra of **79** (top); in presence of DABCO and (*S*)-**50** (bottom).

3.III.13 Study of N-Protected Phenyl Glycine

Natural and unnatural amino acids in optically pure form are important intermediates in the synthesis and study of bioactive molecules. We further extended the scope of our reagent (*S*)-**50** to scan for differently *N*-protected phenyl glycine as a test case. The effectiveness is general for some commonly used derivatives of this amino acid **80** (Table 3.21).

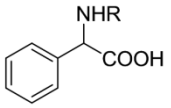

80a-c

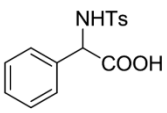

60

Table 3.21: Study of CSA activity for the derivatives of *N*-protected phenyl glycine **80**.

No	R	ArC***H***(NHR)COOH	
		Δδ	ΔΔδ
1	$COCH_3$ **80**a	-0.565	**0.038**
	(CH_3)	[-0.003][a]	**[0.071][a]**
2	COPh **80**b	-0.526	**0.030**
3	Boc **80**c	-0.284[b] [Cα-H_1]	**0.071[b] [Cα-H_1]**
		-0.409[b] [Cα-H_2]	**0.101[b] [Cα-H_2]**
4	Ts **60**	-0.490	**0.065**

[a]For $COCH_3$; [b]For the two rotamers.

3.III.14 Study of alkyl aryl acetic acid and drug intermediate

The importance of chiral drugs in medicinal chemistry is now a well established phenomenon. In the present work we have scanned our CSA (*S*)-**50** for some chiral drugs and drug intermediates. Non steroidal anti-inflammatory agents such as ibuprofen **68**, ketoprofen **81** and flurbiprofen **82** are some of the important chiral drugs. These α-alkyl aryl acetic acids showed significant baseline splitting of signal of $C^{\alpha}H$ in ^{1}H NMR analysis (Table 3.22, Figure 3.48).

Table 3.22: Study of CSA activity of (*S*)-**50** for α-hydroxy/alkoxy acids.

No	α-hydroxy/alkoxy acid	CSA (eq.)	Base (1 eq.)	ArC*H*(OH)COOH Δδ	ΔΔδ
1	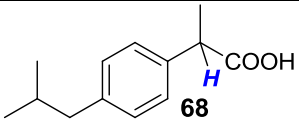 **68**	1.0	DABCO	-0.179	0.049
2	**68**	2.0	DABCO	-0.216	0.075
3	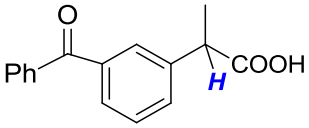	2.0	DABCO	-0.217	0.048
4	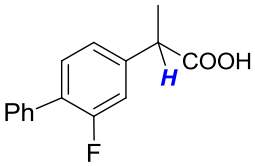	2.0	DABCO	-0.0	0.068
5	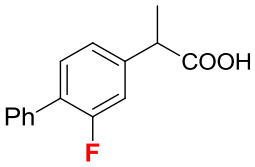	2.0	DABCO	-0.0	0.030
6	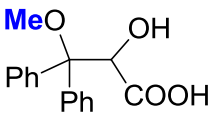	2.0	DABCO	-0.0	0.011
7	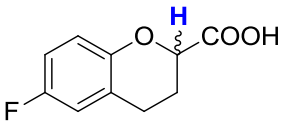	2.0	DABCO	-0.0	0.071
8	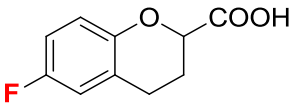	2.0	DABCO	-0.0	0.10

All NMR recorded at 400 MHz in $CDCl_3$ at 10 mM with indicated amount of DABCO.

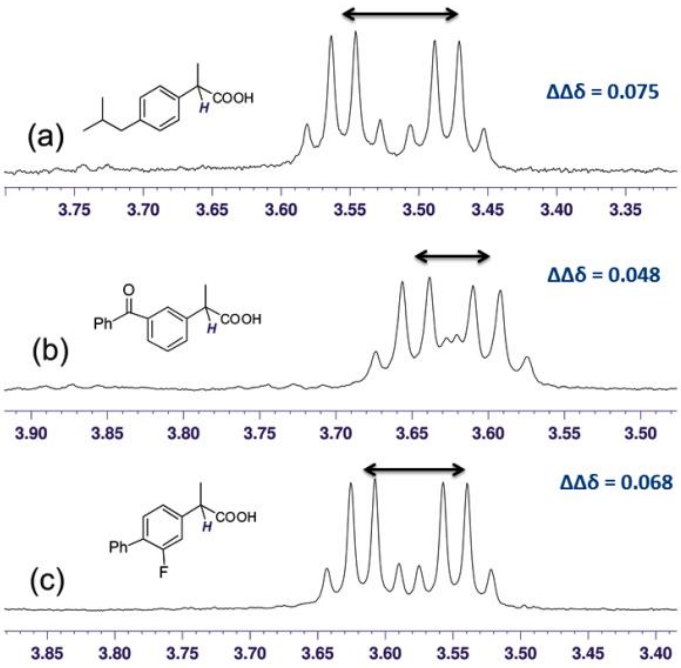

Figure 3.48: Selected region of ^{1}H-NMR spectra in presence of (*S*)-**50 &** DABCO in $CDCl_3$ (a) 68 (b) 81(c) 82

The separation of signals in ^{19}F NMR in flurbiprofen is also observed in case of **82** chemical shift nonequivalence (ΔΔδ) was 0.08 (Figure 3.49).

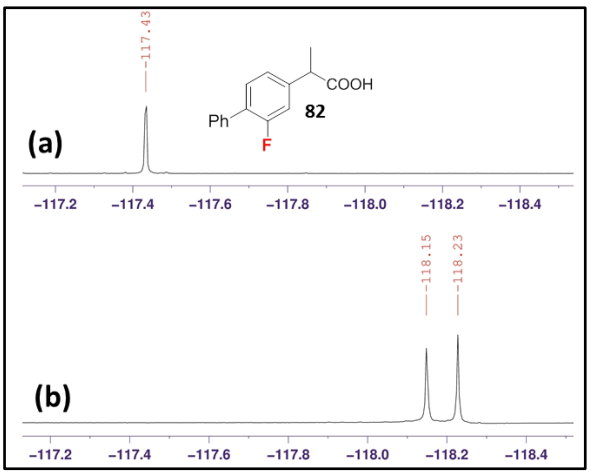

Figure 3.49: ^{19}F NMR spectra of flurbriprofen (a) blank (b) with (*S*)-**50** and DABCO

We extend the study with the analysis of **83**, an intermediate of nebivolol [51] a β blocker agent. In this candidate we could observe very good separation of signals of $C^{\alpha}H$ in ^{1}H NMR (ΔΔδ is 0.071) along with separation of signals in ^{19}F NMR (ΔΔδ is 0.10) (Figure 3.50**b**).

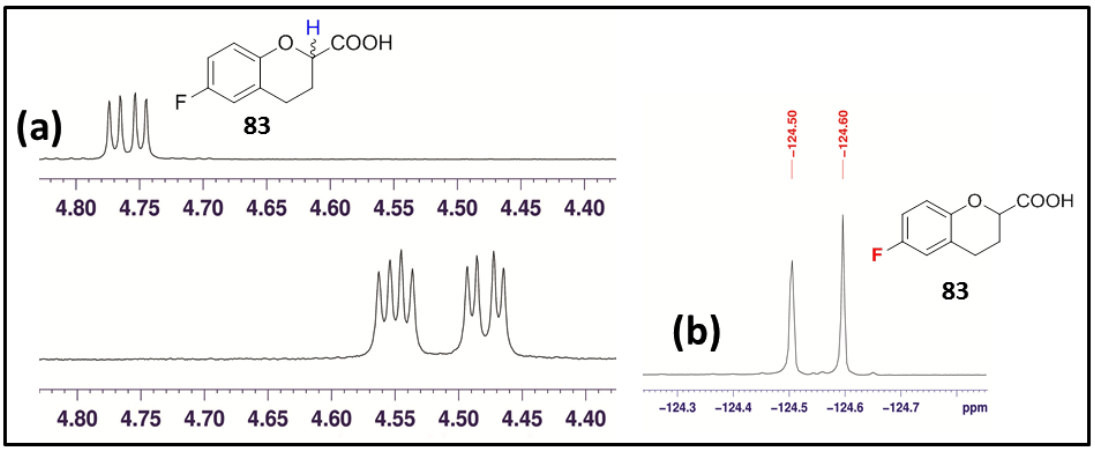

Figure 3.50: (a) Selected region of ^{1}H-NMR spectra **83** [top] in presence of (*S*)-**2 &** DABCO in $CDCl_3$[bottom] (b)^{19}F NMR spectra of **83** in presence of (*S*)-**50** & DABCO

3.III.15 Roof shape Kagan type ligand and their study

Encouraged by result obtained by modified fluorinated Kagan type ligand we also screened roof shape Kagan ligand for various amides, but no discrimination was observed in this modification. We subsequently tested roof shape Kagan type ligand for various the amides and sulphoxide in ^{1}H-NMR spectroscopy but no discrimination was achieved.

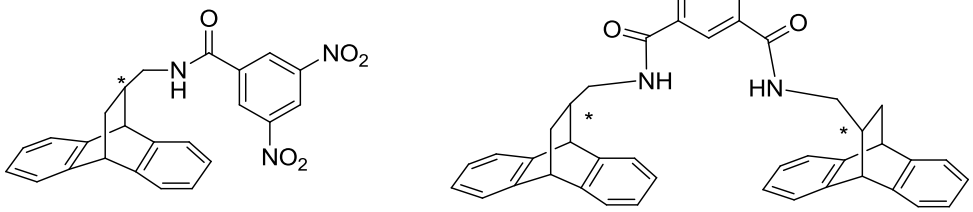

Part II

3.III.16 NMR spectroscopic methods, which depend on a chiral auxiliary such as chiral derivatization agent (CDA), chiral lanthanide shift reagents (CLRS) and chiral solvating agents (CSA) have been discussed in section I. These methods are widely studied for chiral discrimination, measurement of enantiomeric excess and for determination of absolute configuration. In case of CSA, temporary formation of diastereomers with enantiomerically pure reagents results in nonequivalence of the chemical shifts of the protons of the two enantiomers of the analyte. This technique has the distinct advantages of simplicity, more accurate analysis compared to CDA and CLSR. It involves non-covalent interactions between analyte and optically pure molecule of CSA. The efficiency of CSA to recognize two isomers of analyte depends on noncovalent interaction such as Hydrogen bonding, π- π, CH- π charge transfer, and ion-pair interaction. The success of this technique depends on the proper combination of non-covalent interactions between the two partners of the complex.

The recognition properties of CSA can be fine-tuned by introduction of different functionality or group in the structure of CSAs which can consolidate the noncovalent interaction. Thus, even though a large number of CSAs are available, there is a need to design more molecules which can be readily prepared in enantiomerically pure form, while they may be more efficient in chiral discrimination of molecules with diverse functionality. Among different class of compounds of CSAs, amides are especially suited to be used as CSAs as they possess definite and directional nature of noncovalent interactions with substrate. The extent of chemical shift separation between the diastereomeric peaks achieved in the proton spectrum may also depend on the proximity of the non-equivalent interaction such as hydrogen bonding [45]. The chiral Kagan's amide and its ability to discriminate chiral analytes has been discussed earlier, where the beneficial effect of the presence of electron withdrawing group (Figure 3.51, Ring A) has also been elaborated.

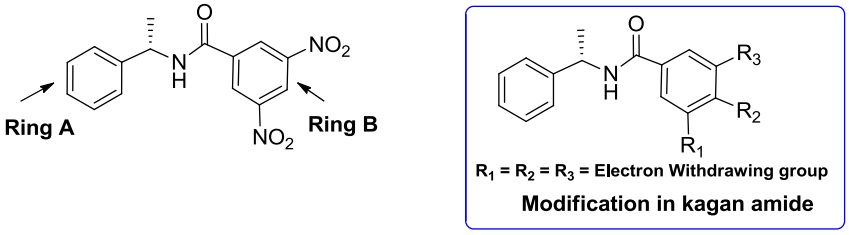

Figure 3.51: Structure of Kagan amide (*S*)-**73** and it`s modification in aromatic ring B

Since our continuation of chiral amide work, here we disclose another modification in Kagan`s amide. To perform systematic studies on substituent studies (Ring B) in the structure of Kagan amide, three different amides containing electron withdrawing group were designed and prepared by simple condensation of (*S*)-α-methylbenzylamine and suitable acid chlorides **84** in presence of a triethylamine as base (Scheme 3.1) in dichloromethane.

Scheme 3.1: Synthesis of amide derivative

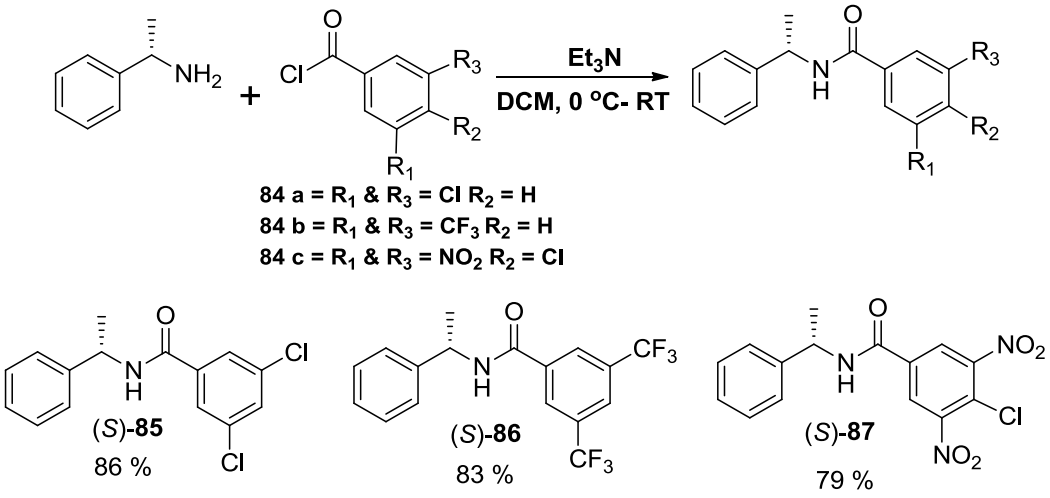

Although Kagan's amide **73** and its modification has been used as a probe to resolve signals of compounds containing sulphoxide, amide and amine. The present set of CSAs, was systematically screened to determine their efficiency to discriminate the isomers PhSO*CH*$_3$ and PhC*H*(*CH*$_3$NHCOC(CH$_3$)) by recording the separation of signals by ^{1}H NMR analysis. The chemical shift nonequivalence values are summarized in Table 3.23.

Scheme 3.2 Chemical structure of analyte and discriminated protons are marked in the structure

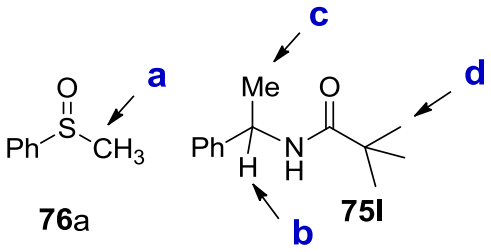

These three derivatives have strong electron withdrawing group attached on the acid

component of the amides. The chemical shift nonequivalence value for (*S*)-**85** and (*S*)-**86** were less than (*S*)-**87** (Figure 3.52). In case of (*S*)-**87** the value of chemical shift equivalence was higher as compared to kagan amide (*S*)-**73** (Table 3.23, entry 1 & 4).

Table 3.23: Comparison of CSA activity of (*S*)-85, (*S*)-86, (*S*)-87 for proton a, b, c, d

No	CSA	$ArSOCH_3$(**76**a)		ArCHMeNHCOR(**75**l)	
		ΔΔδ (a)	**ΔΔδ (b)**	**ΔΔδ (c)**	**ΔΔδ (d)**
1	(*S*)-**73**	0.008	0.061	0.023	-NR-
2	(*S*)-**85**	0.003	-NR-	0.010	-NR-
3	(*S*)-**86**	0.004	0.006	0.003	-NR-
4	(*S*)-**87**	**0.012**	**0.097**	**0.035**	-NR-

[a]Not resolved. R = tBu ^{1}H NMR recorded in $CDCl_3$ in 1:1 ratio (400 MHz).

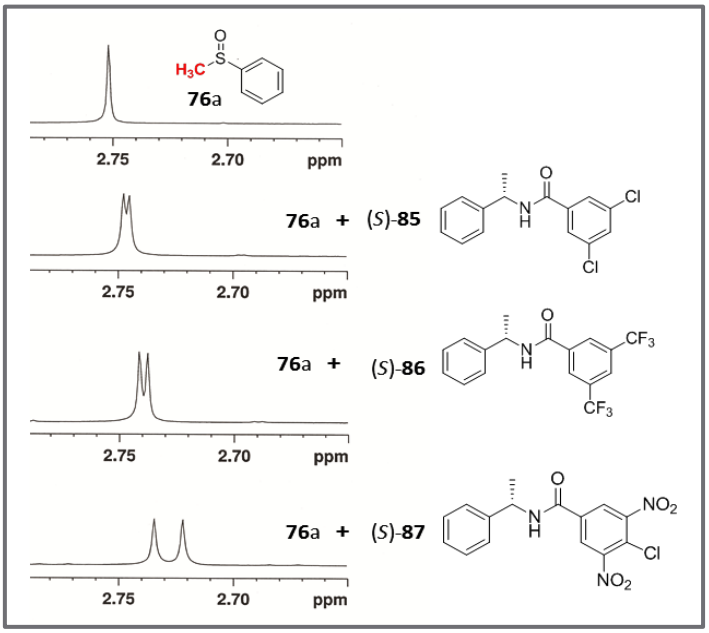

Figure 3.52: ^{1}H NMR spectra of 76a in presence of different amide ligand

The level of CSA activity of (*S*)-**85** and (*S*)-**86** seems quite low, when compared to the results of Kagan amide (*S*)-**73**. In case of (*S*)-**87** CSA activity of these modified amides have higher as compare to (*S*)-**73**. With reasonable confidence we have concluded that introduction of chlorine at para position along with 3,5 dinitro units enhance the CSA activity of chiral amide. We therefore decided to introduce 4-chloro, 3,5-dintro group in to our previously modified amide (*S*)-**50**. For systematic studies we have also introduced this modification in to naphthalene based ligand reported earlier (Scheme 3.4).

Scheme 3.3: Structure of Modified kagan amides (Modification in Ring A)

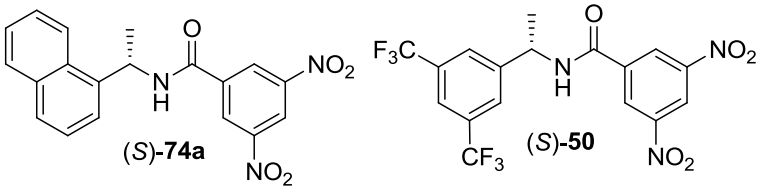

Scheme 3.4: Synthesis of (*S*)-**88** & (*S*)-**89**

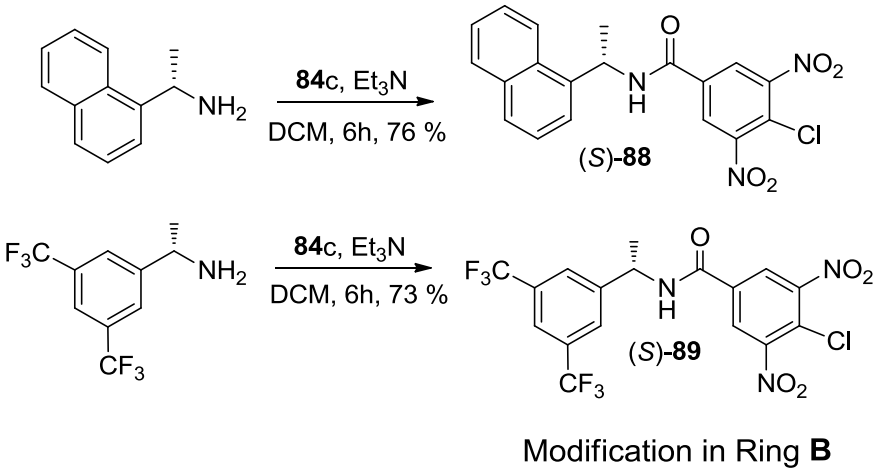

Scheme 3.5: Proposed modification in kagan type CSAs.

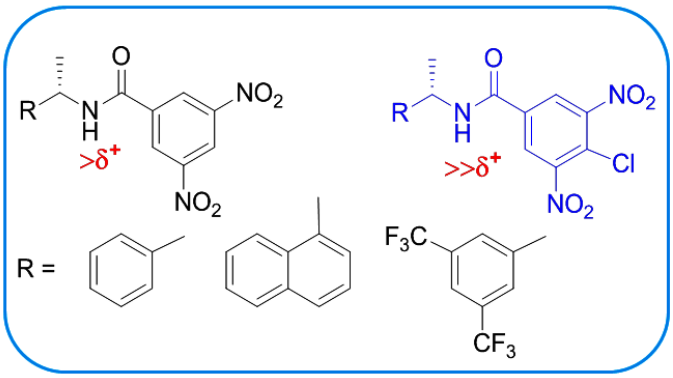

The beneficial effect of the presence of 4-chloro along with 3,5-dinitro functionality in amide structure is that it reduces electron density at the nitrogen, consequently increasing the hydrogen bond strength for effective interactions (Scheme 3.5). This phenomenon was further confirmed by comparing –NH signal in ^{1}H NMR spectra (Figure 3.53). The –NH signal of Kagan`s amide appear at 6.94-6.92 which shifts to upfield region 6.62-6.60 with chloro substitution. Similar trends were also observed

with other two modifications where hydrogen of amide group showed displacement to lower chemical shift (for 1-napthyl 6.95-6.93 to 6.70-6.68 and for 3,5-bis(trifluoromethyl)phenyl 6.91-6.89 to 6.67-6.65). The change in chemical shifts of –NH signals indicate that electron density on the nitrogen of the amide group decrease hence signals were shifted to upfield region. The role of different substituent for effective hydrogen bonding was discussed in literature [52].

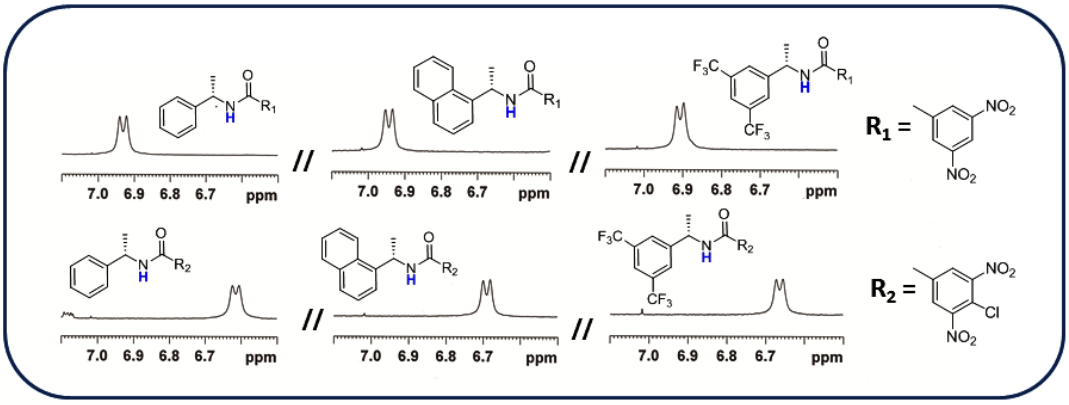

Figure 3.53: Selected region of ^{1}H NMR spectra (top) –NH signal of amide where R_1 is 3,5 dinitro; (bottom) –N**H** signal of amide where R_2 is 4-chloro 3,5-dinitro.

Having prepared two other derivative of modified CSAs (*S*)-**88** and (*S*)-**89,** we next screened them to test their ability to discriminate the signals of sulphoxide PhSO*CH*$_3$ **76**a (Figure 3.54) and amide PhC*H*(C*H*$_3$NHCOC(C*H*$_3$)$_3$) **75**l (Figure 3.55) analyte. It was observed that introduction of chlorine at para positions (Ring B) along with two nitro group at 3, 5 positions enhance the chemical shift nonequivalence (Table 3.24).

It was previously proposed that analyte such as sulphoxide and amide interacts with amide base CSA through -N-H·····O=X (X= C or S) type interaction and forms intermolecular hydrogen bonding, subsequently, other non-covalent interactions such as π-π and CH-π stabilize the complex. Considering the fact that –NH of amide CSA work as hydrogen bond donor, introduction of chlorine group strengthen the H –bond donor ability. This interaction gets intensified because, –NH of CSA acquire more ++δ character for more effective interactions. This hypothesis was then tested by comparing chemical shift separations (ΔΔδ) for previously reported known data of 3,5-dintro based amide ligand and 4-chloro-3,5-dintro amide ligand. Increase in chemical shift nonequivalence (nearly 1.75 to 2 fold enhancement) was observed for the signals supports this concept. It was found to be more effective with reasonably

better value of chemical shift non- equivalence observed compared to (*S*)-**74a** and (*S*)-(*S*)-**50**. Although the value for (*S*)-**88** are higher as compare to (*S*)-**89** but in case of (*S*)-**89** with analyte **75**l three different proton were split with baseline resolution. The analysis will be more accurate if it is confirmed by checking the ratio of more than one protons of the sample. Such types of observations are useful to examine different signals, which shift on the addition of CSA for more effective analysis of the analyte.

Table 3.24: Comparison of chemical shift nonequivalence

No	CSA	ArSO$\underline{CH_3}$(**76**a)	ArC$\underline{H}$Me$\underline{N}$HCOR(**75**l)		
		ΔΔδ (a)	**ΔΔδ (b)**	**ΔΔδ (c)**	**ΔΔδ (d)**
1	(*S*)-**74a**	0.014 (5.6 Hz)	0.141 (56.4 Hz)	0.049 (19.6 Hz)	-NR-
2	(*S*)-**88**	**0.030 (12.0 Hz)**	**0.282 (112.8 Hz)**	**0.102(40.8 Hz)**	**-NR-**
3	(*S*)-**50**	0.008 (3.4 Hz)	0.156 (62.4 Hz)	0.057(22.8 Hz)	0.017(6.8Hz)
4	(*S*)-**89**	**0.013 (5.2 Hz)**	**0.250 (100.0 Hz)**	**0.085(34.0 Hz)**	**0.013(5.2Hz)**

All NMR are recorded in $CDCl_3$ in 1:1 ratio, 400MHz

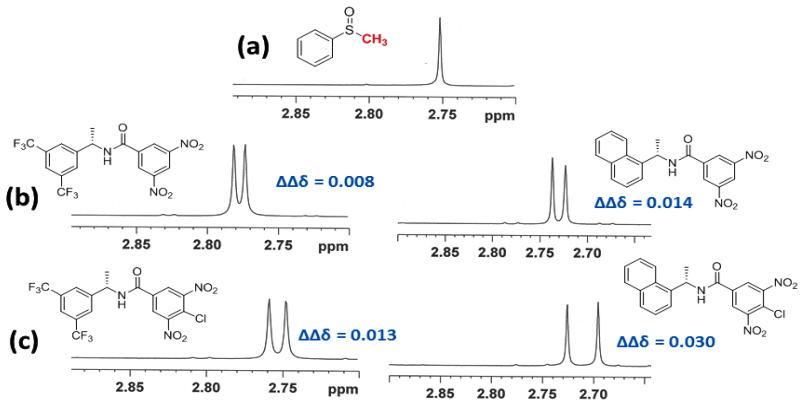

Figure 3.54: Selected region of ^{1}H NMR of **76a** in $CDCl_3$ (a) blank **76a**; (b) racemic sample of **76l** in presence of (*S*)-**50** and (*S*)-**74**a (c) in presence of (*S*)-**88** and (*S*)-**89.**

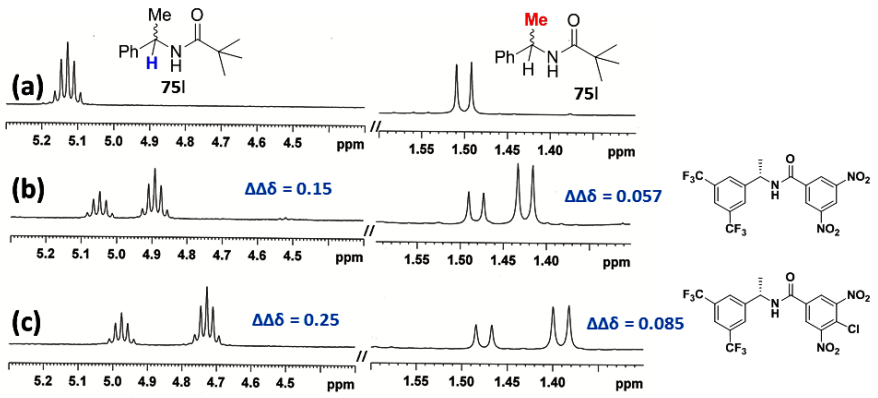

Figure 3.55: Selected region of ^{1}H NMR of **75l** in $CDCl_3$ (a) blank **8l**; (b) non racemic sample of **75l** ratio of *S*:*R* [2:1] in presence of (*S*)-**50**; (c) in presence of (*S*)-**89**

Chart 4.1 Comparison of different amide ligand

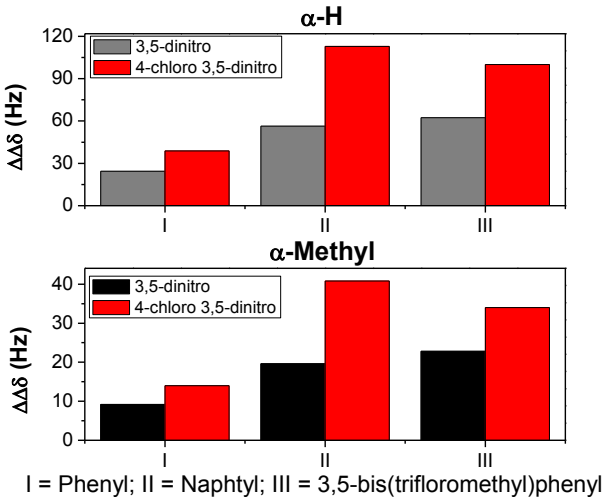

From Chart 4.1 it is clear that beneficial effect of chlorine at *para* position of carbonyl aromatic ring enhance the performance of amide ligand. The resolved signals of analytes remain sharp upon complexation with this chiral amide, which demonstrates that a hydrogen bond-based reagent is suitable for precise measurement of enantiomeric excess.

In view of this observation, we also screened keto epoxide **78** with chlorine substituted modified amide and result are summarised in Table 3.24.

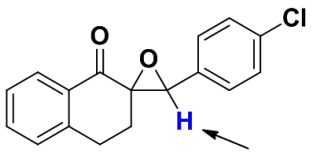

78

Table 3.24: Comparison of chemical shift nonequivalence

No	CSA	**78 ΔΔδ**
		α-H
1	(*S*)-**73**	0.019
2	(*S*)-**87**	**0.023**
3	(*S*)-**74a**	0.029
4	(*S*)-**88**	**0.053**
5	(*S*)-**50**	0.028
6	(*S*)-**89**	**0.044**

All NMR are recorded in $CDCl_3$ in 1:1 ratio.

In conclusion, we have demonstrated that introduction of chlorine alter the electron densities around hydrogen bonding sites which cause enhancement in chiral recognition property.

Experimental

N-(1-(3,5-bis(triflouromethyl)phenyl)ethyl)-3,5-dinitrobenzamide: (*S*)-**85**

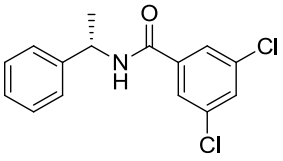

White solid (86%). M.p = 162 ^{o}C

^{1}H-NMR (400 MHz, $CDCl_3$): δ 1.63-1.61 (d, *J* = 7.2 Hz, 3H), 5.27-5.34 (m, 1H) 6.34-6.35 (d, *J* = 6.8 Hz, 1H), 7.31-740 (m, 4H), 7.48-7.49 (t, 1H, 1.6 Hz), 7.63-7.64(d, 1.6 Hz).

^{13}C-NMR (100 MHz, $CDCl_3$): δ 21.5, 49.7, 125.7, 126.3, 127.6, 128.8, 131.3, 135.3, 137.4, 142.5, 164.2.

IR (KBr): υ 3271, 3089. 1639, 1577, 1452, 1385, 1274, 1130, 909, 700 cm.$^{-1}$

N-(1-(3,5-bis(triflouromethyl)phenyl)ethyl)-3,5-dinitrobenzamide: (*S*)-**86**

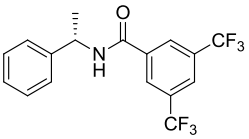

White solid (83 %). M.p = 110 ^{o}C

^{1}H-NMR (400 MHz, $CDCl_3$): δ 1.68-1.67 (d, *J* = 7.2 Hz), 5.33-5.40 (m, 1H) 6. 43-6.42 (d, *J* = 6.8 Hz, 1H), 7.31-7.44 (m, 5H) 8.01 (s, 1H), 8.22 (s, 2H).

^{13}C-NMR (100 MHz, $CDCl_3$): δ 21.4, 49.9, 118.8 (q, $J_{C\text{-}F}$ = 271.0 Hz), 124.2 (septet, $J_{C\text{-}F}$ = 4.4 Hz), 126.2, 126.9, 127.4, 126. 6, 128.7, 131.4 (q, $J_{C\text{-}F}$ = 34.0 Hz), 134.5, 142.4, 163.9.

IR (KBr): υ 33332, 3068, 1630, 1566, 1276, 1092, 804 cm.$^{-1}$

(*S*)-4-chloro-3,5-dintro-N-(1-phenylethyl)benzamide: (*S*)-**87**

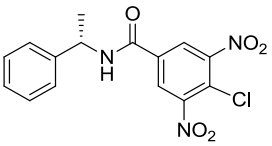

White solid (79 %) M.p = 199-200 ^{o}C

^{1}H-NMR (400 MHz, $CDCl_3$): δ 1.65-1.67 (d, *J* = 7.2 Hz, 3H), 5.27-5.35 (m, 1H) 6.60-6.62 (d, *J* = 6.8 Hz, 1H), 7.28-7.40 (m, 5H), 8.38 (s, 1H).

^{13}C-NMR (100 MHz, $CDCl_3$): δ 21.3, 50.3,123.2, 126.1, 126.3, 128.1, 128.9, 134.9, 141.7, 149.5, 161. 2.

IR (KBr): υ 3278, 3069, 1637, 1542, 1334, 1063, 919 cm.$^{-1}$

(*S*)-4 chloro-N-(1-napthalen-1-yl)ethyl)-3,5-dintrobenzamide: (*S*)-**88**

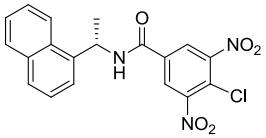

Yellow solid (76%). M.p = 232-235 ^{o}C

^{1}H-NMR (400 MHz, $CDCl_3$): δ 1.75-1.77 (d, *J* = 6.8 Hz, 3H), 5.99-6.06 (m, 1H) 6.68-6.69 (d, *J* = 7.6 Hz, 1H), 7.46-7.57 (m, 4H), 7.84-8.00 (s, 3H), 8.33 (s, 2H).

^{13}C-NMR (100 MHz, $CDCl_3$): δ 20.4, 45.9, 122.7, 122. 8, 123.3, 125.2, 126.2, 127.0, 128.9, 129.0, 130.8, 133.8, 134.5, 136.8, 149. 3, 160. 9.

IR (KBr): υ 3319, 3050, 1624, 1522, 1348, 1274, 1111, 777 cm.$^{-1}$

(*S*)-*N*-(1-(3,5-bis(triflouromethyl)phenyl)ethyl)-4-chloro)-3,5-dintrobenzamide: (*S*)-**89**

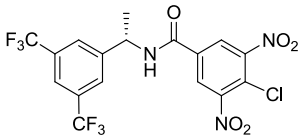

White solid (73%). M.p = 218-19^{o}C

^{1}H-NMR (400 MHz, $CDCl_3$): δ 1.72-1.74 (d, *J* = 6.8 Hz, 3H), 5.39-5.46 (m, 1H) 6.67-6.65 (d, *J* = 7.2 Hz, 1H), 7.85, (s, 3H), 8.43 (s, 1H).

^{19}F-NMR (376 MHz, $CDCl_3$): δ -62.79.

^{13}C-NMR (100 MHz, $CDCl_3$): δ 21.5, 49.8, 122.1 (sep, $J_{C\text{-}F}$ = 4.0 Hz), 122.8 (q, $J_{C\text{-}F}$ = 270.0 Hz), 126.2, 126.6, 132.3 (q, $J_{C\text{-}F}$ = 34 Hz), 134.1, 144.6, 149.6, 161.3.

IR (KBr): υ 3262, 1650, 1546, 1380, 1292, 1175, 1131, 900 cm.$^{-1}$

HRMS (ESI+) m/z calculated for $C_{17}H_{10}F_6NO$ $[M+Na]^+$ 508.0105, found 508.0099.

Conclusion

- In this chapter we have explored roof shape amine and diamine as Chiral Solvating Agents for discrimination of enantiomers of several α-functionalized acids.
- We have observed supramolecular interactions such as π– π, CH-π, acid-base, H-bonding and some steric factors playing role in the recognition of the chiral substrates with CSAs.
- We have screened a number of different α-functionalities and studied their correlation with the ability of discrimination, in some cases we have noted four different types of hydrogens being affected in the ^{1}H NMR although they were remote from stereogenic carbon.
- We have also recorded the recognition by employing other NMR active nuclei ^{13}C, ^{19}F, ^{31}P to determine the CSA efficiency of the chiral roof shape amines.
- We have developed a modified derivative of Kagan's amide capable of distinguishing the protons of the enantiomers in simple ^{1}H NMR experiments.
- We have demonstrated the improved ability of (*S*)-**50** to accurately detect protons of a wide variety of compounds of type amides, sulfoxides, benzoin, α-substituted aryl acetic acids and some drug and drug intermediate with good to excellent separations.
- The proposed mode of the action of recognition of chiral isomers of analytes by CSA is based on hydrogen-bonding.
- Furthermore, conditions are also standardized for quantitative determination of the ratio of enantiomers in the controlled experiment, which opens up possibilities for this technique to be used for determination of *ee* of unknown sample.
- The study of noncovalent interaction such as hydrogen bonding in the amide compound explored by NMR. Introduction of chlorine at para position in kagan amide enhance the chemical shift nonequivalence.

Spectral chart

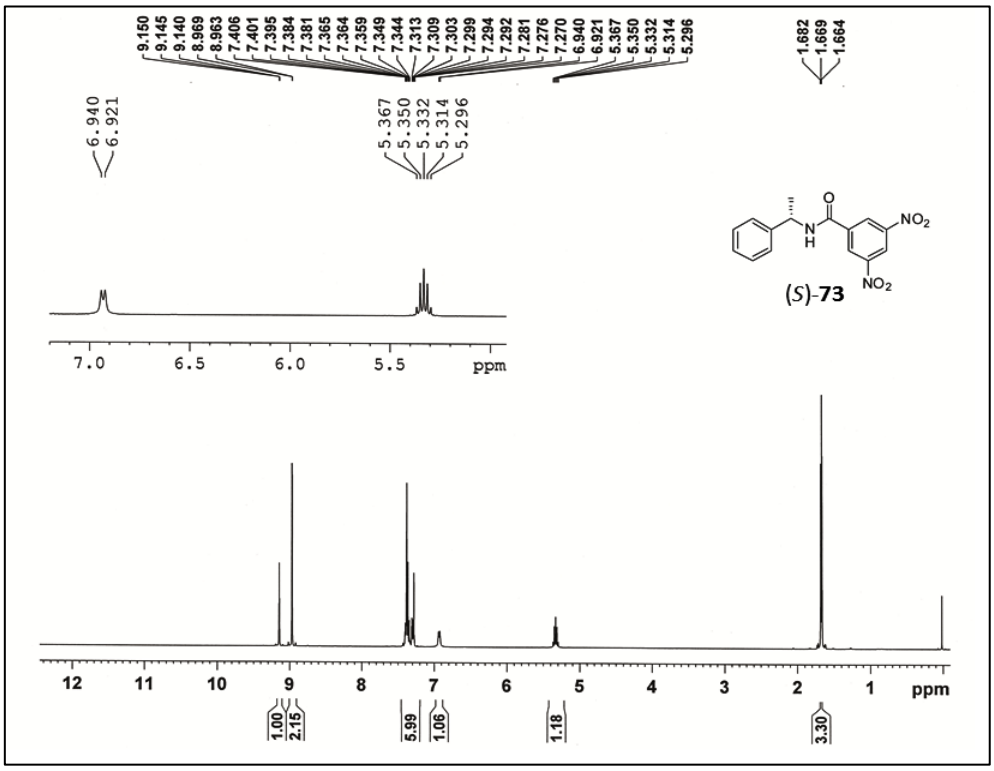

^{1}H NMR spectra of compound (*S*)-73

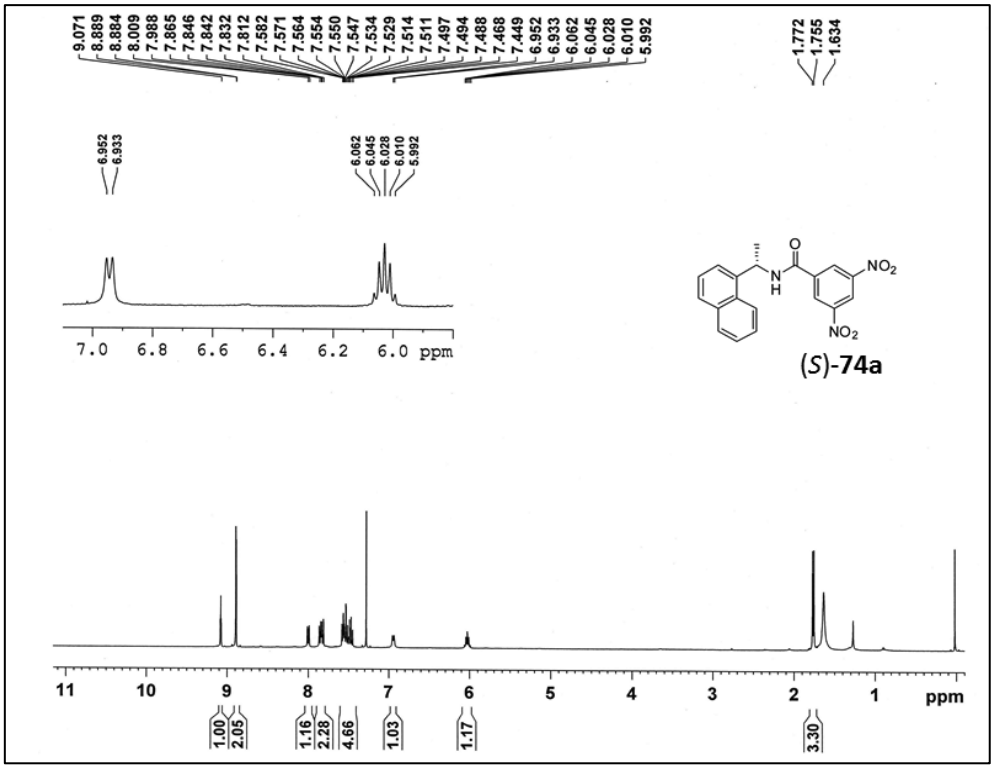

^{1}H NMR spectra of compound (*S*)-73

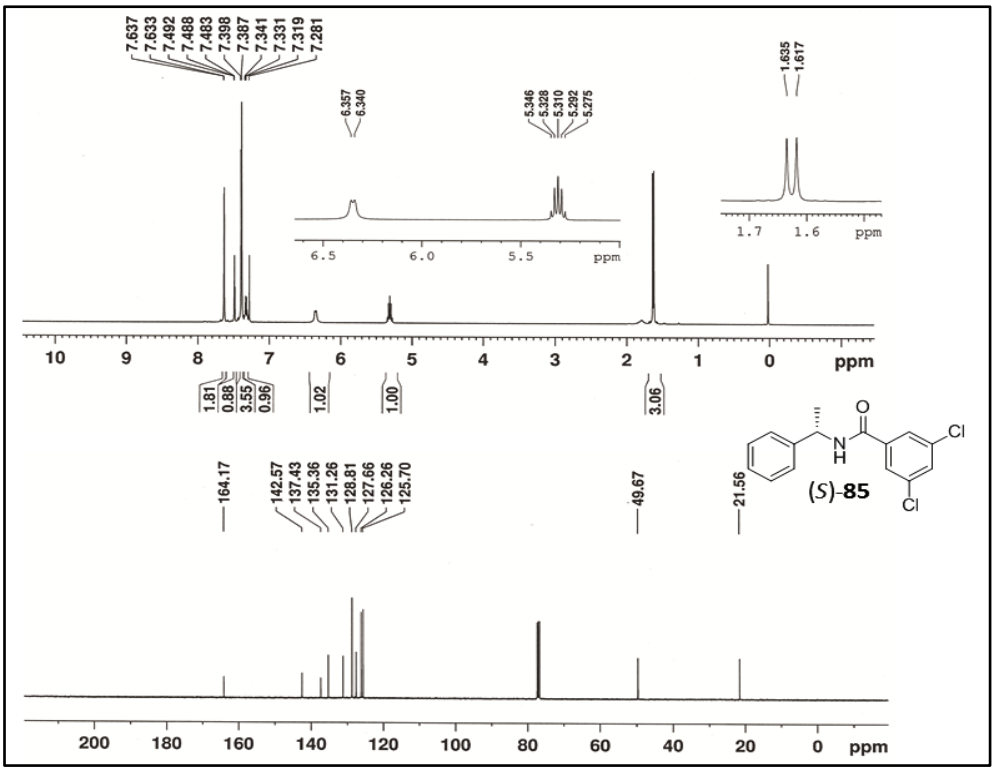

^{1}H NMR & ^{13}C NMR of compound (*S*)-85

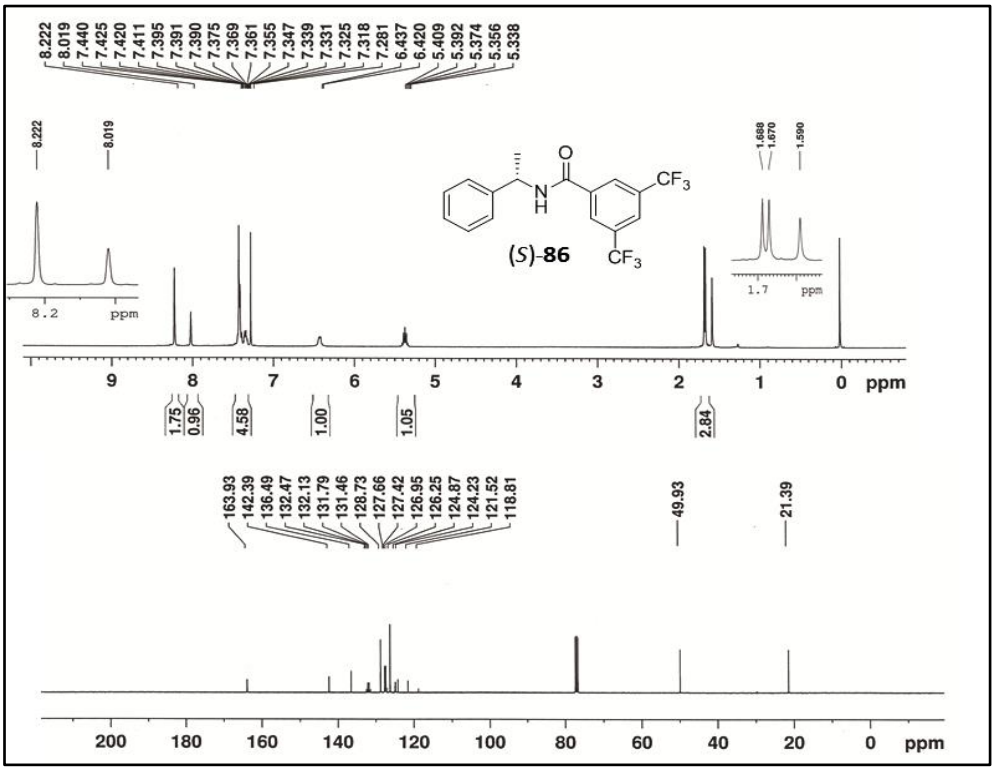

^{1}H NMR & ^{13}C NMR of compound (*S*)-86

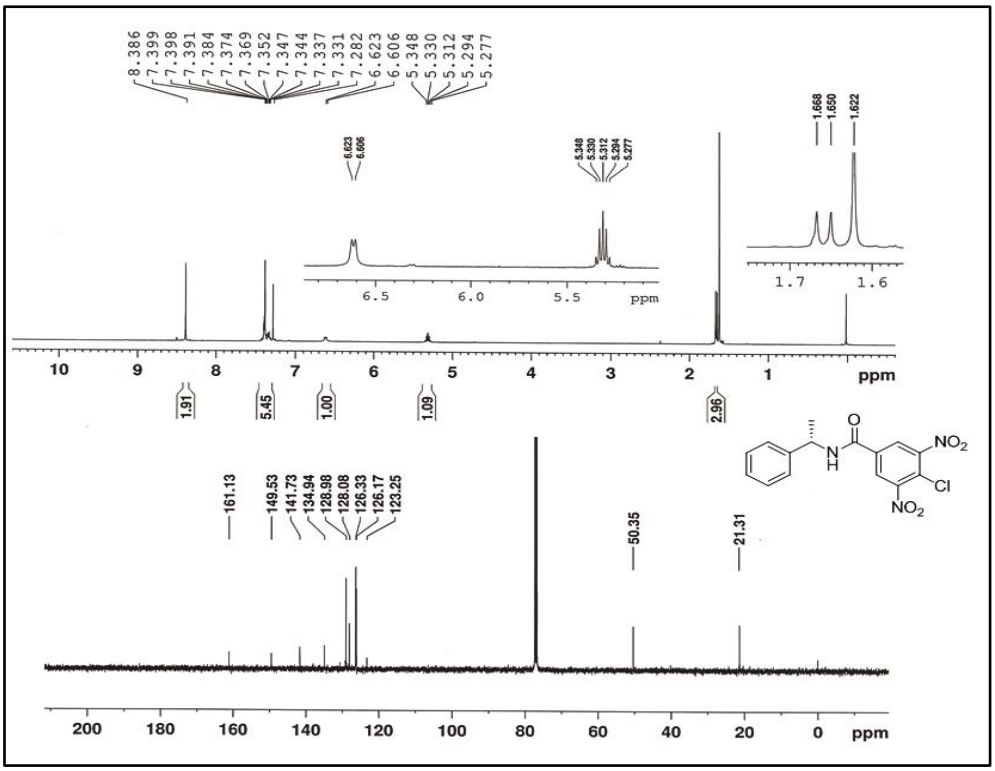

^{1}H NMR & ^{13}C NMR of compound (*S*)-87

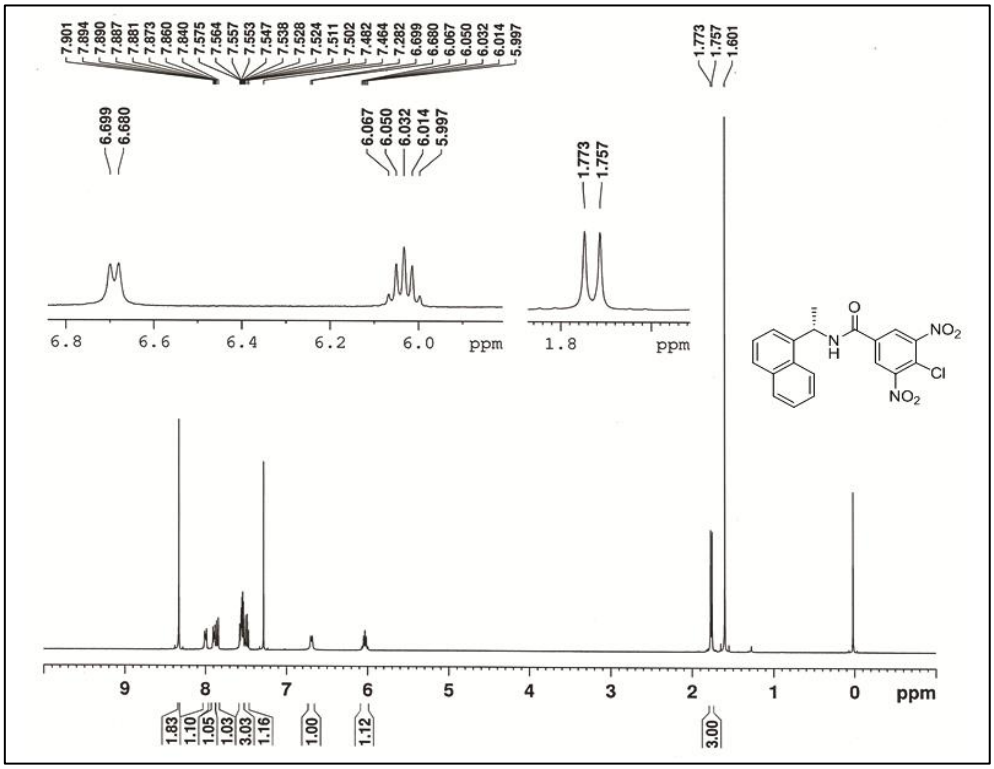

^{1}H NMR of compound (*S*)-88

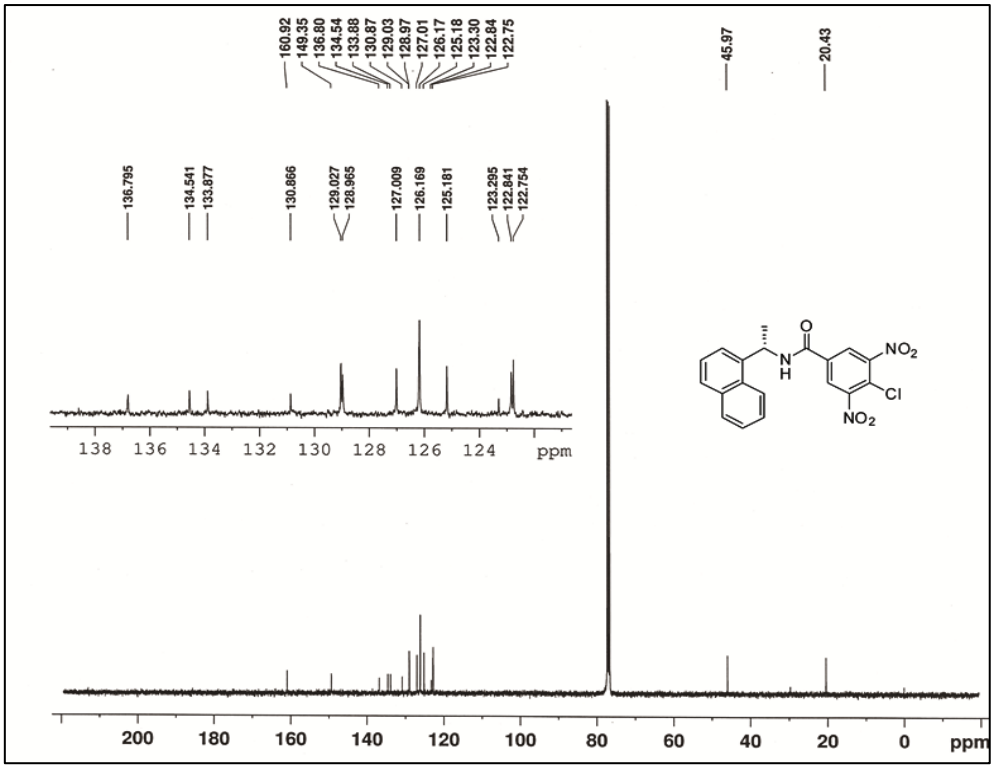

^{13}C NMR of compound (*S*)-88

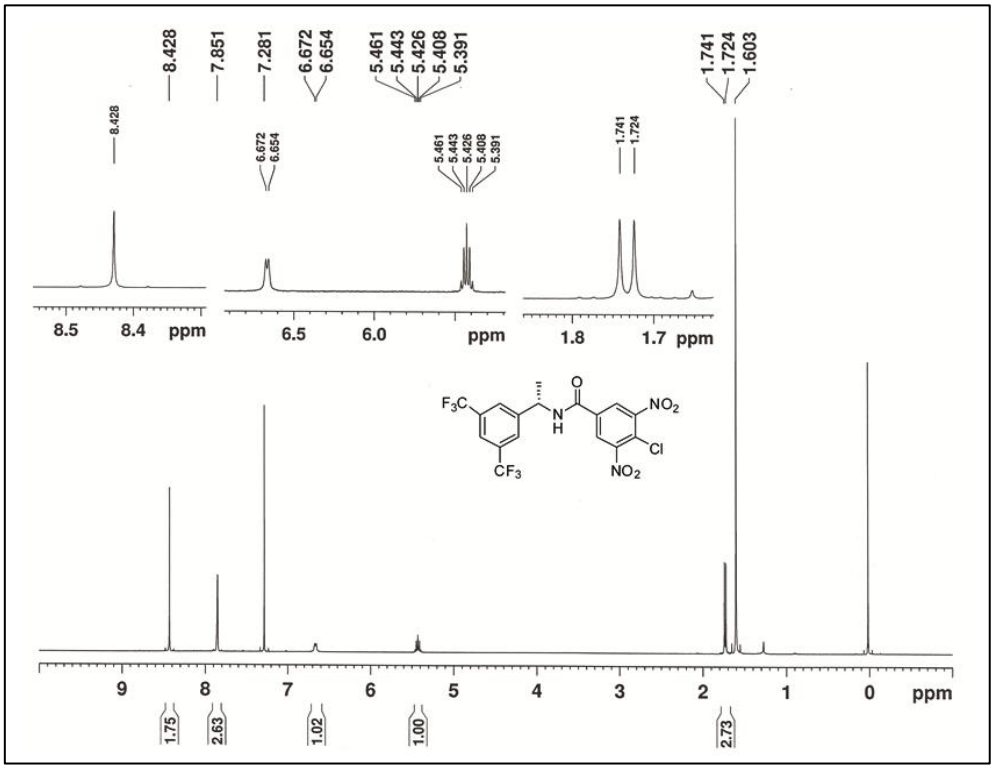

^{1}H NMR of compound (*S*)-89

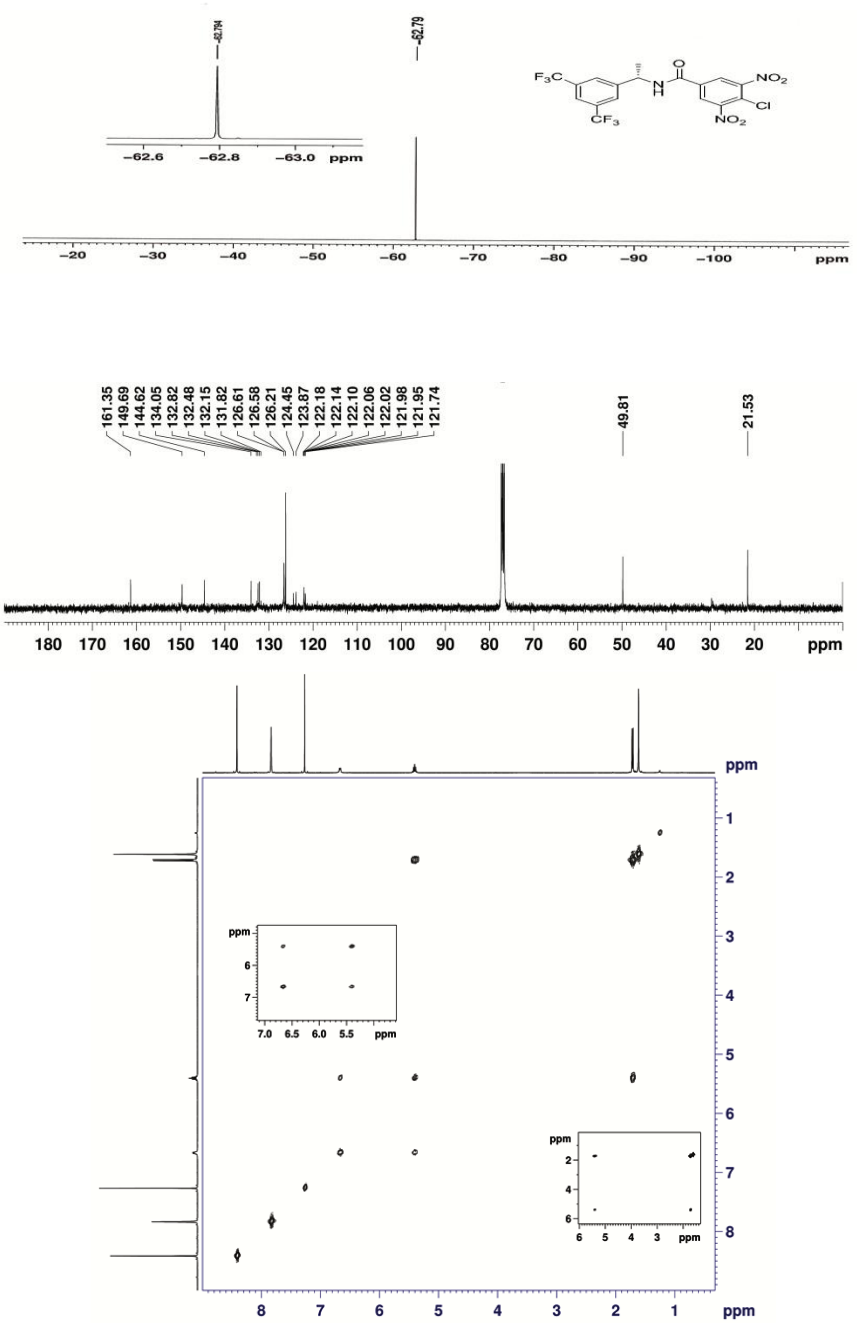

^{19}F NMR ^{13}C NMR, COSY & HRMS of compound (*S*)-89

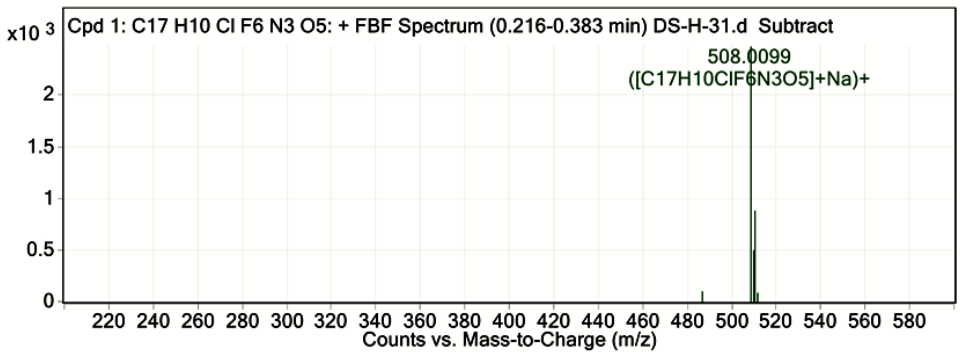

Reference:

1. E. L. Eliel, S. H. Wilen, L. N. Mander, *Stereochemistry of Organic Compounds, Wiley, New York.*

2. (a) D. J. Minick, R. C. B. Copley, J. R. Szewczyk, R. D. Rutkowske, L. A. Miller, *Chirality*, **2007,** *19*, 731. (b) P. J. Stephens, J. J. Pan, K. Krohn, *J. Org. Chem.,* **2007**, *72*, 7641. (c) H. D. Flack, *Acta Chim. Slov.* **2008**, *55*, 689.

3. (a)T. J. Ward, K. D. Ward, *Anal.Chem*, **2010,** *82*, 4712 (b) W. H. Pirkle, Y. Liu, *J. Chromatogr. A* **1996**, *736*, 31 (c) X. Gao, H. B. Kagan, *Chirality* **1998**, *10*, 120 (d) C. Gennary, S. Ceccarelli, U. Piarulli, C. Montalbetti, R. F. W. Jackson, *J. Org. Chem*. **1998**, *63*, 5312 (e) E. Yashima, *J. Chromatogr. A* **2001**, *906*, 105 (f) C. Wolf, P. A. Hawes, *J. Org. Chem*. **2002**, *67*, 2727 (g) A. Duursma, A. J. Minnaard, B. L. Feringa, *Tetrahedron* **2002**, *58*, 5773 (h) X. Lai, S. C. Ng, *Tetrahedron Lett.* **2003**, *44*, 2657. (i) C. Wolf, Z. Fadul, P. A. Hawes, E. C. Volpe, *Tetrahedron: Asymmetry* **2004**, *15*, 1987 (j) C. Moiteiro, N. Fonseca, M .J. M Curto, R. Tavares, A. M. Lobo, P. Ribeiro-Claro, V. Felix, M .G. B Drew, *Tetrahedron: Asymmetry* **2006**, *17*, 3248.

4. (a) L. Polavarapu, L. Prasad, *Chirality* **2002,** *14*, 768. (b) K. Ding, A. Shii, K. Mikami,. *Angew. Chem. Int. Ed.* **1999**, *38*, 497. (c) M. T. Reetz, A. D. Kuhling, H. Hinrichs, D. Belder, *Angew. Chem. Int. Ed.* **2000**, *39*, 3891. (d) S. Nieto, J. M Dragna, E. V. Anslyn, *Chem. Eur. J*. **2010**, *16*, 227. (e) M. W. Ghosn, C. Wolf, *J. Am. Chem. Soc.* **2009**, *131*, 16360. (f) K. Ding, A. Shii, K. Mikami, *Angew. Chem.. Int. Ed.*, **1999**, *38*, 497.

5. (a) P. Abato, C. T. Seto, *J. Am. Chem. Soc.* **2001**, ***123***, 9206. (b) M. Matsushita, K. Yoshida, N. Yamamoto, P. Wirsching, R. A. Lerner, K. D. Janda, *Angew. Chem., Int. Ed.*, **2003,** *42*, 5984.

6. (a) T. J. Wenzel, C.D. Chisholm, *Prog. Nucl. Magn. Reson. Spectrosc.* **2011**, *59*, 1. (b) S. R. Chaudhari, N. Suryaprakash, *Org. Biomol. Chem.* **2012**, *10*, 6410.

7. J. A. Dale, H. S. Mosher, *J. Am. Chem. Soc.* **1973**, *95*, 512.

8. (a) D. Parker, *Chem. Rev.* **1991**, *91*, 1441. (b) T. J. Wenzel, J. D. Wilcox, *Chirality* **2003**, *15*, 256.

9. G. M. Whitesides, D. W. Lewis, *J. Am. Chem. Soc.* **1970**, *92*, 6969.

10. J. A. Dale, D. L. Dull, H. S. Mosher, *J. Org. Chem.* **1969**, *34*, 2543.

11**.** M. Park, Seon-mi Kim, K. Choi, *Org. Biomol. Chem*., **2012**, *10*, 8051.

12. G. M. Whitesides, D. W. Lewis, *J. Am. Chem. Soc.* **1971**, *93*, 5914.

13. (a) W. H. Pirkle, D. L. Sikkenga, M. S. Pavlin, *J. Org. Chem.* **1977**, *42*, 384 (b) Discrimination of Chiral Compounds Using NMR Spectroscopy By Thomas J. Wenzel, John Wiley & Sons, Hoboken 2007. ISBN 978-0-471-76352-9.

14. Crown ether based CSA. (a) E. Bang, J.-W. Jung, W. Lee, D.W. Lee, W. Lee, *J. Chem. Soc. Perkin Trans. 2* **2001**, 1685 (b) T. J. Wenzel, J.E. Thurston, D. C. Sek, J.-P. Joly, *Tetrahedron: Asymmetry* **2001**, *12*, 1125 (c) K. Hirose, A. Fujiwara, K. Matsunaga, N. Aoki, Y. Tobe, *Tetrahedron:Asymmetry* **2003**, *14*, 555 (d) A. González-Alvarez, I. Alfonso, V. Gotor, *Tetrahedron Lett.* **2006**, *47*, 6397 (e) B. Li, X. Yang, X. Wu, Z. Luo, C. Zhong, E. Fu, *Supramol. Chem.* **2006**, *18*, 507 (f) M. Nakamura, T. Taniguchi, N. Ishida, K. Hayashi, M. Muraoka, Y. Nakatsuji, *Tetrahedron* **2011**, *67*, 9298 (g) T. P. Quinn, P. D. Atwood, J. M. Tanski, T. F. Moore ,J. Frantz Folmer-Andersen, *J. Org. Chem.* **2011**, *76*, 10020.

15. Chiral amine based representative examples are cited here. (a) R. Fulwood, D. Parker, *J. Chem. Soc. Perkin Trans 2*, **1994**, 57 (b) D. Enders, C. R. Thomas, J. Runsink, *Tetrahedron:Asymmetry* **1999**, *10*, 323 (c) M. Pomares, F. Sánchez-Ferrando, A. Virgili, A. Alvarez-Larena, J. F. Piniella, *J. Org. Chem.* **2002**, *67*, 753 (d) H. Bergmann, B. Grosch, S. Sitterberg, T. Bach, *J. Org. Chem*. **2004**, *69*, 970 (e) F. Cuevas, P. Ballester M. A. Pericàs, *Org. Lett.* **2005**, *7*, 5485 (f) F. Ma, L. Ai, X. Shen, C. Zhang, *Org. Lett.* **2007**, *9*, 125 (g) S. Shirakawa, A. Moriyama, S. Shimizu, *Org. Lett*. **2007**, 9, 3117 (h) Z. Luo, C. Zhong, X. Wu, E. Fu, *Tetrahedron Lett.* **2008**, *49*, 3385 (i) F. Ma, X. Shen, J. Yang, Z. Deng, C. Zhang, *Tetrahedron:Asymmetry* **2008**, *19*, 31.

16. (a) S. Satishkumar, M. Periasamy, *Tetrahedron:Asymmetry* **2009**, *20*, 2257 (b) B. Altava, M.I. Burguete, N. Carbó, J. Escorihuela, S. V. Luis, *Tetrahedron:Asymmetry* **2010**, *21*, 982. (c) L. S. Moon, M. Pal, Y. Kasetti, P. V. Bharatam, R. S. Jolly, *J. Org. Chem*. **2010**, *75*, 5487. (d) S. Gil, M. Palomino-Schätzlein, K. K. Burusco, C. Jaime, A. Virgili, *Chirality* **2010**, *22*, 548(e) N. H. Pham, T. J. Wenzel, *Tetrahedron: Asymmetry* **2011**, *22*, 641. (f) S. Bozkurt, M. Durmaz, H. N. Nazirogu, M. Yilmaz ,A. Sirit, *Tetrahedron:Asymmetry* **2011**, *22*, 541 (g) A. Gualandi, S. Grilli, D. Savoia, M. Kwit ,J. Gawroński, *Org. Biomol. Chem.* **2011**, *9*, 4234. (g) S.-M. Kim, K. Choi, *Eur. J. Org. Chem.* **2011**, 4747 (h) K. Tanaka, Y. Nakai H. Takahashi, *Tetrahedron:Asymmetry* **2011**, *22*, 178 (i) Q. Ma, M. Ma, H. Tian, X. Ye, H. Xiao, L.-H. Chen, X. Lei, *Org. Lett.* **2012**, *14*, 5813 (j) S. Guo, G. Wang, L. Ai,

Tetrahedron:Asymmetry **2013**, *24*, 480.

17. S. Gaoswami, K. Ghosh, S. Dasgupta, *Tetrahedron* **1996**, *52*, 12223.

18. (a) J. J. Klingenberg *Organic Syntheses, Coll.* Vol.4, **1963**, 110 (b) X. Deng, N. S. Mani *Green Chem* **2006**, *8*, 835. (c) R. Steigerr**,** *J. Org. Chem.*, **1944**,*9*, 396. (d) B. Wang , L. Yanfeng. Liu, D. Zhang , Y. Feng, J. Li, *Tetrahedron:Asymmetry* **2012**, *23*, 1338.

19. (a) M. Perasamy, M. Dalal, M. Padamja, *J. Chem Sci.* **2010**, *122*, 561, (b) S. R. Chaudhari, N. Suryaprakash, *Org. Biomol. Chem.* **2012**, *10*, 6410.

20. S. R. Chaudhari, Srinivasa, N. Suryaprakash, *RSC Advances*, **2012**, *2*, 8689.

21. N. Lokesh, S. L. Sachin, L. V. Narendra, K. Arun, N. Suryaprakash *Org. Biomol. Chem.* **2015**, ASSP.

22. S. Y. Han, K. M. Kim *Tetrahedron* **2004,** *60*, 2447.

23. S. L Manjinder, K. R. Yeeman, N. G. J. Michael, C. V John, *J. Org. Chem.* **2002**, *67*, 1536.

24. (a) Z. Tomasz, A. Michał, J Janusz, *Tetrahedron:Asymmetry* **2002**, *13*, 2053. (b) J. Kim, S. Song, O. Jung; H. Suh, *J. Incl. Phenom. Macrocycl. Chem.* **2007**, *58*, 187. (c). G. Pollini, N. Baricordi, S Benetti, C. De Risi, V Zanirato, *Tetrahedron Lett.* **2005**, *46*, 3699. (d) N. Atsushi, M. Toyoharu, K Hiroto, E. Takeshi, *Macromolecules* **2003**, *36*, 9335.

25. T. Kolasa, M. V Miller, *Tetrahedron* **1989**, *45*, 3075.

26. (a) W. Amberg, S. Hergenröder, H. Hillen, R. Jansen, G. Kettschau, A. Kling, D. Klinge, M. Raschack, H. Riechers, L. Unger, *J. Med. Chem.* **1999**, *42*, 3026. (b) R. Jansen, M. Knopp, W. Amberg, H. Bernard, S. Koser, S. Müller, I. Münster, T. Pfeiffer, H. Riechers, *Org. Process Res. Dev.* **2001**, *5*, 16.(c) B. M. Nestl, S. M. Glueck, M. Hall, W. Kroutil, R. Stuermer, B. Hauer, K. Faber, *Eur. J. Org. Chem*. **2006**, 4573.

27. (a) R. Noyori, K. Sato, Q. Yao, Encyclopedia of reagents for organic synthesis, 2008, Wiley.(b) S. H. Wilen and J.Z. Qi, *J. Org. Chem*. **1991**, *56*, 487. (c) J. Inanaga, Y. Sugimoto, T. Hanamoto, *New J. Chem.* **1995**, *19*, 707 (d) H. Furuno, T. Hanamoto, Y. Sugimoto, J. Inanaga, *Org. Lett.* **2000**, *2*, 49.

28. (a) Y. Turgut, H. Hosgoren, *Tetrahedron:Asymmetry* **2003**, *14*, 3815 (b) M. Karakaplan, T. Aral, *Tetrahedron:Asymmetry* **2005**, *16*, 2129 (c) Y. Nakatsuji, Y. Nakahar, A. Muramastu, T. Kidq, M. Akashi *Tetrahedron Lett.* **2005**, *46*, 4331

29. (a) C. J. Pedersen *J. Am. Chem. Soc* **1967,** *89*, 7017 (b) C. J. Pedersen *J. Am. Chem. Soc* **1967,** *89*, 2495

30. (a) G. A. Jeffrey, W. Saenger, Hydrogen Bonding in Biological Structures; Springer: Berlin, 1991 (b) G. R. Desiraju *Angew. Chem., Int. Ed.* Engl**. 2011,** 50.

31. S. Sambasivan, D. Kim, K.H. Ahn, *Chem. Commun*. **2010**, *46*, 541.

32. W. M Latimer, W. H Rudebush, *J. Am. Chem. Soc*. **1920**, *42*, 1431,

33**.** L**.** Maurice, Huggins, *Angew. Chem., Int. Ed.* Engl **1971**, *10*, 147

34. (a) S. Tothadi, G. R. Desiraju, Crysl. Growth Des., **2012**, *12*, 6188 [Acid Amide refernce] (b) G. K. Surya Prakash, F. Wang, M. Rahm, J. Shen, R. Haiges, G. A Olah, *Angew.Chem.Int. Ed.* **2011,** *50*, 11761 and reference therein.

35. M. Tsuboi, *Bull. Chem.Soc.Jpn* **1951**, *24*, 75.

36.(a) P. Pitchen, E. Duñach, M. Deshmukh, H. B. Kagan, *J. Am. Chem. Soc.*, **1984,** *106*, 8188 (b) M. Deshmukh, E. Duñach, S. Juge , H. B. Kagan, *Tetrahedron Lett.*, **1984**, *25*, 3467 (c) E. Duñach, H. B. Kagan, *Tetrahedron Lett.*, **1985**, *26*, 2649. (d) P. Chaprin, E. Duñach, H. B. Kagan, F.R. Theobald, *Tetrahedron Lett.*, **1986**, *27*, 2989.

37. W.H. Pirkle, P. L. Spence, B. Lamm, *J. Org. Chem.*, **1992**, *57*, 3854 (b) W.H. Pirkle, C.J. Welch, *J. Liq. Chromatogr.*, **1992**, *15*, 1947 (c) W.H. Pirkle, L. J. Brice, G. J. Terfloth, *J. Chromatogr. A*, **1996**, *753*, 109.

38. (a) Z. Pakulski, O.M. Demchuk, R. Kwiatosz, P.W. Osiński, W. Świerczyńska and K.M. Pietrusiewicz, *Tetrahedron:Asymmetry*, **2003**, *14*, 1459. (b) M. E. Koscho, P.L. Spence , W. H. Pirkle, *Tetrahedron:Asymmetry*, **2005**, *16*, 3147. (c) C. Wolf, A. M. Cook, J. E., Dannatt, *Tetrahedron:Asymmetry*, **2014**, *25*, 163.

39. D. P. Iwaniuk , C. Wolf, *J. Org. Chem.*, **2010**, *75*, 6724.

40. A. Bilz, T. Stork, G. Helmchen, *Tetrahedron:Asymmetry*, **1997**, *8*, 3999.

41. X. Mei, C Wolf, *Chem. Commun.* **2004**, 2078.

42. Crystallographic data for the structures of compound (*S*)-**2** have been deposited with the Cambridge Crystallographic Data Centre (CCDC No. 1042105). Copies of the data can be obtained from http://www.ccdc.cam.ac.uk/conts/retrieving.html or from the Cambridge Crystallographic Data Centre, 12 Union Road, Cambridge CD21EZ, UK (fax: +44-1223-336-033).

43. (a) C. R Johnson, J. E Keiser. **2003**. Methyl Phenyl Sulfoxide *Organic Syntheses, Coll*. **1973,** *5*,791

44. (a) B. C. Hamann, N. R. Branda , J. Rebek, Jr. *Tetrahedron Lett*., **1993**, *34*, 6837.

(b) G. M. Kyne, M.E. Light, M. B. Hursthouse, J. D. Mendoza, J. D. Kilburn, *J. Chem. Soc., Perkin Trans. 1,* **2001**, 1258 (c) J. Wagger, S. G. Grdadolnik, U. Grošelj, A. Meden, B. Stanovnik, J. Svete, *Tetrahedron:Asymmetry,* **2007**, *18,* 464 (d) M. Hernandez-Rodriguez , E. Juaristi, *Tetrahedron*, **2007**, *63*, 7673 (e) S. R. Chaudhari, N. Suryaprakash, *J. Mol. Struct*., **2012**, *1016*, 163 (f) S. R. Chaudhari, N. Suryaprakash, *New J. Chem.*, **2013**, ***37***, 4025.

45. T. Ema, D. Tanida, T. Sakai, *J. Am. Chem. Soc*., **2007**, *129*, 10591.

46. T. J. Wenzel, K.L. Brogan, *Enantiomer,* **2000**, ***5***, 293.

47. (a) C. Meyer, H. Duddeck, *Magn. Reson. Chem*. **2000**, *38*, 29. (b) A. E. Tremblay, N. Tan, E. Whittle, D. J. Hodgson, B. Dawson, P. H. Buist, J. Shanklin, *Org. Biomol. Chem*., **2010**, *8*, 1322. (c) C. Zonta, A. Kolarovic, M. Mba, M. Pontini, E. P. Kündig G. Licini, *Chirality,* **2011,** *23*, 796.

48. Omeprazole reference (a) P. Lindberg, A. Brandstrom, B. Wallmark, H. Mattsson, L. Rikner, K. L. Hoffman, *Med. Res. Rev*., **1990**, *10*, 1 (c) H. Cotton, T. Elebring, M. Larsson, L. Li, H. Sorensen, S. von Unge, *Tetrahedron:Asymmetry*, **2000**, *11*, 3819.

49. Refernce for Benzoin T. Ema, D. Tanida, K. Sugita, T. Sakai, K. I. Miyazawa, A. Ohnishi, *Org. Lett.,* **2008**, ***10***, 2365.

50. G. Bian, H. Fan, S. Yang, H. Yue, H. Huang, H. Zong, L. Song, *J. Org. Chem.,* **20 13**, *78*, 9137.

51. A. Veverka, D. S. Nuzum, J. L. Jolly, *Ann. Pharmacother*., **2006**, *40*, 1353.

52. S. Y. Chang, H. P. kim, K. Chang, K. Jeong *Org. Lett.*, **2004**, ***6***, 181.